Miller, K.D. (1990).
"Correlation-Based Models of
Neural Development."
pp. 267-353 in
Neuroscience and Connectionist
Theory, M.A. Gluck and
D.E. Rumelhart (eds.).
Hillsdale, NJ: Lawrence Erlbaum
Associates.

7

Correlation-Based Models of Neural Development

Kenneth D. Miller
University of California, San Francisco
Department of Physiology
San Francisco, CA 94143-0444

The task of constructing the vertebrate central nervous system is tremendously complex. Perhaps 10^{12} neurons must migrate to their proper locations, send axons to the proper targets, and make hundreds or thousands of precise synaptic connections onto other neurons. The genome does not contain sufficient information to prespecify each connection. General genetic prespecification must be supplemented by dynamical rules whose result is to construct the nervous system in a useful and precise way.

Early stages of this process, in which neurons find their proper locations and send axons to roughly the right region of the correct target structure, are known in many instances to occur properly even when all electrical activity of neurons is blocked (Harris, 1981; Schmidt & Edwards, 1983; Shatz & Stryker, 1988). Later stages of this process in many structures, however, depend on patterns of neuronal electrical activity to achieve the final precision of synaptic connections. What is known about these activity-dependent processes of synaptic modification is generally consistent with a hypothetical rule first proposed by Hebb (1949): Synapses are strengthened if there is temporal correlation between their pre- and postsynaptic patterns of activity, and weakened otherwise.

In this chapter, I review some of the evidence that correlation-based mechanisms of synaptic modification operate in biological development. I then review theoretical studies to determine the expected outcomes of development under such mechanisms. These studies have been conducted in the context of models of the visual system, the system in which the existence of such correlation-based mechanisms is best established, but many of the conclusions are more general.

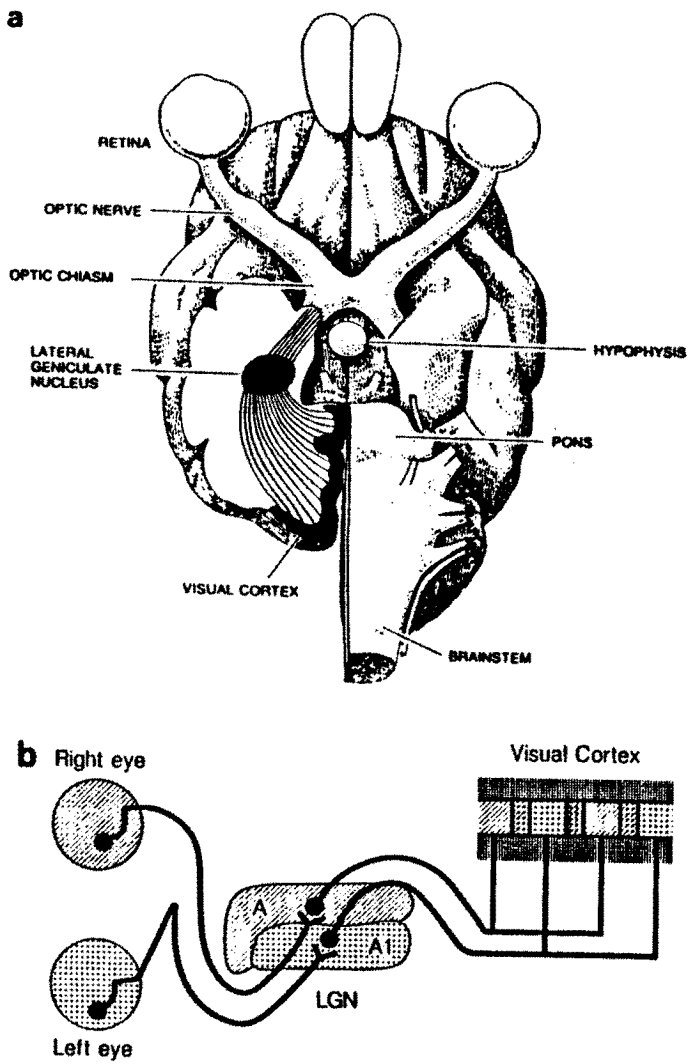

FIG. 7.1. Visual pathways in the cat. (a) The cat's brain, viewed from below. Portions of the right hemisphere (left in picture) have been dissected away to reveal the visual pathways, including the lateral geniculate nucleus (LGN) and visual cortex. Ganglion cells from each retina project axons to the LGN. LGN cells in turn project axons to the visual cortex. The right halves of each retina, which see the left half-field of vision, project axons to the LGN of the right hemisphere. That LGN in turn projects axons to the visual cortex of the same hemisphere. Thus the right LGN and right visual cortex receive inputs representing the left visual half-field in both eyes. The sorting of fibers, so that fibers from both right retinae go to the right LGN, and fibers from both left retinae go to the left LGN, occurs in the optic chiasm. Adapted from Guillery, 1974. Copyright © 1974 by SCIENTIFIC AMERICAN, Inc. All rights reserved. (b) Cartoon of the visual pathway, showing in more detail the fate of fibers representing each eye in the right hemisphere. Fibers from each eye project to separate laminae of the LGN. The two major such laminae in the cat, known as layers A and A1, are illustrated. Fibers from the eye contralateral to the LGN (the left eye, for the right LGN) project to layer A, while fibers from the ipsilateral eye (the right eye, for the right LGN) project to layer A1. Fibers representing similar receptive field points in each eye project to vertically aligned portions of layers A and A1. Retinotopically aligned geniculate cells, in turn, project axons to a retinotopically appropriate region of visual cortex, where they terminate in cortical layer 4. The axons representing each eye terminate in separate stripes or patches within this region. In the cat, as shown, there is some overlap at the borders of the two eyes' patches in layer 4; in the monkey, the two eyes' patches are cleanly separated. The cortex is depicted in cross-section, so that layers 1-3 are above and layers 5-6 below the layer 4 projection region. From Miller, Keller and Stryker, 1989. Copyright © 1989 by the AAAS.

The mechanisms to be studied here are unsupervised: there is no teacher, error signal, or reinforcement signal. All the information for synaptic modification is found in the statistics of the input patterns of activity, and in the connectivity of the nervous system receiving the input. The line between supervised and unsupervised learning is sometimes unclear. For example, a teaching signal may be incorporated into the statistics of neural activity (Rumelhart & Zipser, 1986). Nonetheless, the mechanisms studied should be thought of as refining initially diffuse projections and developing a match between input signals and neural processing structure, rather than contributing to learning from reinforcement or error signals.

CORRELATION-BASED MECHANISMS OF SYNAPTIC MODIFICATION IN NEURAL DEVELOPMENT

Ocular Dominance Segregation in Mammalian Visual Cortex and Lateral Geniculate

The first neural evidence for correlation-based mechanisms of synaptic modification was provided by the pioneering studies of Hubel and Wiesel on the primary visual cortex of cats and monkeys, reviewed in Hubel and Wiesel (1977). More recent reviews of the field include Movshon and Van

Sluyters (1981); Sherman and Spear (1982); Stryker (1986); LeVay and Nelson (1989); and Rauschecker (1989). The visual cortex (area 17) is the first receiving area in cerebral cortex for visual sensory information. It receives signals from the lateral geniculate nucleus of the thalamus (LGN), which in turn receives signals directly from the two eyes (Fig. 7.1a).

The visual cortex extends many millimeters in each of the two dimensions along the cortical surface. These two dimensions contain a continuous map of the world as seen through the two eyes, so that neighboring areas of retina are represented by neighboring areas of cortex. The cortex thus contains a "retinotopic" map, a continuous map of the retinal surface. Visual cortical cells at any given point in the cortex respond to light stimulation from only a small "receptive field" area in the visual world, and this area shifts continuously across these two dimensions of cortex to yield a map of the visual world. In the third dimension, the cortex is about 2 mm in depth, consisting of six layers. The area of the visual world represented by visual cortical cells remains essentially constant through this depth. Such organization of cortical properties in a manner that is invariant through the depth of cortex is known as *vertical* or *columnar* organization. Columnar organization appears to be a general cortical feature (Mountcastle, 1978).

Cells from the two eyes project to separate laminae of the LGN (Fig. 7.1b), so that cells in the LGN are *monocular*, responding exclusively to stimulation of a single eye. Cells from the LGN project to layer 4 of the cortex, where they terminate in separate stripes or patches largely restricted to terminals representing a single eye. Many or, in some species, all visual cortical cells in layer 4 are monocular. Most visual cortical cells in other layers respond to stimulation through either eye, but respond preferentially to the eye that dominates layer 4 at that central location. Thus, visual cortical cells may be characterized by their *ocular dominance*, or eye preference, as first described by Hubel and Wiesel (1962). The stripes or patches of cortex that are dominated across the cortical depth by a single eye are known as *ocular dominance columns* (Fig. 7.2).

This patchy, segregated projection of LGN inputs to layer 4 of cortex develops from an initially diffuse, overlapping projection (Fig. 7.3a) (LeVay, Stryker, & Shatz, 1978). Initially, LGN inputs project to layer 4 in a single retinotopic map without apparent distinction by eye represented. Individual geniculate (LGN) cells project treelike arbors of terminal processes, the largest of which appear initially to extend uniformly over regions of cortex 2 mm in diameter (Levay & Stryker, 1979) (Fig. 7.3b). The geniculate cells are likely to be making synaptic contacts with cortical cells throughout the region of arborization. Subsequently, these arbors rearrange, so that inputs representing each eye become confined to alternating, approximately half-millimeter wide ocular dominance patches. This segregation of inputs by eye represented begins at about 3 weeks of age in kittens (Shatz & Stryker, 1978), but prenatally in monkeys (Hubel, Wiesel, & Levay, 1977; Rakic, 1976, 1977).

FIG. 7.2. Ocular dominance patches in layer 4 of cat visual cortex. Photomontage was constructed from sections taken through layer 4 of one hemisphere of flattened cortex. Geniculocortical afferent terminals serving the eye ipsilateral to the cortex (the right eye, if viewing the right visual cortex) were labelled and appear white. The large dark region is the representation in cortex of the portion of the visual field corresponding to the ipsilateral eye's blind spot (its optic disc). That region of cortex receives inputs only from the unlabeled eye. From Fig. 6D of Anderson et al., 1988. Reprinted by permission of the *Journal of Neuroscience*.

The role of correlations among neuronal activities in this segregation process was first suggested by experiments demonstrating that abnormal visual experience leads to abnormal development of ocular dominance columns (Hubel & Wiesel, 1965; Wiesel & Hubel, 1965). When one eye is closed for even a few days in a young kitten (monocular deprivation), the LGN inputs representing the open eye take over far more than their normal share of visual cortex (Fig. 7.4) (Wiesel & Hubel, 1965; Shatz & Stryker, 1978). This effect occurs only during a critical period for developmental plasticity, and occurs most strongly from approximately $3\frac{1}{2}$ to 6 weeks of age in the kitten. The loss of cortical territory by the closed eye is due to competition with the open eye rather than to disuse, as can be seen in at least two ways. First, binocular deprivation (closing of both eyes) for a

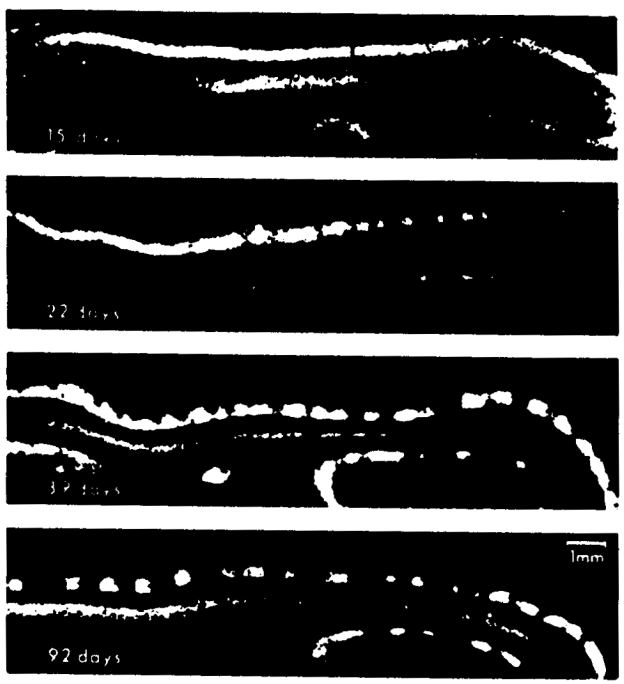

FIG. 7.3 Development of the geniculocortical projection in the cat. (a) Development of the input to layer 4 representing one eye. These are horizontal sections through one hemisphere of visual cortex, showing a cross-section of cortex as in Fig. 7.1b. Sections from cats of four different ages are shown. Geniculocortical afferent terminals serving the eye ipsilateral to the cortex were labelled and appear white. At 15 days of age, the innervation is uniform throughout layer 4. At later ages, inputs from that eye become progressively segregated into discrete patches of layer 4. Label is also present in axons in the white matter, visible as fainter, continuous label below layer 4. From LeVay and Stryker, 1979. Reprinted with permission from the Society for Neuroscience. (b) Development of the projections of individual geniculocortical afferent arbors. (1) At an early age, a putative geniculocortical afferent appears to project uniformly over an area of cortex about 2 mm in diameter. This afferent is believed to be of the type that projects the largest arbors. (2) At a later age, an afferent of the same type has its projection restricted to discrete patches of layer 4, presumably corresponding to the ocular dominance patches of its eye. (1), from LeVay and Stryker, 1979. Reprinted with permission from the Society for Neuroscience. (2), from Ferster and LeVay, 1978. Reprinted by permission of the *Journal of Comparative Neurology*.

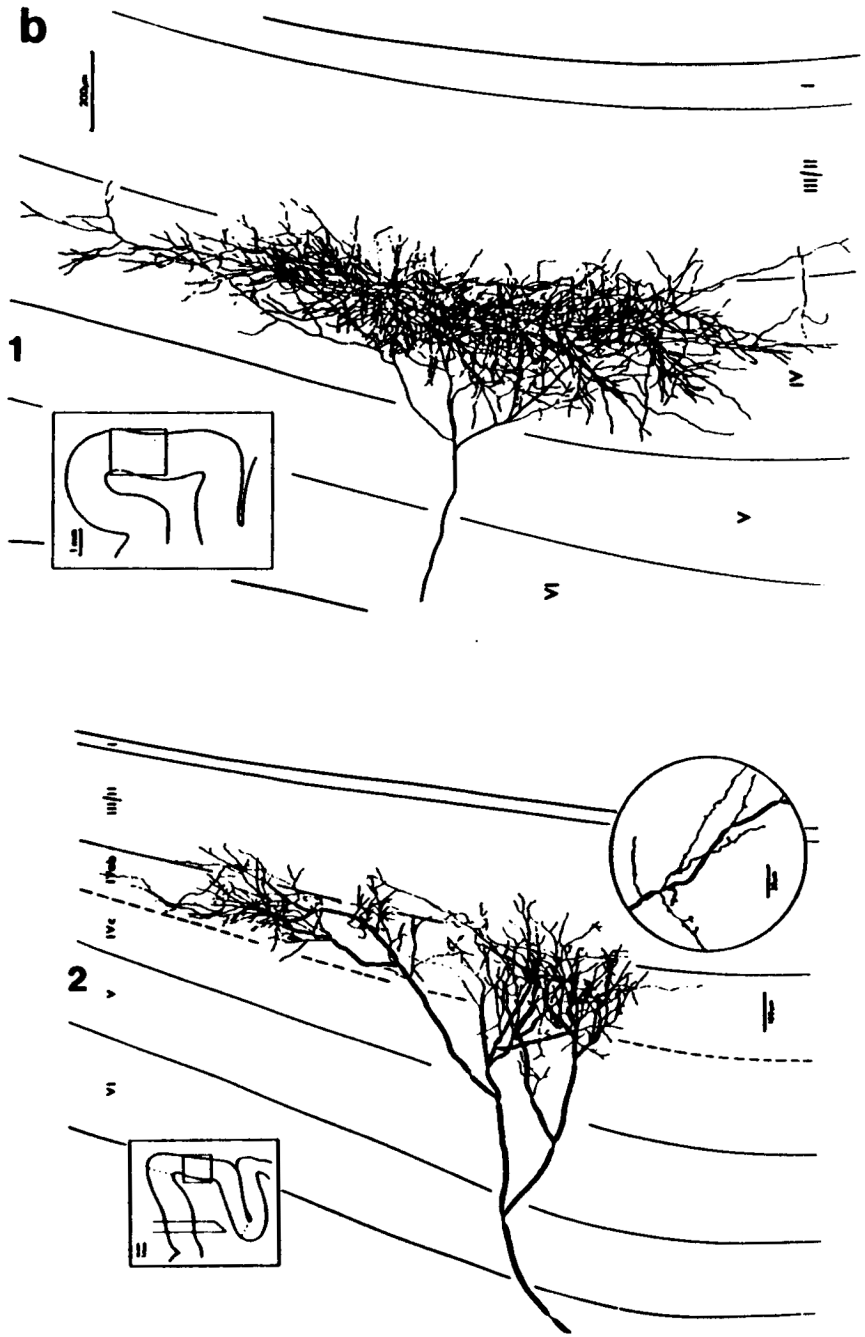

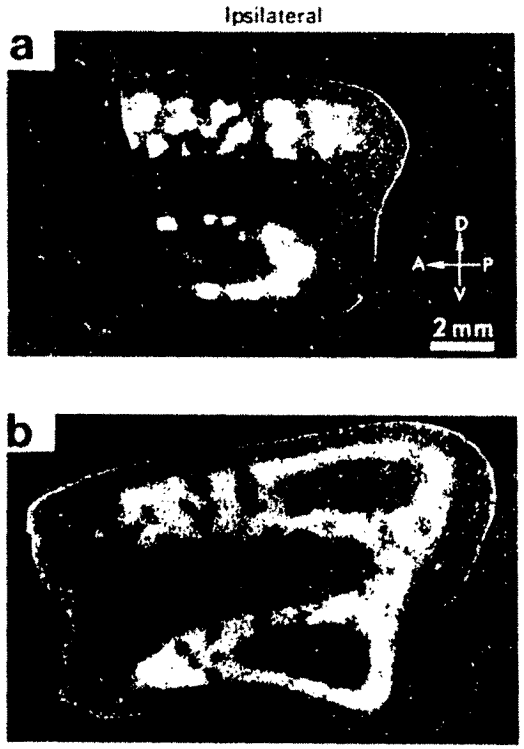

FIG 7.4. Effects of monocular deprivation in cats. Parasaggital sections (cut parallel to the midline) from visual cortex are shown. These sections intersect several portions of layer 4. Geniculocortical terminals serving the ipsilateral eye were labelled and appear white. (a): Hemisphere ipsilateral to the labelled eye in a normally reared cat, showing the normal pattern of geniculocortical termination restricted to discrete patches. (b): Hemisphere ipsilateral to the open eye in a cat which was monocularly deprived. Open eye terminals occupy most of layer 4. This animal had one eyelid sutured shut for many months, beginning prior to eye opening. Arrows indicate directions: A: anterior; P: posterior; D: dorsal; V: ventral. From Shatz and Stryker, 1978. Reprinted by permission of the Physiological Society.

similar time during the critical period causes no abnormal effect to either eye's connections to cortex or ability to drive cortical cells. In addition, monocular deprivation causes no abnormal effects in regions of cortex that receive inputs from only one eye, where the closed-eye inputs face no competition from open-eye inputs (Guillery & Stelzner, 1970; Guillery, 1972). The changes due to monocular deprivation occur in cortex, rather than at a previous level of the visual system, as ocular dominance distribution in the LGN is completely normal after deprivation.

Treatments that preserve the equality of the two eyes' activities, but destroy the correlations or cause anticorrelations between them, also alter cortical ocular dominance organization during a critical period (Hubel & Wiesel, 1965). In artificial strabismus, the extraocular muscles are altered so that the two eyes point in different directions and thus never see the same scene at the same time. Alternating monocular deprivation, in which each eye is covered on alternate days, similarly disrupts correlations between the two eyes. After either treatment, the two eyes are unable to coactivate single cortical cells. Most cortical cells in all layers of cortex become monocular, driven exclusively by the eye that dominates the corresponding region of layer 4.

The role of neural activity in ocular dominance segregation was demonstrated most clearly in recent experiments by Stryker and Harris (1986) and Stryker and Strickland (1984) (Stryker, 1986). Pharmacological blockade was used to silence all neuronal activity in both eyes of kittens beginning before the normal onset of ocular dominance segregation. As a result of this treatment, the normal ocular dominance segregation of geniculate inputs did not occur. Subsequently, nearly all cortical cells responded well to stimulation of either eye. Other kittens received artificial electrical stimulation of the nerves from the two eyes while the eyes themselves were silenced. If inputs from both eyes were stimulated synchronously, the outcome was the same as in the absence of activity. When the same pattern of electrical stimulation was given to each eye, but in a manner that was binocularly asynchronous, the result was a cortex in which virtually all cells were monocularly driven, as in artificial strabismus or alternating monocular deprivation. Thus, neuronal activity is crucial to ocular dominance segregation, but the simple presence of activity does not determine that segregation will occur. Rather, the degree of synchrony or correlation of activity between the two eyes is key.

Recent experiments have proven that activity in the cortex, rather than simply in the eyes or the LGN, is crucial to cortical ocular dominance plasticity (Reiter, Waitzman, & Stryker, 1986). A blockade of all activity in cortex, both pre- and postsynaptic, without effects on activity in the eyes or the LGN, was sufficient to prevent monocular deprivation from causing any changes in cortical ocular dominance. Furthermore, the plasticity crucially depends on both postsynaptic and presynaptic cortical activity[1] (Reiter & Stryker, 1988; see also Bear & Cooper, chap. 2 in this volume[2]). This was shown by infusion of the drug muscimol into cortex. This drug mimics the inhibitory neurotransmitter GABA to hyperpolarize

[1]Previous evidence for a critical role of postsynaptic cells existed, based on the relation between orientation selectivity and ocular dominance in animals deprived of certain orientations in only one eye or of different orientations in each eye. (See reviews in Stryker, 1977, and Rauschecker, 1989).

[2]Reiter and Stryker infused muscimol into cortex. Muscimol hyperpolarizes postsynaptic cells, and thus both blocks their activity and prevents any currents through NMDA-receptor mediated channels. In the region in which all postsynaptic action potentials were blocked, the ocular dominance shift was to the closed eye; outside this region, the normal shift to the open eye was seen. Bear and colleagues infused APV, which blocks activation of NMDA receptors on postsynaptic cells (see discussion of NMDA receptors later in this chapter). No assessment was made of the region over which NMDA receptors were blocked. Close to the cannula, where the block should be most complete, the shift was to the closed eye. Further from the cannula, a population of cells with no shift was seen. We have shown that such APV infusion severely depresses or eliminates postsynaptic action potentials in response to visual stimulation, in a manner closely correlated to the degree of NMDA receptor blockade (Miller, Chapman, & Stryker, 1989). Hence, both treatments could be achieving their effects either by the depression or elimination of postsynaptic activity, or by the blockade of NMDA-receptor activated currents, or by some combination. In any case, the effect appears to result from alterations of postsynaptic rather than presynaptic responses.

and thus silence all postsynaptic cells, without apparent affect on presynaptic activity. After monocular deprivation in the presence of muscimol, there was an ocular dominance shift in favor of the closed, less-active eye. Hence the same pattern of geniculate input may lead to a strengthening or weakening of synaptic strengths, depending on the activation of the postsynaptic cell. In particular, inputs that are more active are strengthened relative to less active inputs when they can activate the postsynaptic cell, but weakened when the postsynaptic cell is hyperpolarized and silenced.

A reasonable interpretation of this evidence is that geniculate terminals serving the two eyes compete on the basis of their patterns of activity. Correlated inputs serving a single eye successfully coactivate cortical cells and are mutually strengthened. If one eye is slightly more successful in activating a cortical cell than the other, the synapses serving it are strengthened and those serving the less successful eye are correspondingly weakened. Inputs serving one eye thus may come to dominate a region of cortex, while inputs serving the opposite eye become weakened and are ultimately excluded. Such an interpretation requires that inputs from each eye be locally correlated in the absence of visual experience, because segregation begins prenatally in monkeys and is seen even in dark-reared kittens (Wiesel & Hubel, 1965). In adult cats, the maintained activity in darkness of neighboring retinal ganglion cells is correlated within each eye over tens of milliseconds (Mastronarde, 1983a, 1983b, 1989), and correlations may exist across all retinal ganglion cells within an eye over seconds or minutes (Rodieck & Smith, 1966; Levick & Williams, 1964). These correlations have not yet been studied in younger animals, but it is known that such maintained activity exists in the fetus in rats (Galli & Maffei, 1988; see also Shatz & Kirkwood, 1984).

Thus, correlations in maintained activity among neighboring neurons may serve to guide even fetal neural development. Indeed, recent work has shown that segregation of retinal ganglion cell axons into eye-specific layers in the LGN, a process that occurs entirely prenatally in some species such as cats, may also occur through activity-dependent competition between the two eyes. The fetal LGN, analogously to the visual cortex, initially receives an overlapping innervation by the retinal ganglion cells from the two eyes. These inputs subsequently segregate to form the eye-specific laminae (Shatz, 1983; Sretavan & Shatz, 1986; Rakic, 1976, 1977). Blockade of all neural activity in fetal cats, initiated before the normal onset of segregation, prevents segregation of these laminae in the fetal LGN (Shatz & Stryker, 1988). Studies of the development of retinal ganglion cell arbors in the fetal LGN under varying conditions of intraocular competition have also suggested a role for activity-dependent competition in development of laminar segregation (Garraghty, Shatz, Sretavan, & Sur, 1988; Garraghty, Shatz, & Sur, 1988; Sretavan & Shatz, 1987; Sretavan, Shatz, & Stryker, 1988; Sur, 1988; see reviews in Garraghty & Sur, 1988; Shatz, 1988).

Activity-Dependent Development in the Optic Tectum

Correlation-based mechanisms have been implicated in the development of the projection from the retina to the optic tectum of fish and amphibia (reviewed in Fawcett & O'Leary, 1985; Schmidt, 1985; Schmidt & Tieman, 1985; Udin & Fawcett, 1988). The optic tectum is the primary recipient of visual inputs in these species, which lack a cerebral cortex. The inputs to the optic tectum come directly from the contralateral eye; each tectum normally receives direct inputs from only a single eye. It is known that the activities of neighboring retinal ganglion cells are correlated in at least one such species (Arnett, 1978; Ginsburg, Johnsen, & Levine, 1984), so the substrate exists for a correlation-based mechanism.

During development, and after regeneration of a cut optic nerve, the tectum initially receives diffuse and only coarsely topographic projections from the retina. The axons of individual retinal cells arborize over regions of tectum many times larger than will their final arbors, and individual points in tectum receive input from visual areas much larger than in the mature tectum. Complete refinement of this diffuse map to its more precise adult state does not occur when all neural activity in the eye is pharmacologically blocked (Fig. 7.5) (Meyer, 1983; Schmidt & Edwards, 1983). Complete refinement also does not occur if all retinal ganglion cells are forced to fire synchronously by raising the animal with stroboscopic lighting in the absence of patterned visual images (Cook, 1987; Cook & Rankin, 1986; Eisele & Schmidt,1988; Schmidt & Eisele, 1985). Recent evidence indicates that interference with aspects of postsynaptic tectal cell responses is sufficient to suppress refinement of the map (Cline & Constantine-Paton, 1988; Schmidt, 1988).

Although the tectum is normally monocular, it is possible artificially to force two eyes to innervate a single tectum. When this occurs, the inputs from the two eyes in many cases segregate into eye-specific patches or stripes (Fig. 7.6) (Boss & Schmidt, 1984; Constantine-Paton & Law, 1978; Levine & Jacobson, 1975; Meyer, 1979). This provides intriguing evidence that ocular dominance patches can develop simply as a by-product of activity-dependent processes that exist for other purposes, as in this system the inputs from the two eyes never naturally interact. Although biochemical markers specific for retinotopic position, and potentially for eye of origin, appear to play an important role in normal retinotectal development, convincing evidence exists that such markers are not involved in patch formation (Fawcett & Willshaw, 1982; Ide, Fraser, & Meyer, 1983). Blockade of all activity in both eyes (Boss & Schmidt, 1984; Meyer, 1982; Reh & Constantine-Paton, 1985) prevents segregation of the stripes. Interference with elements of postsynaptic tectal responses alone appears sufficient to prevent stripe formation (Cline, Debski, & Constantine-Paton, 1987). Curiously, unlike in mammalian visual cortex, there is no monocular

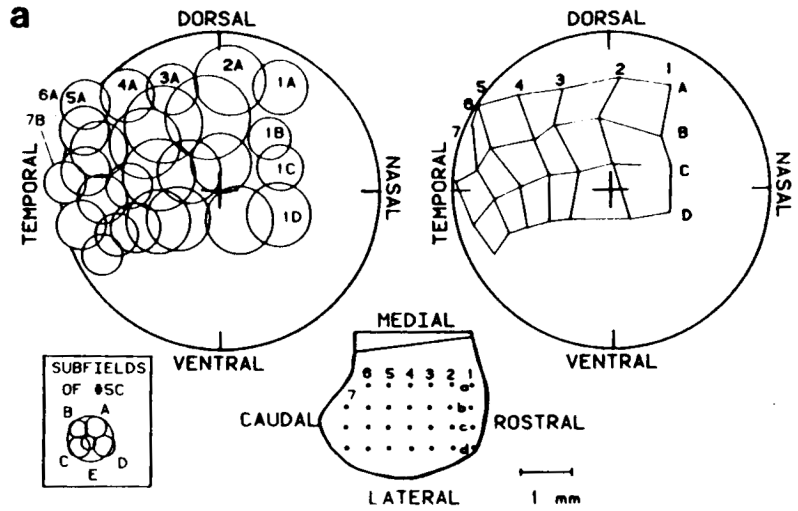

FIG. 7.5. Refinement of the visual map in fish optic tectum, and its prevention by blockade of neural activity. Optic nerves in adult animals were crushed, and a new projection from retina to tectum was then allowed to grow. (a) Retinotectal map in a fish in which all neural activity in the retina was pharmacologically blocked during regrowth. Multiunit recordings of retinal inputs were made from a regular grid of points in the tectum. Above, the two large

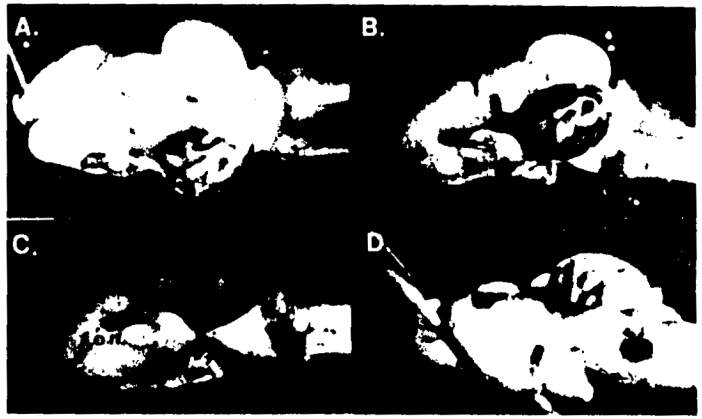

FIG. 7.6. Ocular dominance stripes on the frog optic tectum. Such stripes form when two eyes are forced to innervate a single tectum, in this case by transplantion of a third eye. Figure shows four views of the same three-eyed tadpole brain after labeling the transplanted optic nerve (t.o.n.) and tract with HRP. Terminals from the transplanted eye appear dark. Total tectal length at this stage is approximately 2 mm. Photograph supplied by Dr. Martha Constantine-Paton.

deprivation effect (Meyer, 1982); complete blockade of activity in only one eye leads to apparently normal segregation.

The optic tectum in some species also receives an indirect innervation, via an intermediate nucleus, representing the ipsilateral eye. In at least one such species, but not in several other species tested, retinotopic matching of this

circles represent the visual field, and show the centers (right) and outer boundaries (left) of the receptive fields recorded at each point in tectum. Below is a drawing of the tectal surface, showing the grid of recording locations. Centers of receptive fields form a regular grid in the visual field, demonstrating that a coarse retinotopic map exists. However, receptive fields are large and extensively overlapping. The inset shows that a typical receptive field, number 5C, was composed of many, only partially overlapping retinal inputs. (b) Retinotectal map in a fish in which normal retinal activity existed during regrowth. The tectal surface is at right, with the grid of recording points again indicated. The visual field is at left, and the outer boundary of each receptive field is shown. Receptive fields are small, approximately the size of the receptive field of a single retinal input, and largely non-overlapping. From Schmidt and Edwards, 1983. Reprinted by permission of Elsevier Science Publishers BV.

indirect ipsilateral input with the direct contralateral input appears to occur via an activity-dependent mechanism (Keating, 1975; Udin, 1983; reviewed in Udin, 1985). Following rotation of one eye, which leaves neurons physically unchanged but alters their activity patterns, the ipsilateral input to the tectum adjusts to be in register with the input from the contralateral eye. The adjustment does not occur if the animal is reared in the dark. Again, interference with aspects of postsynaptic response is sufficient to prevent this adjustment (Scherer & Udin, 1988).

Activity-Dependent Development and Plasticity in Other Neural Systems

Many neural systems exhibit phenomena that may be explained by hypothesizing an activity-dependent, perhaps correlation-based mechanism of plasticity, but in which the location, activity-dependence, or correlation-dependence of the changes is not as well established as in the phenomena previously discussed.

Cells in mammalian visual cortex exhibit many properties besides ocular dominance. One of the most characteristic properties in many species is orientation selectivity: most cells respond best to an oriented bar or edge of light, rather than to a circular spot of light, and these cells each respond largely or only to a narrow range of orientations. Like ocular dominance, orientation selectivity is organized in columns: cells throughout the depth of cortex have the same preferred orientation, and this preferred orientation changes continuously as one moves across the cortex. It is clear that a mature orientation structure can develop without visual experience (Hubel & Wiesel, 1963; Wiesel & Hubel, 1974). Whether this development depends on prenatal maintained neuronal activity is not known. There is conflicting evidence as to whether preferred orientations of cells can be modified by visual experience. Some authors have concluded that such modification can occur during the critical period for ocular dominance plasticity in young kittens (reviewed in Fregnac & Imbert, 1984; Rauschecker, 1989). However, lack of exposure to certain orientations during the critical period leads to deterioration of responses of cortical cells that preferred those orientations. This effect would seem to reflect disuse rather than competition. Results that have been interpreted to demonstrate competitive modification of preferred orientations can be adequately explained by this disuse effect (Stryker, Sherk, Leventhal, & Hirsch, 1978). It remains of great interest to determine both theoretically and experimentally the possible role of activity-dependent competition in the development of orientation selectivity.

Mammalian retinal ganglion cells may be either on-center or off-center, and in adults maintained activity in darkness of these two types of cells is anticorrelated (Mastronarde, 1983a, 1983b, 1989). Individual cells in the

LGN normally receive only on-center or only off-center input. In the cat, action-potential blockade in one eye from birth leads most LGN cells responding to that eye to develop mixed on-center/off-center excitatory input (Dubin, Stark, & Archer, 1986). This treatment also leads to much greater than normal mixing onto LGN cells of two normally segregated types of retinal ganglion cells known as X-cells and Y-cells. In some species, on-center and off-center LGN cells are found in separate geniculate sublaminae (Conway & Schiller, 1983; LeVay & McConnell, 1982; Schiller & Malpeli, 1978; Stryker & Zahs, 1983). In two such species, inputs to cortex from on-center and off-center geniculate cells are segregated in cortex into separate patches much like ocular dominance patches (McConnell & LeVay, 1984; Zahs & Stryker, 1988). It is intriguing to think that one might be able to account for the various patterns of segregation observed simply with a correlation-based mechanism.

The left and right visual cortices are connected via axons passing through the corpus callosum. The left and right visual cortices represent the right and left visual hemifields, respectively. In the adult cat, these visual callosal connections come from and connect to the representation of the vertical midline, the only area represented in both hemispheres. Earlier in development these projections are more widespread. Alterations in visual experience during a critical period alter the final sources and/or terminations of these projections in a manner that could be explained by selection for a correlation in firing between callosal and geniculate inputs to cortical cells (Innocenti & Frost, 1979, 1980; Innocenti, Frost, & Illes, 1985).

In rat or mouse somatosensory cortex, individual whiskers are represented in discrete cylindrical columns known as "barrels." These barrels develop between postnatal days 2 and 5 or 6. Removal of whiskers during this time leads to rearrangements and shrinkage of the corresponding barrels and in some cases expansions of adjacent barrels (Belford & Killackey, 1980; Durham & Woolsey, 1984; Jeanmonod, Rice, & Van der Loos, 1981). This suggests that more active inputs may take over more cortical space during this critical period, but this interpretation is complicated by the potential presence of alterations, including cell death and degeneration, at intermediate stages of the somatosensory input from periphery to cortex (Jeanmonod et al., 1981).

Although this anatomical plasticity occurs only during a critical period, there is a great deal of physiological evidence that correlation-based mechanisms of plasticity may be active in somatosensory cortex of many species throughout adult life[3] (reviewed in Allard, 1989; Wall, 1988;

[3]Anatomy refers to structure, for example the physical locations and patterns of nerves and their connections. Physiology refers to function, in particular the patterns of electrical response of nerve cells. Thus, changes in synaptic strengths or weights, that is the effectiveness

Merzenich, Allard, Jenkins, & Recanzone, 1988). The body is mapped in a locally continuous way onto the cortex. This map can change throughout adult life with changing patterns of peripheral activity,[4] so that a more active peripheral area can come to activate a larger area of cortex while less active peripheral areas correspondingly lose cortical space (Merzenich, Kaas, Wall, Sur, Nelsen, & Felleman, 1983; Wall, Kaas, Sur, Nelson, Felleman, & Merzenich, 1986). Interpretation of many of these results is complicated by the fact that these changes, though assessed in cortex, may originate at any of several levels from the periphery to the cortex.

Some of the most striking results in adult somatosensory cortex are those in which only peripheral correlations, not amounts of activity, are altered. The monkey's fingers are represented in discrete, though adjacent, patches of somatosensory cortex. As a rule, individual cortical cells in these areas have receptive fields restricted to a single finger. Thus, the transition from the representation of one finger to that of the next is normally sudden and discontinuous. Patterns of correlation were altered by sewing together the skin surfaces of two adjacent fingers (Clark, Allard, Jenkins, & Merzenich, 1988). This leads the normally uncorrelated skin surfaces at the surgical boundary, which originate from separate fingers, to become correlated in their activity much as adjacent skin surfaces on any other continuous patch of skin. After several months, the cortical map was found to vary continuously from one finger to another. A large intermediate region of cortex was activated by both fingers.

Representations in adult somatosensory cortex generally can be moved in these experiments by no more than 600-700 μm across cortex (Allard, 1989; Merzenich et al., 1988). This distance limit has been interpreted to mean that the plasticity involves the strengthening or weakening of existing synapses rather than the movement of synapses to entirely new areas of cortex. That is, areas of the periphery might be represented by inputs that project effective synapses to the normal area of representation, and weak or relatively ineffective synapses to adjacent areas over 600-700μm; these relative strengths might be dynamically maintained by activity patterns, and alter when activity patterns alter.

In many regions in which two neural inputs innervate a single output region, a segregation of the two inputs into discrete columnar patches or stripes resembling ocular dominance columns is seen. In somatosensory cortex, neurons representing rapidly adapting and slowly adapting peripheral receptors are organized into patches, as are those representing glabrous and dorsal portions of skin (Merzenich, Nelson, Kaas, Stryker, Jenkins, Zook, Cynader, & Schoppmann, 1987; Sur, Wall, & Kaas, 1984). In primate prefrontal cortex (Goldman & Nauta, 1977; Goldman-Rakic & Schwartz, 1982; reviewed in Goldman-Rakic, 1984) and somatosensory cortex (Jones, Burton, & Porter, 1975; Jones, Coulter, & Wise, 1979), intra-hemispheric and inter-hemispheric (callosal) cortico-cortical connections terminate in alternating columns. Inputs from prefrontal and temporal cortices to caudate nucleus similarly are interdigitated (Selemon & Goldman-Rakic, 1985). In some cases the cells projecting to two different regions from one region are somewhat segregated and interdigitating (Arikuni, Sakai, & Kubota, 1983; Caminiti, Zeger, Johnson, Urbano, & Georgopoulos, 1985; Jones & Wise, 1977; Schwartz & Goldman-Rakic, 1984). There is no evidence at present as to whether these various patterns are established in an activity-dependent manner. However, these patterns are suggestive that the activity-dependent processes that lead to ocular dominance segregation may not be specific to the visual or sensory systems, but rather may occur more generally.

The optic tectum in mammals is known as the superior colliculus. In some higher mammals, it receives direct inputs from both eyes, which terminate in ocular dominance patches (reviewed in Fawcett & O'Leary, 1985; Schmidt & Tieman, 1985). These patches develop from an initially uniform, overlapping innervation by the two eyes. Activity dependence is indicated by the fact that monocular deprivation, if initiated sufficiently early in the segregation process, leads to a change in the size of the ipsilateral projection. The segregation process in this case involves death of some input cells rather than simply rearrangements and movement of terminal arbors.

The superior colliculus or optic tectum of mammals and birds contains a map of auditory space as well as a map of visual space (reviewed in Knudsen, Du Lac, & Esterly, 1987). The map of auditory space is synthesized from cues of inter-ear time and intensity differences that are changing rapidly during development as the animal's head and ears grow. Hence there is developmentally a need for plasticity to adjust the auditory space map to changing cues. In the barn owl, vision appears to calibrate the auditory map, as binocular visual deprivation from birth leads to a less precise and somewhat abnormal auditory spatial map (Knudsen, 1988). Developmental plasticity in the barn owl keeps the auditory map in register with the visual map. During a sensitive period in a young owl, plugging of one ear leads to an abnormal auditory map that is in register with the visual map only when the ear remains plugged (Knudsen, 1985). Once the head and ears reach adult size, this capacity to develop an abnormal map in response to abnormal auditory experience is lost. During a longer, critical

of synapses in activating the postsynaptic cell, without broad changes in the patterns of physical connectivity, would with current techniques only be detectable as a physiological change in the responses of the cells.

[4]Peripheral in this context refers essentially to the skin; more generally, to those areas that have receptors to detect somatosensory stimulation.

period, exposure to normal auditory cues can reestablish a normal auditory map in a previously earplugged owl. This readjustment, as assessed behaviorally, occurs only if visual cues are present, and will match the auditory map to even a distorted visual map created by prisms (Knudsen & Knudsen, 1985). These phenomena may involve error-correcting mechanisms, in which visual assessment of errors in localization are used to correct the auditory map, rather than simple correlation-based mechanisms, in which visual and auditory inputs whose activities are correlated come to coinnervate tectal cells.

Other auditory maps may also show developmental dependence on patterns of neural activity. In the inferior colliculus of the mouse, an auditory area, cells normally sharpen their tuning for frequency of auditory inputs during the second and third postnatal weeks. Forcing all afferents to fire synchronously during this time by choice of an appropriate auditory stimulus prevents this sharpening (Sanes & Constantine-Paton, 1985), suggesting that sharpening may normally be caused by correlated firing among afferents tuned to similar frequencies. Circumstantial arguments based on contrasting the diffuse nature of anatomical projections with the precision and specificity of physiological responses suggest that many features of the auditory projection in mammals may require correlation-based mechanisms for their development and maintenance (Merzenich, Jenkins, & Middlebrooks, 1984).

In summary, in two well-studied systems, the mammalian visual cortex and optic tectum of fish and amphibia, strong evidence exists for correlation-based mechanisms of activity-dependent plasticity. Such mechanisms are strongly implicated in visual cortex in the development of ocular dominance columns, and in optic tectum in the development of ocular dominance stripes, receptive field refinement and, in one species, retinotopic matching of inputs. A wide variety of other systems display phenomena suggestive that similar mechanisms are active.

The selection of systems presented here should not blind one to the existence of many neural systems whose development may not depend on activity. A great variety of mechanisms underlie neural development and plasticity (Purves & Lichtman, 1985). For example, exchange of trophic (nutritive) factors between neurons and their targets allows nerve cells to dynamically adjust themselves to changing conditions presented by evolutionary development and individual growth (Purves, 1988; Purves, Snider, & Voyvodic, 1988). Similarly, biochemical markers of location, gradients of differential adhesion and fiber-fiber interactions can be used to organize topographic maps and to match innervation to target size and shape (Fraser, 1980; Willshaw & von der Malsburg, 1979). Activity-dependent mechanisms are of special interest because they make use of the functional activity of nerve cells to effect such dynamic adjustments. These mechanisms allow the nervous system to be altered and shaped by the animal's

experience, and so provide a potential substrate for learning. Evolution has likely led to a precise selection of those times and locations in which the nervous system may be so altered by neural activity.

Having reviewed systems in which correlation-based mechanisms of synaptic plasticity may be active, I now turn briefly to consider the biological mechanisms that may underlie such plasticity.

BIOLOGICAL SUBSTRATES FOR CORRELATION-BASED MECHANISMS

At this writing, there is a single elegant and well-established mechanism known to embody a Hebbian mechanism of correlation-based synaptic plasticity. This is plasticity mediated by the N-methyl-D-aspartate (NMDA) receptor in certain areas of hippocampus (also discussed in McNaughton & Nadel, chap. 1 in this volume; Bear & Cooper, chap. 2 in this volume).

Synaptic currents triggered by activation of the NMDA receptor are both transmitter-activated and voltage-dependent (see reviews in Mayer & Westbrook, 1987; Nicoll, Kauer, & Melenka, 1988). Thus, the currents are activated only if the presynaptic cell is active, releasing transmitter to bind to the receptor, and the postsynaptic cell is at least locally depolarized, alleviating a voltage-dependent block of the NMDA receptor-activated channels. This means that NMDA receptors provide precisely the trigger required by a Hebbian mechanism: a signal of correlated pre- and postsynaptic activation. When the NMDA-activated channels are opened they, unlike other related channels, allow calcium to enter the postsynaptic cell. Calcium in turn can trigger many events that may lead to strengthening of the synapse. Thus, in response to the signal of correlated activity, a calcium current passes that may be capable of enhancing synaptic strength. Because this calcium current can be local to a single synapse, the potentiation can be specific to active synapses.

This elegant mechanism has been implicated in a form of plasticity known as long term potentiation (LTP) in one region of hippocampus (McNaughton & Nadel, chap. 1 in this volume; reviewed in Brown, Chapman, Kairiss, & Keenan, 1988; Nicoll et al., 1988). It has clearly been shown that the conjunction of presynaptic activity and postsynaptic depolarization leads to a long-term strengthening of synaptic inputs specific to those inputs that were active. This provides a basis for cooperation and association among inputs: if a sufficient number of inputs are activated to depolarize the cell, all will be potentiated; as will any other input active while the cell remains depolarized. This potentiation occurs only if NMDA receptors are activated and if calcium is able to enter the cell through the channels activated by NMDA receptors. However, postsynaptic depolarization, transmitter activation of NMDA receptors and calcium entry is not sufficient to cause long-lasting potentiation; presynaptic activation is also

necessary, perhaps to supply an additional unidentified factor (Kauer, Malenka, & Nicoll, 1988). Persistent activation of a calcium-dependent protein kinase appears necessary to the maintenance of the potentiation: blocking such kinases reversibly blocks LTP after it has been initiated (Malinow, Madison, & Tsien, 1988).

In the visual cortex and optic tectum, there is provocative, but far less compelling, evidence that NMDA receptors may be involved in activity-dependent plasticity. Understanding of the mechanisms underlying plasticity proceeds much more slowly in these systems than in hippocampus, for technical reasons. In these systems blockade of postsynaptic NMDA receptors prevents or alters the normally seen plasticity. This has been shown for ocular dominance plasticity in visual cortex (Kleinschmidt, Bear, & Singer, 1987; Bear & Cooper, chap. 2 in this volume), refinement of receptive fields in optic tectum (Cline & Constantine-Paton, 1988; Schmidt, 1988), ocular dominance segregation in optic tectum (Cline et al., 1987), and matching of the direct contralateral and indirect ipsilateral retinotopic maps in optic tectum (Scherer & Udin, 1988).

However, many mechanisms may be responsible for plasticity. It is well established that interference with the patterns of activity will disrupt or alter plasticity. Therefore, to show that activation of NMDA receptors is serving as a specific signal for activity-dependent plasticity, it is critical to show that blockade of those receptors does not otherwise interfere with activity. NMDA receptors appear to be involved in sensory-driven neural activity in many systems. We have shown that in visual cortex, normal sensory responses of cortical cells depend upon activation of NMDA receptors (Miller, Chapman, & Stryker, 1989). A similar result has been shown in somatosensory thalamus (Salt, 1986, 1987), and preliminary evidence of this exists in the LGN (Moody & Sillito, 1988) and optic tectum (Fox & Fraser, 1987). Hence, the effects of NMDA-receptor blockade on plasticity in visual cortex and optic tectum may simply represent the effect of blocking postsynaptic activity. It therefore remains unclear whether the NMDA-receptor mechanism of Hebbian plasticity is operating either in visual cortex or in optic tectum.

Many mechanisms have been proposed to underly plasticity. The final mechanism maintaining LTP in hippocampus appears to involve activation of a protein kinase. At least two different kinases may be capable of causing such potentiation, protein kinase C and type II calcium/calmodulin-dependent protein kinase (CaM kinase II) (Brown et al., 1988; Nicoll et al., 1988). Protein kinase C can be activated either by calcium or by activation of phosphatidyl inositol metabolism, while CaM Kinase II is activated by calcium (reviewed in Schwartz & Greenberg, 1987). Activation of phosphatidyl inositol metabolism can itself trigger release of intracellular calcium (reviewed in Nahorski, 1988). Each kinase can constitute a biochemical

"switch": brief activation can alter the kinase so that it remains activated for a long period independent of the activating agent (Schwartz & Greenberg, 1987). CaM kinase II is localized in large quantities at the postsynaptic density in mammalian brain. Theoretical study has suggested that the kinetic properties of CaM kinase II allow the many molecules in the postsynaptic density to collectively store graded information (Lisman & Goldring, 1988), which presumably could be translated into graded levels of synaptic strength.

There may be many routes to the same final mechanism of plasticity. Calcium can enter the cell through activation of NMDA receptors, but it may also enter through voltage-dependent calcium channels or be released from intracellular stores. Voltage-dependent calcium channels, if located on dendritic spines, might contribute to a Hebbian mechanism (Gamble & Koch, 1987; see also Coss & Perkel, 1985; Miller, Rall, & Rinzel, 1985). Both voltage-dependent calcium channels and phophatidyl inositol metabolism can be activated or modulated by a wide variety of neurotransmitters and receptors (reviewed in Nahorski, 1988; Tsien, Lipscombe, Madison, Bley, & Fox, 1988).

Similarly, there may be many final mechanisms by which plasticity can be achieved. Cortical cells might, when active, release diffusible modulatory or trophic factors that are taken up in an activity-dependent way by presynaptic terminals and alter their synaptic strength (Fawcett & O'Leary, 1985; Garthwaite, Charles, & Chess-Williams, 1988; Lichtman & Purves, 1981; Piomelli, Volterra, Dale, Siegelbaum, Kandel, Schwartz, & Belardetti, 1987; Purves, 1988).[5] Such factors may also act on glial cells, which in turn may cause synaptic modification (Garthwaite et al., 1988; Muller, Engel, & Singer, 1988). Lynch and Baudry (1984) suggested that activation of a postsynaptic calcium-activated protease may expose postsynaptic receptors and thus enhance synaptic response. This protease when activated may also cause long-term activation of the protein kinases discussed earlier (Schwartz & Greenberg, 1987). At the neuromuscular junction, plasticity may be mediated by activity-dependent release by postsynaptic cells of proteases that destroy synaptic terminals, combined with protection from the effects of these proteases by presynaptic activity (O'Brien, Ostberg, & Vrbova, 1980). Theoretical proposals had previously been made that Hebb-type rules could be achieved by degradation of nonstabilized synapses, and stabilization of synapses by correlated pre- and postsynaptic activity (Changeux & Danchin, 1976; Stent, 1973). Mechanisms by which

[5]This proposal also provides a possible alternative or additional mechanism by which activation of NMDA receptors may lead to synaptic plasticity. Two candidate diffusible modulatory factors are released by neurons in some systems specifically in response to NMDA receptor activation (Dumuis, Sebben, Haynes, Pin, & Bockaert, 1988; Garthwaite et al., 1988).

calcium and synaptic activity might stabilize synapses have been suggested (Kater, Mattson, Cohan, & Conner, 1988).

Thus, evolution has had many tools available to construct the correlation-dependent mechanisms that we have seen acting in development. Although we lack detailed biochemical knowledge of the mechanisms underlying plasticity in these systems, it is profitable to study theoretically the outcomes to be expected from the general correlation-based rules shared by such mechanisms. Aspects of development common to such rules may be determined in a manner largely independent of the underlying details. This can allow distinctions to be drawn between general classes of mechanisms, such that each class produces a distinct developmental outcome. These points will be illustrated through theoretical studies of the development of ocular dominance columns in visual cortex.

THEORETICAL STUDIES OF DEVELOPMENT WITH A CORRELATION-BASED MECHANISM

The system of ocular dominance columns in mammalian visual cortex, which we have studied (Miller, 1989a; Miller, Keller, & Stryker, 1986, 1988, 1989; Miller & Stryker, 1988, 1989; Miller, Stryker, & Keller, 1988), has a number of advantages as a model system for the study of correlation-based mechanisms. First, it is the system that is best explored phenomenologically. Second, the nature of the competition simplifies the analysis. The competition is binary, between left- and right-eye inputs, rather than between larger numbers of patterns. The two sets of inputs begin from nearly equal strengths, so that one can assume a symmetry between them. Third, a large-scale structure organized across many postsynaptic cells develops. This enables distinctions to be drawn between mechanisms that would be indistinguishable in their action on a single isolated postsynaptic cell. The second and third advantages apply equally to ocular dominance stripes in frog optic tectum. There is a fourth advantage of visual cortex. Geniculate and visual cortical cells have all been born, and the geniculocortical projection has grown into layer 4, before column development begins (Luskin & Shatz, 1985; Rakic, 1976, 1977; Shatz, 1983; Shatz & Luskin, 1986). In cats, where column development begins after birth, it is clear that this projection is retinotopically ordered before column development begins (Hubel & Wiesel, 1963; Sherk & Stryker, 1976). One can therefore regard the retinotopic map as largely fixed while columns are forming, and thus ignore movement of synapses as opposed to changes in

their strengths.[6] In the frog, in contrast, new cells are continuously born in both the eyes and the tectum. Differential patterns of growth of the eyes and the tectum force the retinotopic map to continuously reorganize, and this involves a mixture of activity-dependent and activity-independent interactions (Easter & Stuermer, 1984; Fraser, 1985; Reh & Constantine-Paton, 1984).

Formulation of a Simple Model

We model the LGN as two two-dimensional layers, one responding to each eye, and the cortex as a single two-dimensional layer representing layer 4. This model could apply equally to any situation in which two input layers innervate a single output layer. We let roman letters $x,y, \ldots$ represent two-dimensional positions in cortex, and greek letters $\alpha,\beta, \ldots$ represent two-dimensional positions in the LGN (Fig. 7.7). These positions are taken to be *retinotopic* positions, so that the position α can refer to a position either in the left- or right-eye LGN layer, and so that $x - \alpha$ can be meaningfully defined as the distance across cortex between the position x and the retinotopic position in cortex corresponding to α. $S^L(x,\alpha,t)$, $S^R(x,\alpha,t)$ designate the total synaptic strength or weight between LGN position α in the left or right eye, respectively, and cortical position x, at time t.

A few elements are crucial to any correlation-based model of development (Fig. 7.7). These are the elements that determine how synapses can influence one another's development. One element is correlation in the activities of the inputs. This is described by a set of correlation functions, $C^{LL}(\alpha - \beta)$, $C^{LR}(\alpha - \beta)$, which tell the correlation in activity between the left-eye input from α and, respectively, the left- or right-eye input from β. C^{RL} and C^{RR} are defined similarly. A second element is the initial connectivity. This is described by an arbor function, so called because it characterizes the extent of the terminal arborizations of inputs, as well as the dendritic spread of cortical cells. This is also known in connectionist literature as a fan-in or fan-out function. The arbor function, $A(x - \alpha)$, tells the number of synapses made between position α and position x. A third element is interaction across cortex, by which activity at one cortical location

[6] Although the retinotopic map does not substantially change during the period of column formation, it remains possible that the synaptic plasticity associated with development of ocular dominance occurs through continual local sprouting and retraction of synapses, rather than through modification of the strengths of fixed synapses as we assume here. It is likely that a model involving local sprouting and retraction would require only small additions to the framework we develop here, but this remains an important issue for analysis.

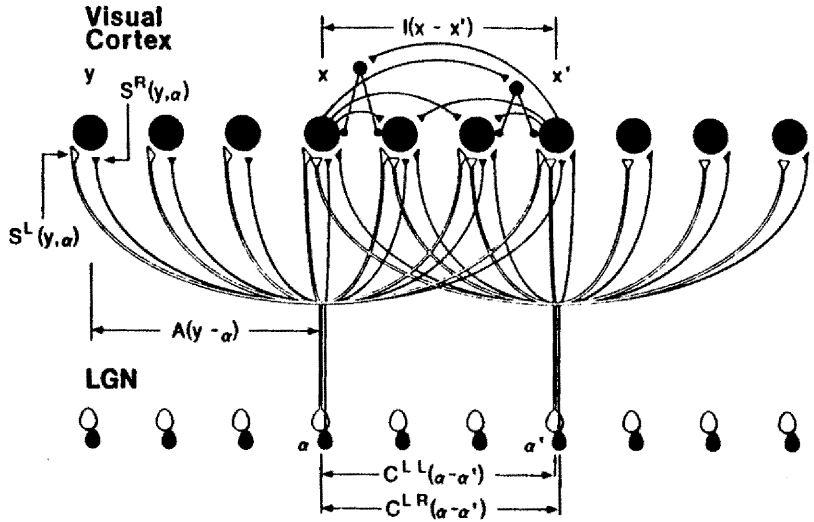

FIG. 7.7. Illustration of the major elements of the model and the notation. The LGN is modeled as consisting of two layers, one serving each eye. Each layer is two-dimensional, though only one dimension is illustrated. Greek letters α, α' label two-dimensional geniculate positions. The cortex is modeled as a single, two-dimensional layer with positions labeled by roman letters x, x', y. In the figure, x and x' are taken to be the cortical positions retinotopically corresponding to α and α', respectively. Geniculate cells project synapses to a range of cortical cells, centered about the retinotopically corresponding cortical position. The anatomical strength of the projection (the number of synapses) from the geniculate cell of either eye at α to the cortical cell at position y is proportional to the arbor function $A(y - \alpha)$. $A(y - \alpha)$ depends on the distance between y and the point x that corresponds retinotopically to α. The physiological strength of the projection (the effectiveness of the geniculate cell's activity in driving the cortical cell) is given by the total synaptic strength, $S^L(y,\alpha)$ for the left eye or $S^R(y,\alpha)$ for the right eye. S^L and S^R change during development in the model, while the arbor function A is held fixed; the assumption is made that anatomical changes occur late in development, after a pattern of synaptic strengths is established. Geniculate inputs are locally correlated in their firing. The correlation of a left-eye afferent at α with a left-eye afferent at α' is given by $C^{LL}(\alpha - \alpha')$, while its correlation with a right-eye afferent at α' is given by $C^{LR}(\alpha - \alpha')$. There is an influence across cortex, by which activation at the point x' influences growth of synapses at the point x. The sign and strength of this influence is given by the intracortical interaction function, $I(x - x')$.

From Miller, Keller, and Stryker, 1989. © 1989 by the AAAS.

influences the effectiveness of correlated synapses on different cortical cells at nearby locations. In the absence of such interactions, the competition occurring on each cortical cell would be independent, and hence one would not expect to see development of large-scale clustering of cortical properties such as ocular dominance. This intracortical influence is summarized by a cortical interaction function, $I(x - y)$, described further later. A fourth element is some means of stabilization to ensure that the strengths of individual synapses, and the total synaptic strength over any cell, stay within some bounded ranges. This framework can be used to study a variety of biological mechanisms. With knowledge of the three functions characterizing a neural system—the correlation functions, arbor function, and cortical interaction function—many aspects of development can be predicted, in ways that depend only very generally on the mode of stabilization.

The cortical interaction function is particularly dependent on the biological mechanism proposed to underlie plasticity. Therefore, understanding the dependence of developmental outcome on this function provides one of the key means of distinguishing between classes of mechanisms. In a Hebbian mechanism, the cortical interaction function is determined by intracortical synaptic connections. Two synapses firing in synchrony at distinct points in cortex will both tend to excite their postsynaptic cells. If the two postsynaptic cells excite one another, the two synapses will therefore increase the chance that the other's postsynaptic cell will be excited and hence will tend to enhance one another's growth via a Hebbian mechanism. Conversely if the two postsynaptic cells inhibit one another, the two synapses will tend to inhibit one another's growth. Thus, the cortical interaction function for a Hebbian mechanism is positive over distances at which cortical cells tend to excite one another, and negative over distances at which cortical cells tend to inhibit one another. For mechanisms that involve the release and uptake of a trophic or modification factor, the cortical interaction function must also describe spread of influence across cortex due to diffusion.

We ignore the detailed temporal structure of cortical activation, and regard interactions as instantaneous. We hypothesize that the tendency of two inputs to fire in a correlated way is the key feature to be abstracted, and the finer details of activity patterns can be ignored. We also assume that the time scale over which inputs must be correlated in order to influence one another's growth is much smaller than the time scale over which synapses are appreciably changing their strengths.

After averaging over input patterns, and ignoring the problem of stabilization for the moment, we arrive at an equation describing correlation-based mechanisms of development (derived in appendix 1). This equation expresses the changes in synaptic strengths with time, as a function of the

correlations among afferents, the spread of arbors, the intracortical interactions, and the synaptic strengths themselves:

$$\frac{d}{dt}S^L(x,\alpha,t) = \lambda A(x-\alpha)\sum_{y,\beta} I(x-y)[C^{LL}(\alpha-\beta)S^L(y,\beta,t) + C^{LR}(\alpha-\beta)S^R(y,\beta,t)] - \gamma S^L(x,\alpha,t) - \epsilon^L A(x-\alpha)$$

$$\frac{d}{dt}S^R(x,\alpha,t) = \lambda A(x-\alpha)\sum_{y,\beta} I(x-y)[C^{RR}(\alpha-\beta)S^R(y,\beta,t) + C^{RL}(\alpha-\beta)S^L(y,\beta,t)] - \gamma S^R(x,\alpha,t) - \epsilon^R A(x-\alpha) \quad (1)$$

λ, γ, ϵ^L and ϵ^R are constants. The last two terms of each equation express decay or growth of synapses in the absense of interactions between them. The first term expresses interactions between synapses, and can be summarized as follows. First, the influence exerted by any one synapse on another, is a product of the correlation in activity between those two synapses (how likely are they to be firing together?), the intracortical interaction (if they are firing together, how do they influence one another?), and the strength of the influencing synapse. For two synapses on the same postsynaptic cell, this is just the product of their correlations and the influencing synaptic strength, weighted by the constant $I(0)$. For synapses on different postsynaptic cells, this influence is weighted by the intracortical interaction $I(x-y)$ between the respective postsynaptic locations. Second, interactions are linear: The change in one synapse is a simple sum of the influences exerted on it by each other synapse. Linearity is not necessary to the analysis, but is used for simplicity at this stage. Third, to find the change in total synaptic strength, sum over all influencing synapses, then multiply by the arbor function, which represents the number of synapses being influenced. We have taken the three functions, correlations, connectivity, and cortical interactions, to be fixed (time-invariant) as ocular dominance columns develop.

Several types of stabilization are considered. We assume that individual synapses cannot increase beyond some maximum strength, nor decrease below some minimum. For synapses from LGN to cortex, the minimum synaptic strength is zero: these synapses biologically are exclusively excitatory. We also consider the effects of conserving total synaptic strength over a cortical cell or a geniculate cell, or of limiting these totals to remain within a bounded range. Some justification for such limits is provided by biological evidence for intrinsic limits to the total number of synapses

supported by a cell, though there is no direct evidence as to limits to total synaptic strength. In monkey visual cortex synapse number does not appear to be affected by visual experience during the time of ocular dominance column development (Bourgeois, Jastreboff, & Rakic, 1989). Similarly, in the goldfish optic tectum, total synapse number appears conserved in an activity-independent manner during post-regeneration map refinement (Hayes & Meyer, 1989a, 1989b). These findings suggest that activity is involved in determining the arrangements or strengths of synapses but not their number. When the full complement of retinal cells are forced to innervate only half a tectum, the number of synapses per tectal cell remains normal, indicating that on average each retinal cell makes only half the normal number of synapses (Hayes & Meyer, 1988b; Murray, Sharma, & Edwards, 1982). This suggests that there is a limited number of postsynaptic sites per tectal cell, for which incoming neurons must compete. Conversely, in several systems, if inputs are given a larger than normal target structure, they are unable to innervate the target cells with normal density, indicating intrinsic limits in the total innervation that can be supported by an input cell (Brown, Jansen, & Van Essen, 1976; Fladby & Jansen, 1987; Hayes & Meyer, 1988a; see also Schneider, 1973).

To understand how development proceeds under correlation-based mechanisms as modeled in these equations, we begin by considering development of a single, isolated cortical cell receiving inputs from the LGN. We then consider the reverse, the development of two isolated geniculate cells, one from each eye, projecting to the cortex. Finally, we consider how these two processes are knit together, and what new features are added, in development of the full system: two layers of geniculate cells projecting to a cortical layer.

How An Isolated Cortical Cell Develops

For an isolated cortical cell, the equations simplify. Suppressing the cortical index, x, letting $x = \alpha = 0$ be the cortical and LGN locations retinotopically corresponding to the position of the cortical cell, and taking $I(0) = 1$, the equations become

$$\frac{d}{dt}S^L(\alpha,t) = \lambda A(\alpha)\sum_{\beta}[C^{LL}(\alpha-\beta)S^L(\beta,t) + C^{LR}(\alpha-\beta)S^R(\beta,t)] - \gamma S^L(\alpha,t) - \epsilon^L A(\alpha)$$

$$\frac{d}{dt}S^R(\alpha,t) = \lambda A(\alpha)\sum_{\beta}[C^{RR}(\alpha-\beta)S^R(\beta,t) + C^{RL}(\alpha-\beta)S^L(\beta,t)] - \gamma S^R(\alpha,t) - \epsilon^R A(\alpha) \quad (2)$$

Figure 7.8 shows a typical developmental sequence for a cell under this equation. For this sequence, we have considered a 13 by 13 square of geniculate cells from each eye, with a connectivity $A(\alpha)$ to the cortical cell that tapered in strength gradually from the center of the square and was set to zero outside a circle of radius $6\frac{1}{2}$. Correlations between inputs from the

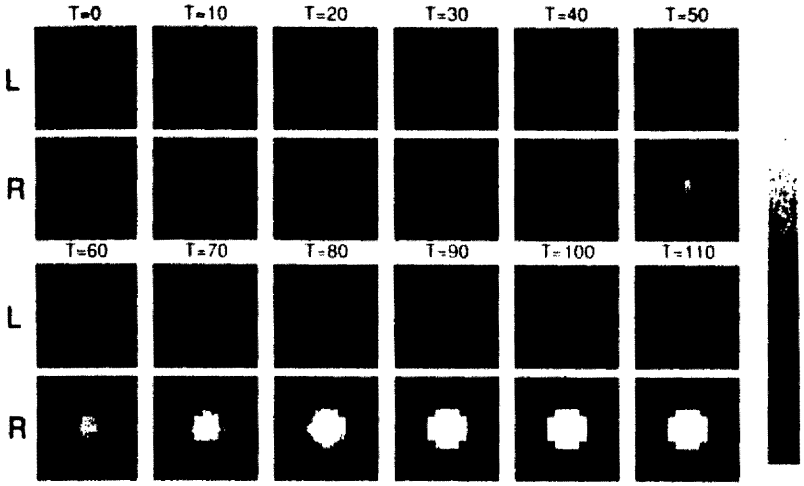

FIG.7.8. Development of an isolated cortical cell under equation 2. Vertically paired 13 by 13 squares show synaptic strengths of left- and right-eye inputs from each of 13 by 13 retinotopic positions at one time. The greyscale codes total synaptic strength from each input position, from strength 0 (black) to 11.2 (the maximum value of $8A(\alpha)$, white). Synaptic strengths at 12 successive times are shown. Time proceeds from left to right and top to bottom, beginning with the randomly assigned initial condition ($T = 0$) at top left and concluding with the 110th iteration ($T = 110$) at bottom right. Synaptic strength becomes concentrated in the center of the receptive field, and then becomes monocular as right-eye inputs grow at the expense of left-eye inputs. The cortical cell was constrained to keep a constant synaptic strength. This constraint was achieved by subtracting $\epsilon(t)A(\alpha)$ from each total synaptic strength after each iteration, where $\epsilon(t) = \frac{\Sigma_\alpha [\frac{d}{dt}S^L(\alpha,t) + \frac{d}{dt}S^R(\alpha,t)]}{\Sigma_\alpha [A^L(\alpha) + A^R(\alpha)]}$ and $A^L = A^R = A$. Synaptic strengths were frozen if their value reached zero: they were no longer allowed to change, assigned derivatives of zero and omitted from the constraint. Parameters used were $\lambda = 0.0025$, $\gamma = \epsilon^L = \epsilon^R = 0$. The arbor function $A(\alpha)$ was that illustrated in Fig. 7.9. The correlation function was the same-eye correlation function with gaussian parameter 0.3 of Fig. 7.9.

same eye, C^{LL} and C^{RR}, were taken to fall gradually from one to zero as separation between the two inputs varied from zero to about six grid points; opposite eyes were neither correlated nor anticorrelated ($C^{LR} = C^{RL} = 0$). The arbor function and correlation function used are illustrated in Fig. 7.9. The cortical cell was constrained to keep a constant synaptic strength, so that one synapse's gain must be some other synapse's loss. Individual total synaptic strengths $S(\alpha)$ began with a randomly assigned synaptic strength near $A(\alpha)$. These synaptic strengths were then allowed to decrease until they reached zero, or increase until they reached $8A(\alpha)$.

Two features are immediately apparent from the simulation. First, central synapses in the receptive field grow more rapidly than do peripheral synapses, leading receptive fields to refine in size. Second, the synapses of one eye gradually come to grow faster than the synapses of the other, leading to a monocular cortical cell that receives inputs from only one eye. Development of monocularity occurs more slowly than refinement of the receptive field. These results are robust: they occur for all initial conditions tried, and are relatively insensitive to variations in the functions as will be discussed.

These features are easy to understand. Inputs in the center of the receptive field have more correlated neighbors than inputs in the periphery, provided that the correlations decrease with distance. Hence, the center of the receptive field will grow faster than the periphery. Similarly, one eye is likely initially to have slightly more total or central synaptic strength than the other due to the random initial conditions. This eye tends to gain slightly more strength than the other at each iteration, leading it to increase its advantage in a feedforward, accelerating process. This occurs more slowly than refinement, because the two eyes start out much more equal in numbers and strengths of correlated neighbors than do central versus peripheral synapses.

This understanding can be made more precise from consideration of the model equations. The equations are most illuminating if we transform them from right- and left-eye variables, S^R and S^L, to sum and difference variables: $S^S = S^R + S^L$, $S^D = S^R - S^L$. We assume the two eyes are equal in all respects as in the simulation, so that $C^{LL} = C^{RR} = C^{\text{SameEye}}$, $C^{LR} = C^{RL} = C^{\text{OppEye}}$, $\epsilon^L = \epsilon^R = \epsilon$. Define $C^S = C^{\text{SameEye}} + C^{\text{OppEye}}$, $C^D = C^{\text{SameEye}} - C^{\text{OppEye}}$. Then Eq. 2 becomes

$$\frac{d}{dt}S^S(\alpha,t) = \lambda A(\alpha)\sum_\beta C^S(\alpha - \beta)S^S(\beta,t) - \gamma S^S(\alpha,t) - 2\epsilon A(\alpha)$$

$$\frac{d}{dt}S^D(\alpha,t) = \lambda A(\alpha)\sum_\beta C^D(\alpha - \beta)S^D(\beta,t) - \gamma S^D(\alpha,t) \qquad (3)$$

FIG 7.8

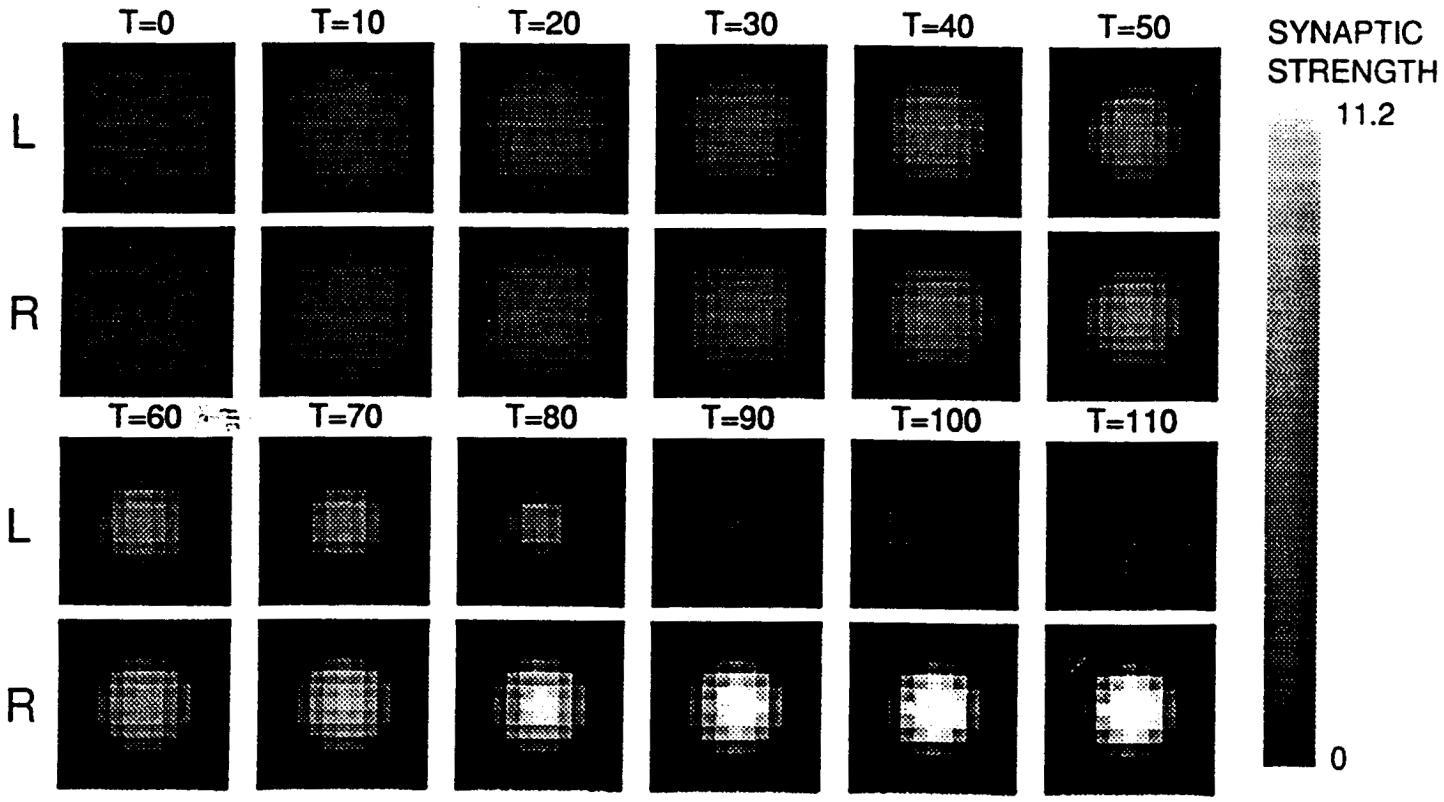
T=0
T=10
T=20
T=30
T=40
T=50
L
R
T=60
T=70
T=80
T=90
T=100
T=110
L
R
SYNAPTIC STRENGTH
11.2
0

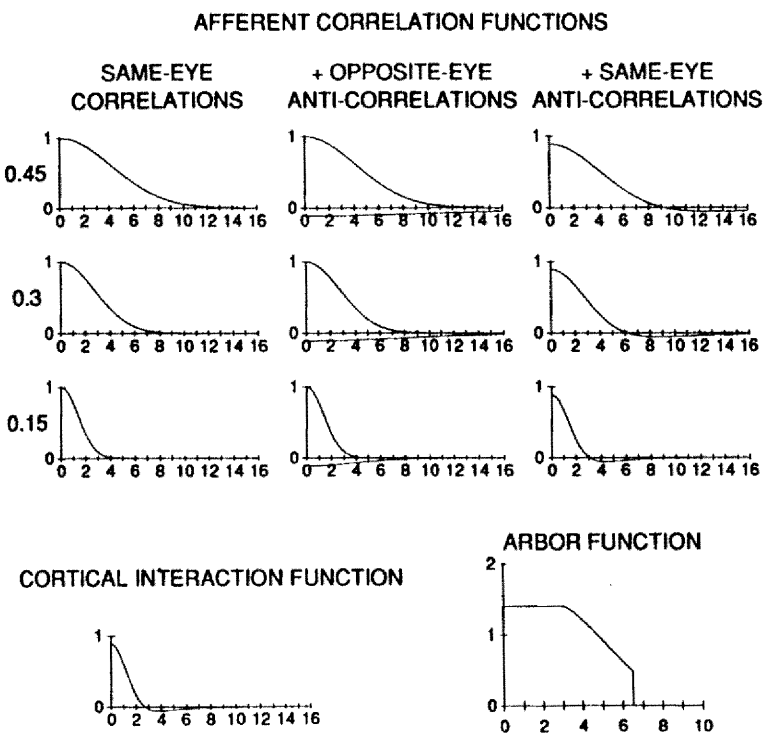

FIG. 7.9. Functions used in simulations and numerical calculations for isolated cortical or geniculate cells. Value of function, vertical axis, versus distance in grid intervals, horizontal axis. All functions are circularly symmetric in two dimensions. A 13 by 13 square grid of inputs potentially connects to a single cortical cell, and conversely an input potentially connects to a 13 by 13 grid of cortical cells. Top: Correlation functions $C(\alpha)$. These summarize the correlation in activity between two afferents separated by a retinotopic distance α, either serving the same eye ($C^{LL}(\alpha)$ or $C^{RR}(\alpha)$, assumed equal), or serving opposite eyes ($C^{LR}(\alpha)$ or $C^{RL}(\alpha)$, assumed equal). The correlation functions in the left column (same-eye correlations) are positive within each eye, and zero between the two eyes: $C^{LL}(\alpha) = e^{-\alpha^2/(\varkappa D)^2}$, where $D = 13$ is the arbor diameter and $\varkappa = 0.45$, 0.3 or 0.15 for the top, middle, or bottom row respectively, and $C^{LR} = 0$. The positive correlations within each eye are shown. The correlation functions in the middle column (+ opposite-eye anticorrelations) are positive within each eye as in the left column, as shown by the curves above the horizontal axes; but in addition there are weaker, more broadly ranging negative correlations between the two eyes, shown by the curves below the horizontal axes. These negative correlations are given by $C^{LR}(\alpha) = \frac{1}{9}e^{-\alpha^2/(3\varkappa D)^2}$. The correlation functions in the right row (+ same-eye anticorrelations) have these same negative correlations added to the positive correlations within each eye, and have zero correlation between the two eyes. This creates a "Mexican hat" function within each eye, so that inputs are correlated at shorter distances and anticorrelated at longer distances, as illustrated. Bottom left: Cortical interaction function $I(x)$. This is a Mexican hat function, given by gaussians as for the correlation functions but with $\varkappa = 0.1333$. Bottom right: Arbor function $A(\alpha)$, representing the relative number of synapses made by an input to a cortical cell when the retinotopic position of the two differs by α. The arbor function tapers from the center of the 13 by 13 grid of inputs, so that more outlying inputs project less densely, and is set to zero for $\alpha > 6.5$. The function is constructed as follows: Inputs are modeled as projecting uniform circular arborizations of radius 6, and cortical cells as extending uniform circular dendritic fields of radius 3. The arbor function $A(\alpha)$ is taken proportional to the overlap of such an input arborization and cortical dendritic field when the two cells are separated by $\alpha < 6.5$. While these scales are arbitrary, they determine a scale in terms of which the other functions can be defined: One can characterize the correlation function by its variation over an arbor radius, in this case approximately ± 6 grid intervals.

Note that S^S and S^D have become decoupled, each developing independently of the other, which simplifies analysis.[7]

Individual total synaptic strengths $S(\alpha)$ begin with a randomly assigned synaptic strength $(1.0 + \eta(\alpha))A(\alpha)$ where $\eta(\alpha)$ is a number randomly drawn from a uniform distribution between -0.2 and 0.2. At the initial condition, then, $S^S(\alpha) = (2 + \eta^S(\alpha))A(\alpha)$, $S^D(\alpha) = \eta^D(\alpha)A(\alpha)$, where $\eta^S = \eta^L + \eta^R$, $\eta^D = \eta^L - \eta^R$, and η^S and η^D both range between -0.4 and 0.4. Since η^S is small, near the initial condition we can approximate $S^S(\alpha) \approx 2A(\alpha)$. Hence near the initial condition our equations become (ignoring the decay terms)

$$\begin{aligned} \frac{d}{dt}S^S(\alpha) &= 2\lambda A(\alpha)(C^S * A)(\alpha) \\ \frac{d}{dt}S^D(\alpha) &= \lambda A(\alpha)(C^D * (\eta A))(\alpha) \end{aligned} \tag{4}$$

where the * indicates convolution, $X * Y(\alpha) = \Sigma_\beta X(\alpha - \beta)Y(\beta)$.

Refinement of the receptive field is determined by the equation for S^S, the summed synaptic strength. Sites in the receptive field where $C^S * A$ is larger will initially grow faster. A is always positive or zero, and either flat or decreasing with increasing distance. Therefore if C^S is nonnegative and

[7] S^I and S^R appeared decoupled also, for our choice of correlation functions for which $C^{LR} = C^{RL} = 0$. However, they were coupled by the constraints, which fix $\Sigma_\alpha S^S(\alpha)$ to be a constant but do not modify the equation for S^D.

decreases over the distance across a receptive field, central synapses will grow faster than peripheral ones. If C^S is perfectly flat, refinement will not occur. If C^S is "Mexican hat," positive at short distances and negative at longer distances, then, depending on the shapes of C^S and A, central synapses may grow more slowly than peripheral ones, by virtue of having more negatively correlated neighbors.

Development of monocularity is determined by the equation for S^D, the difference in strength between the two eyes. The initial condition for S^D is a small, random perturbation of $S^D = 0$, which may be positive or negative at each point α. This initial condition can be described as a mixture of very small amounts of a set of *characteristic patterns* of S^D, much as a curve can be decomposed by fourier analysis into a set of sine and cosine waves. Technically, these characteristic patterns of ocular dominance are the *eigenfunctions* of the operator that determines the time development of S^D. This is described more fully in appendix 2. The characteristic patterns are distinguished by the fact that each grows independently of the others, each at its own rate. The patterns grow exponentially, so that the fastest-growing pattern quickly dominates. A pattern is monocular if it is all positive or all negative, representing domination throughout the receptive field by a single eye.

The initial condition of S^D is a random mixture of small amounts of each characteristic pattern. Hence, the development of monocularity is determined by the answers to two questions. First, is the fastest-growing characteristic pattern of S^D monocular? If it is, there will be an intrinsic tendency for the cell to develop ocular dominance. Second, if it is monocular, what determines its relative advantage in growth rate over binocular patterns and over the tendency of S^S to refine and perhaps reach saturation? These will determine the speed and robustness with which ocular dominance will emerge.

The nature of the fastest-growing pattern is determined in large part by the fastest-growing eigenfunction of the correlation function C^D, though the arbor function also plays a role.[8]. The dependence on C^D is illustrated in Fig. 7.10. This shows the three fastest-growing characteristic patterns that result from each choice of correlation function illustrated in Fig. 7.9.

[8]To a reasonable approximation, one can think of the characteristic patterns as the eigenfunctions of the correlation function, restricted to the region over which $A(\alpha)$ is nonzero, but in truth they depend upon both the arbor function and the correlation function. Some authors, looking at similar equations, have described the solutions as the *principal components*, or eigenfunctions, of the correlation matrix (Baldi & Hornik, 1989; Linsker, 1988; Oja, 1982; Sanger, 1989). This is true if the correlation matrix tells the correlation between each pair of inputs, irrespective of their locations. If we wish the correlation function to describe the correlation between inputs just as a function of their locations, however, then the solutions must also take into account the arbor function, which describes the number of inputs from each location.

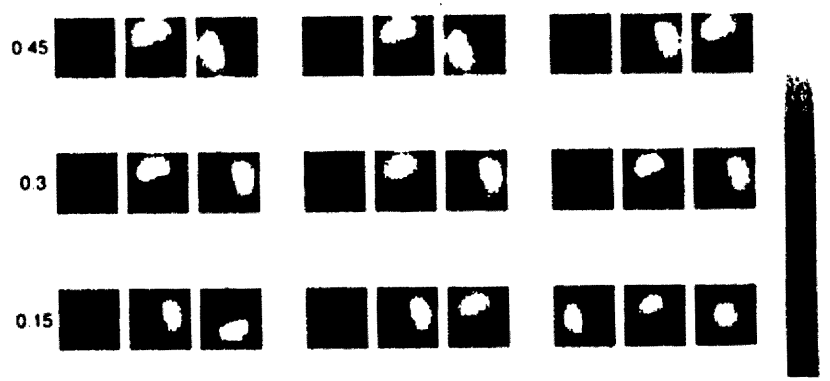

FIG. 7.10. The three fastest-growing characteristic patterns of ocular dominance, for each of the nine correlation functions of Fig. 7.9. The arbor function of Fig. 7.9 is used. These are the patterns of $S^D \equiv S^R - S^L$ which grow most quickly from an initial condition in which the two eyes' innervations are nearly equal. Each 13 by 13 square shows a pattern of S^D across a cortical cell's receptive field. The greyscale ranges from domination by one eye (white, S^D positive) to domination by the other (black, S^D negative). The sign of a pattern is arbitrary, because each pattern grows at the same rate if all its elements are multiplied by a constant such as -1. Hence, the important aspect of a pattern is not which eye dominates a region of the receptive field, but rather whether the receptive field is dominated everywhere by a single eye and hence is monocular, or is dominated by opposite eyes in different regions and hence is binocular. Each set of three patterns decreases in growth rate from left to right; the corresponding growth rates are shown in table 1.

The fastest-growing pattern of each set of three is at the set's left. This pattern is monocular provided C^D does not include significant anticorrelations within an arbor radius (about ± 6 grid intervals). In the one case with such anticorrelations, the fastest-growing pattern is binocular (Fig. 7.10, lower right). The less rapidly C^D decreases with distance, the less rapidly the fastest-growing pattern decreases with distance and the more closely the pattern mimics the arbor function in shape. In the limit in which C^D is constant across an arbor diameter, the fastest-growing pattern is precisely given by the arbor function, meaning a pattern of dominance develops with equal strength at all synapses in the receptive field. This makes sense, because if C^D is constant, location in the receptive field loses all significance with respect to the synaptic modification rule for S^D. A less rapid decrease of C^D is achieved either by broadening of correlations within each eye (upward in Fig. 7.10), or by addition of broader anticorrelations between the two eyes (opposite-eye anticorrelations). A more rapidly decreasing C^D

FIG 7.10

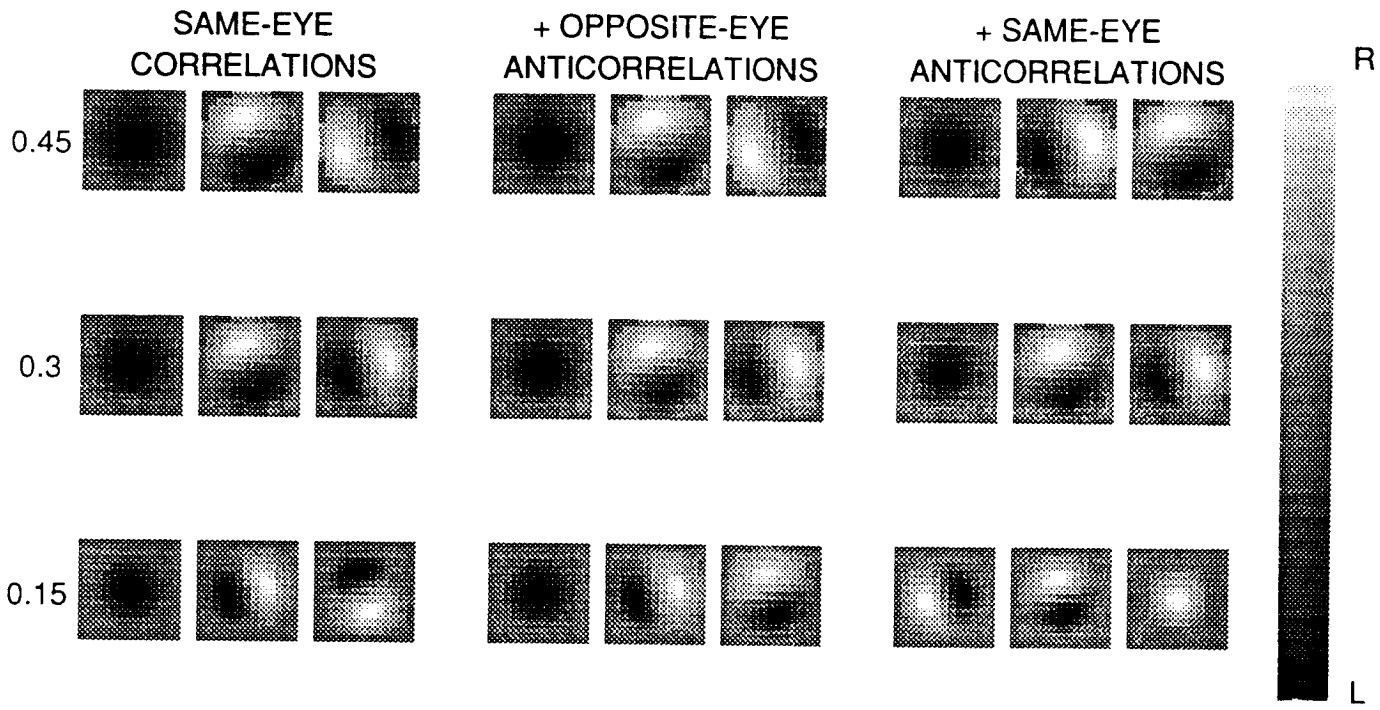
SAME-EYE CORRELATIONS
+ OPPOSITE-EYE ANTICORRELATIONS
+ SAME-EYE ANTICORRELATIONS
0.45
0.3
0.15
R
L

is achieved by the reverse, or by addition of anticorrelations within each eye (same-eye anticorrelations).

A spatially broader correlation function C^D, in addition to leading to a spatially broader pattern of ocular dominance, also leads to a greater advantage in growth rate of the dominant monocular pattern relative to the other patterns (Table 7.1). In the limit of a constant C^D, the monocular pattern is the only one with a positive growth rate, all other patterns decaying away at the rate γ. This advantage in growth rate of the monocular over binocular paterns develops, because the broader correlation function increases the number of locations at which S^D's of like sign will contribute to one another's growth, and at which S^D's of opposite sign will detract from one another's growth. Opposite-eye anticorrelations also enhance the development of monocularity even if they only increase the amplitude of C^D without broadening it. This is so because they enhance the growth rates of the patterns of S^D relative to the growth rates of the patterns of S^S. A simple change in amplitude of both C^D and C^S would not enhance monocularity; it would be equivalent to a change in λ, changing the speed of development but, within a reasonable range, not altering the outcome. Opposite-eye anticorrelations, however, increase the amplitude of C^D while decreasing the amplitude of, and adding anticorrelations to, C^S. This enhances the growth of S^D relative to that of S^S. The speed of development of monocularity thus becomes proportionately faster relative to the speed of development of receptive field refinement, potentially allowing ocular dominance to develop further before saturation halts the development process.

Figure 7.11 displays the results of simulated time developments for the functions whose characteristic patterns were illustrated in Figure 7.10. As

TABLE 7.1
Growth Rates of Characteristic Patterns of Fig. 7.10.

Correlation Function	*1st Pattern*	*2nd Pattern*	*3rd Pattern*
Same-eye corr 0.45	67.6	23.0	23.0
+ Opp-eye anti-corr 0.45	81.0	23.8	23.8
+ Same-eye anti-corr 0.45	54.4	22.3	22.3
Same-eye corr 0.3	41.7	21.8	21.8
+ Opp-eye anti-corr 0.3	53.3	23.1	23.1
+ Same-eye anti-corr 0.3	30.7	20.5	20.5
Same-eye corr 0.15	14.0	10.9	10.9
+ Opp-eye anti-corr 0.15	21.1	13.1	13.1
+ Same-eye anti-corr 0.15	9.0	9.0	8.9

Growth rates are shown for $\lambda = 1$, $\gamma = 0$ in Eq. 3 for S^D. For other values, all growth rates would be multiplied by λ and decreased by subtraction of γ. Each pattern's growth rate is its eigenvalue, as explained in appendix 2.

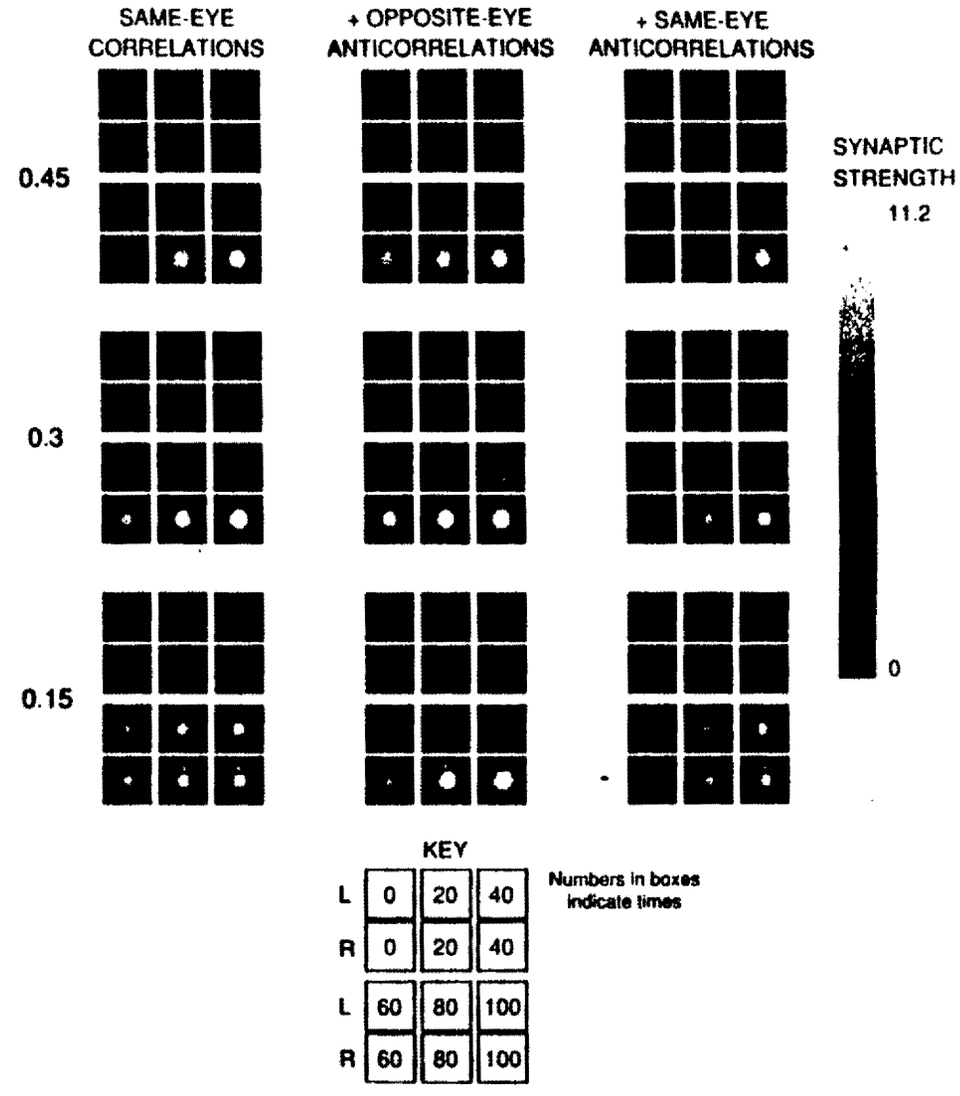

FIG. 7.11. Time development of an isolated cortical cell for each of the nine correlation functions of Fig. 7.9. As indicated in the key, for each correlation function the upper row of three left-right pairs shows inputs at times 0, 20, and 40, while the lower row of three left/right pairs shows inputs at times 60, 80, and 100. Synaptic strengths at each time are displayed as in Fig. 7.8. Broader correlations, or addition of opposite-eye anticorrelations, lead to more robust development of monocularity, while narrower correlations, or addition of same-eye anticorrelations, slow or prevent the development of monocularity. Each run used the same initial condition (time 0), arbor function, constraints, and parameters as used for Fig. 7.8, except that λ was adjusted to make initial changes in synaptic strengths more nearly equal with varying breadth of correlation function: $\lambda = 0.00075/\varkappa$, where $\varkappa = 0.45$, 0.3 or 0.15 is the parameter characterizing the breadth of the correlation functions.

FIG 7.11

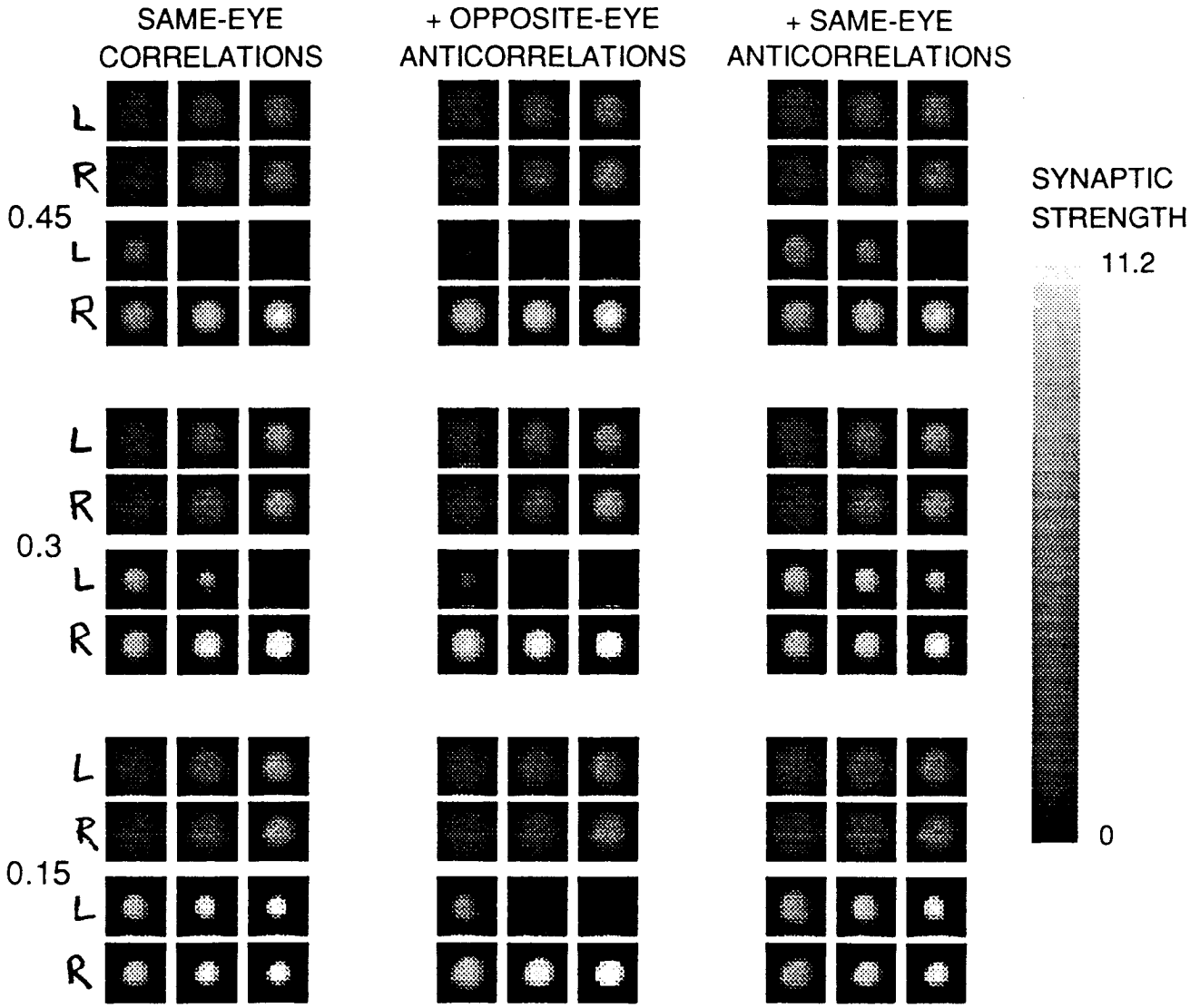
SAME-EYE CORRELATIONS
+ OPPOSITE-EYE ANTICORRELATIONS
+ SAME-EYE ANTICORRELATIONS
L
R
0.45
L
R
L
R
0.3
L
R
L
R
0.15
L
R
SYNAPTIC STRENGTH
11.2
0

expected from the analysis of the characteristic patterns, broader correlations within each eye, or addition of opposite-eye anticorrelations, enhance the development of monocularity, whereas addition of same-eye anticorrelations reduces ocular dominance. Note that when ocular dominance develops slowly, the less dominant, more slowly growing eye may, as predicted, grow to saturation before significant monocularity can develop. When same-eye anticorrelations are present within an arbor radius, development of monocularity is suppressed, as predicted by the fastest-growing characteristic pattern for that case. That pattern shows segregation of the synapses serving the two eyes into separate parts of the receptive field, whereas the time development leads to concentration of both eye's synapses in the receptive field center. This difference can be understood as resulting from the saturating nonlinearities.[9]

The basic features of our analysis of S^D remain accurate in the presence of nonlinearities. This is true for two reasons. First, near the initial condition nonlinearities can be ignored. The initial condition is a small perturbation of $S^D \equiv 0$, so that S^D is initially small everywhere. Nonlinear terms in S^D such as $(S^D)^2$ are therefore negligibly small in comparison to linear terms. Thus, although the true biological equation describing the time evolution of S^D is not likely to be linear, the equation will be linear near the initial condition. Second, the fastest-growing patterns of S^D near the initial condition will dominate the final, fully nonlinear results. This occurs because in the linear realm, the characteristic patterns grow exponentially. Therefore the fastest-growing patterns quickly become very dominant, even while the amplitudes of these patterns are still quite small and the equations still effectively linear. The final pattern will result from nonlinear interactions among these dominant patterns, and the more slowly growing patterns

[9]In the absence of opposite-eye anticorrelations, synapses serving the two eyes have no information as to the internal structure of one another's receptive field. Instead, interaction between the eyes, via the constraints, couples the synapses serving one eye only to the total synaptic strength serving the other eye. Hence it is not possible for the growth of the synapses serving the two eyes to be coordinated so as to occur in separate receptive field locations. The leading eigenfunction for S^D is nonetheless striped because, for synapses representing each eye, a striped pattern, positive in one part of the receptive field and negative in the other, grows faster than any other pattern in the absence of nonlinearities. This pattern is then the fastest-growing pattern of S^D, that is this pattern of initial differences between the two eyes grows faster than any other pattern of initial differences, because the two eyes grow independently except for constraints. In the presence of the saturating nonlinearities, which prevent synapses from having negative strengths, a circularly symmetric pattern representing each eye turns out to grow more rapidly than a pattern that has a positive stripe and a stripe of zero synaptic strength. Before the saturating nonlinearities are reached, a striped pattern of S^D grows, so that synapses representing each eye have a small advantage in opposite halves of the receptive field. After saturation, the pattern of S^D which emerges is approximately zero everywhere. Note that this final pattern of S^D, like that which develops early, sums to zero, so that no ocular dominance develops.

will not significantly contribute. Therefore, features common to all of the fastest-growing patterns, such as development of monocularity or, as discussed later, a wavelength of ocular dominance organization across cortex, will be robust to nonlinearities.[10] Our description of these aspects of cortical organization correctly describes the biology provided only that our postulated linear equation for S^D is a reasonable approximation to the true linear equation describing the development of S^D near the initial condition. We have shown elsewhere a specific example of the derivation of our equation for S^D as the linearization of a more complicated, nonlinear model of neural development (Miller & Stryker, 1989).

The precise developmental results will depend on the conditions that stabilize and limit synaptic growth. For example, if total synaptic strength over the cortical cell is conserved, the faster growth of the central synapses forces the peripheral synapses to lose strength and disappear. Alternative stabilization conditions might lead to retention of the peripheral synapses, but the receptive field would nonetheless become dominated, at least initially, by the faster-growing central synapses. Similarly, whether a cell becomes completely monocular or becomes dominated by one eye depends on the degree to which one eye's greater growth can force the other's to shrink before both reach saturation. Though the precise results of development or of simulation, and the absolute rates of growth, thus may depend greatly on the details, the tendencies to refinement and to ocular dominance, and the effects of features such as broader correlations or opposite-eye anticorrelations on relative rates of growth, are general.

The simple rules we have postulated are sufficient to understand the effects of experimental modifications of the normal patterns of activity. Alternating monocular deprivation or artificially induced strabismus lead to a virtual elimination of binocular cells. These treatments can be thought of as reducing opposite-eye correlations or inducing opposite-eye anticorrelations and thus enhancing the development of monocularity. Monocular deprivation, closing one eye in a young animal during a critical period, leads to dominance of most cortical cells by the open eye. We can model this in two ways. First, there will be a decrease in the amount of activity within the closed eye. This will decrease the size but not change the shape of the correlation function that describes correlations within that eye. In addition, there may be a disruption of correlated activity within the eye, which would

[10]It is possible for the initial pattern which develops out of linear interactions to be metastable. This means that it may eventually reorganize into a pattern with a different wavelength, determined by nonlinearities. This is unlikely in the ocular dominance system, as developmental studies (LeVay, Stryker & Shatz, 1978) show no obvious change in ocular dominance periodicity between its earliest detection and the final adult pattern. It may be possible to test this by following development of the columns within a single animal, using voltage sensitive dyes (Blasdel & Salama, 1986).

narrow the correlation function or otherwise change its shape. In either case, the closed eye would clearly be at a disadvantage, receiving less reinforcement through correlations at each timestep and hence growing more slowly than the open eye.[11]

The effects of brief monocular deprivation, modeled as a simple decrease in the amplitude of the correlation function within one eye, are illustrated in Fig. 7.12. Developmental sequences are shown with initial conditions and functions identical to those used for Fig. 7.8, except that during a period of 20 iterations the right eye is monocularly deprived. The figure shows the effects of depriving from times 0-20, 20-40, 40-60, 60-80, or 80-100, compared to the results without deprivation. Early deprivation leads to a complete shift in favor of the open eye, whereas later deprivation causes no distinguishable change from the nondeprived outcome. This is analogous to the biological result that monocular deprivation only leads to an ocular dominance shift during a critical period of development. Results in similations are virtually unchanged if deprivation remains in effect from the time of onset to time 100. Biologically, brief monocular deprivation during the critical period has nearly as strong a physiological effect as long-term deprivation (Hubel & Wiesel, 1970; reviewed in Movshon & Van Sluyters, 1981).[12]

The critical period in this simulation does not depend on stabilization of saturated synapses, or on other changes in the rules governing plasticity. Instead, the critical period in this simulation is a dynamical result. The influence of one synapse on another, as shown in the derivation of Eq. 2, is a product of two factors: the level of activity of the influencing synapse, and its synaptic strength. Hence, for any given disparity in activity level between the two eyes, there is a corresponding disparity in synaptic

[11]We have noted that in optic tectum, there is no effect of monocular deprivation. One possible explanation would arise if there are constraints in optic tectum conserving, or ensuring the equality of, the total synaptic strength over individual input cells from each eye. This might occur, for example if activity-dependent effects were much weaker than activity-independent effects that yield such conservation or symmetry. Ideas of a hierarchy of effects in the optic tectum have been developed by Fraser (1980, 1985).

[12]The physiological results of a few days of monocular deprivation may consist predominantly of a shift, to the open eye, of cells that were driven relatively equally by the two eyes (Hubel & Wiesel, 1970). Cells originally dominated by the closed eye may require slightly longer periods to undergo an ocular dominance shift. Deprivation for six days appears adequate to cause a physiological shift to the open eye about as strong as that resulting from long deprivation (Hubel & Wiesel, 1970). Anatomical results may show similar stages. After ten dys of deprivation, the anatomy shows only a greater clarity, as though deprived eye afferents were withdrawn from areas that had been innervated by both eyes (Shatz, Lindstrom, & Wiesel, 1977). Long deprivation leads the geniculocortical innervation to anatomically alter, so that the open eye's stripes become wider and the closed eye's become narrower or become islands in a sea of open-eye inputs (Shatz & Stryker, 1978).

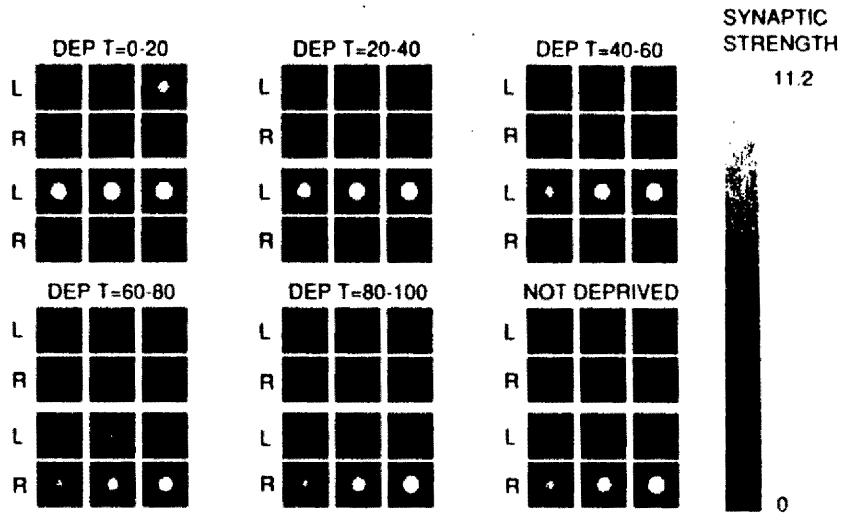

FIG. 7.12. The effects of monocular deprivation from times 0-20, 20-40, 40-60, 60-80, or 80-100, compared to the results without deprivation. Display is as in Fig. 7.11. Early deprivation leads to a complete shift in favor of the open (left) eye, while late deprivation causes no distinguishable change from the nondeprived outcome. All parameters, functions, and initial conditions are identical to those used in Fig. 7.8, except that the deprived eye's correlation function was multiplied by 0.7 during the 20 iterations of deprivation. Results are indistinguishable if deprivation remains in effect from the time of onset to time 100, except that deprivation from times 60-100 leads the two eyes' inputs to become more nearly equal in strength than does deprivation from times 60-80.

strengths that is sufficient to overcome the activity differential. Once an eye has a sufficient advantage in synaptic strength, it will continue to grow faster than the opposite eye even if deprived and rendered less active, and hence monocular deprivation will no longer cause an ocular dominance shift. Thus, brief deprivation initiated early in development, when the two eyes are nearly equal, leads the open eye to gain an advantage in synaptic strength sufficient for it to dominate the cell even if deprivation then ceases. Deprivation initiated late in development, in contrast, is no longer able to shift the final balance between the two eyes, even if deprivation persists and synapses are not stabilized.

This dynamical explanation of the critical period applies only to cells that are normally destined to become monocular. A binocular cell will always be subject to a monocular deprivation effect by this reasoning. In cats, many cells in the adult cortical layer 4 at the borders between ocular dominance

FIG 7.12

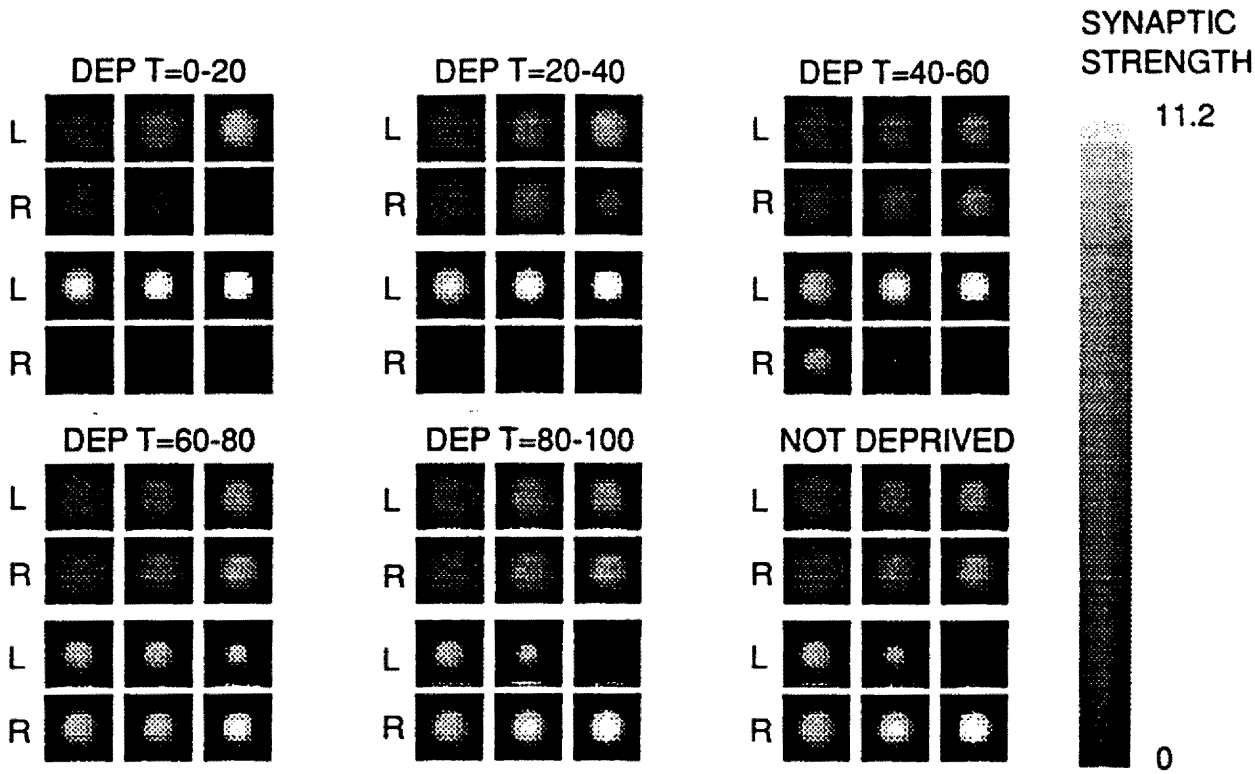
DEP T=0-20
DEP T=20-40
DEP T=40-60
DEP T=60-80
DEP T=80-100
NOT DEPRIVED
L
R
SYNAPTIC STRENGTH
11.2
0

stripes are binocular (Shatz & Stryker, 1978), an effect that occurs in the model when correlations within each eye are narrow compared to an arbor radius. Yet adult cats appear to show absolutely no effect of monocular deprivation (Hubel & Wiesel, 1970). Hence, to fully explain the biologically seen critical period, stabilization of saturated synapses or other biochemical changes in plasticity rules must be invoked. Nonetheless, it is possible that many aspects of the observed critical period are dynamical in origin.

An alternative experimental modification of normal development occurs when muscimol is infused into cortex to inhibit all cortical activity, as previously described. In this case, monocular deprivation causes a shift in favor of the *closed* eye. This is easily modeled if we assume a mechanism, such as a Hebbian mechanism, in which the correlation-based reward for coactivated synapses depends on postsynaptic activity. Synapses then will not be able to influence one another, because all cortical cells are always inhibited in the presence of muscimol. The influence between synapses is normally due to their excitatory or inhibitory influences on one another's postsynaptic cell, but now the synapses are without effect on the activity of the postsynaptic cell. Thus, as can be seen from the derivation of the equations from a Hebb synapse mechanism (appendix 1), the term involving synaptic interactions is eliminated from our equation. Instead, each synapse decays at a rate proportional to its mean activity. The more active, open-eye synapses decay more rapidly, leading the closed eye to dominate the cell, as observed experimentally.

In summary, under a correlation-based rule, if a set of inputs is correlated in a way that falls off with distance, without anticorrelations, two conclusions follow. First, central synapses in a receptive field will grow more rapidly than peripheral synapses. The more rapidly the correlations fall off with distance, the more pronounced this tendency. Second, if two different such sets of inputs, not mutually correlated, innervate a single cortical layer, there is a tendency for one set, selected randomly by the initial conditions, to grow more rapidly and come to dominate the cell. Greater amounts of correlation over a broader distance range within each input set enhance this tendency, by enhancing the rate of growth of monocular over binocular patterns of synaptic differences. Opposite-eye anticorrelations also enhance this tendency, both by broadening correlations and by enhancing the growth of ocular dominance over the development of receptive field refinement. The precise developmental results depend on the conditions that stabilize and limit synaptic growth, but the tendencies to refinement and to ocular dominance are general. The tendency to ocular dominance, in particular, is robust to nonlinearities. Results of development with more complicated correlation functions involving same-eye anticorrelations, or with experimental modifications of activity such as monocular deprivation or postsynaptic inhibition, can also be understood as we have described.

These results agree with the biological results attributed to correlation-based mechanisms: receptive fields sharpen, ocular dominance develops, and experimental modifications of activity during a critical period modify developmental outcomes in the manner predicted. Cases in which different sets of correlated inputs become matched based on their mutual correlations can be regarded as a particular case of the sharpening of receptive fields to a highly correlated group of inputs, in the case when correlations are not simply determined by distances between the inputs.

The development of large-scale patterns of receptive fields, such as ocular dominance stripes, requires consideration of a full layer of cortical cells. Before turning to this topic, we briefly reverse perspective and consider the development of the terminal arbors of an isolated pair of geniculate cells projecting to a layer of cortical cells.

How Isolated Geniculate Cells Develop

For the case of two geniculate cells, representing a single retinotopic position in each eye, innervating a cortical layer, the model equations simplify in a manner formally identical to Eq. 2 for a single cortical cell:

$$\begin{aligned}\frac{d}{dt}S^L(x,t) &= \lambda A(x)\sum_y [C^{LL}(0)I(x-y)S^L(y,t) + \\ &\qquad C^{LR}(0)I(x-y)S^R(y,t)] - \gamma S^L(x,t) - \epsilon^L(x)\\ \frac{d}{dt}S^R(x,t) &= \lambda A(x)\sum_y [C^{RR}(0)I(x-y)S^R(y,t) + \\ &\qquad C^{RL}(0)I(x-y)S^L(y,t)] - \gamma S^R(x,t) - \epsilon^R(x)\end{aligned} \tag{5}$$

Hence, letting $I^S(x-y) = I(x-y)[C^{\text{SameEye}}(0) + C^{\text{OppEye}}(0)]$, $I^D(x-y) = I(x-y)[C^{\text{SameEye}}(0) - C^{\text{OppEye}}(0)]$, the conclusions for development of the arbors of two isolated geniculate cells are identical, in terms of I^S, I^D and A, to the previous conclusions for the receptive field of an isolated cortical cell in terms of C^S, C^D, and A.

Assume $C^{\text{SameEye}}(0) > |C^{\text{OppEye}}(0)|$, so that the factors multiplying I in both I^S and I^D are positive and thus both I^S and I^D are simply scaled versions of I. Then if $I(x-y)$ is Mexican hat, with short-distance excitation and broader-ranging inhibition both found within an arbor radius, the arbors of the two inputs will tend to segregate from one another into separate patches of cortex, as in the case for receptive fields when same-eye anticorrelations are present and C^D is Mexican hat. Simulation of time development under this condition is shown in Fig. 7.13, for a case in which

$C^{\text{OppEye}}(0) = -\frac{C^{\text{SameEye}}(0)}{4}$.[13] If $I(x)$ is purely excitatory, one geniculate cell would be expected to grow faster than the other and to dominate the inputs to cortex from the given retinotopic position, as in the simulations of receptive field development for a purely excitatory correlation function.

There is an important difference in the case of isolated geniculate cells as opposed to an isolated cortical cell. The constraints used for stabilization now affect both S^S and S^D, whereas previously they affected only S^S. Previously, constraints on total synaptic strength over a cell were over a cortical cell, and the constraint drew no distinction between left- and right-eye synapses.[14] In the present case, the cells are two distinct geniculate cells, and any constraints on total synaptic strength over a cell must be placed separately on each cell. If total synaptic strength were strictly conserved over a cell, the arbors of each cell could rearrange and segregate from one another, but neither eye could gain or lose total synaptic strength. Then a pattern in which one eye's patches were wider than an arbor radius could not grow, because such a pattern would involve one eye's cell gaining more synaptic strength than the other's. A purely excitatory $I(x)$, or a Mexican hat $I(x)$ whose central excitatory part is sufficiently wide, would select such a pattern in the absence of constraints. With such functions, then, constraints can significantly alter ocular dominance segregation. In the presence of constraints, either each arbor would refine to its central part, or the two arbors would segregate from one another into separate patches of cortex, each about an arbor radius in width.

Development of the Geniculocortical Innervation

We are now prepared to understand many aspects of development when a left-eye and a right-eye geniculate layer innervate a cortical layer. In the simplest case there are positive local correlations within each eye, and a Mexican hat cortical interaction function. Cortical cells will each tend toward monocularity. Greater breadth of local correlations or opposite-eye anticorrelations will yield an increased tendency toward monocularity. Arbors will tend to segregate into patches. The scale of the patches will be determined by the cortical interaction function, up to a limit imposed by the arbor function if synaptic strength over an input arbor is conserved. For the tendencies of cortical cells and geniculate arbors to mesh compatibly, cortical cells as a whole must segregate into alternating patches of cells dominated by a single eye, with the scale of the patches determined in the same manner as the scale of the patches of individual arbors.

Another way to understand the formation and scale of cortical patches is the following. Suppose each cortical cell becomes monocular. Their interactions via the cortical interaction function will then be most favorable, in

[13] In the absence of opposite-eye anticorrelations, the saturating nonlinearities defeat the tendency of S^D to develop a striped pattern, as discussed in footnote 9. The constraints of meshing the innervations of multiple cells when a complete geniculocortical innervation is considered, however, lead to patchy geniculate arbors even in the absence of opposite-eye anticorrelations. Hence the case with opposite-eye anticorrelations is illustrated here, for pedagogical purposes.

[14] Such a constraint could have drawn a distinction between left- and right-eye synapses. For example, if the constraint were multiplicative, achieved by multiplying each synaptic weight by a constant rather than by subtracting a constraint from each synaptic weight, stronger synapses would be more heavily affected by the constraint. If total synaptic strength were growing in the absence of constraints, this constraint would penalize the dominant eye and tend to retard the development of ocular dominance segregation, as is briefly discussed later. The important point is that a constraint over a cortical cell can be formulated so as to have no effect on the equation for S^D and hence no effect on ocular dominance, whereas a constraint on geniculate cells must affect the equation for S^D.

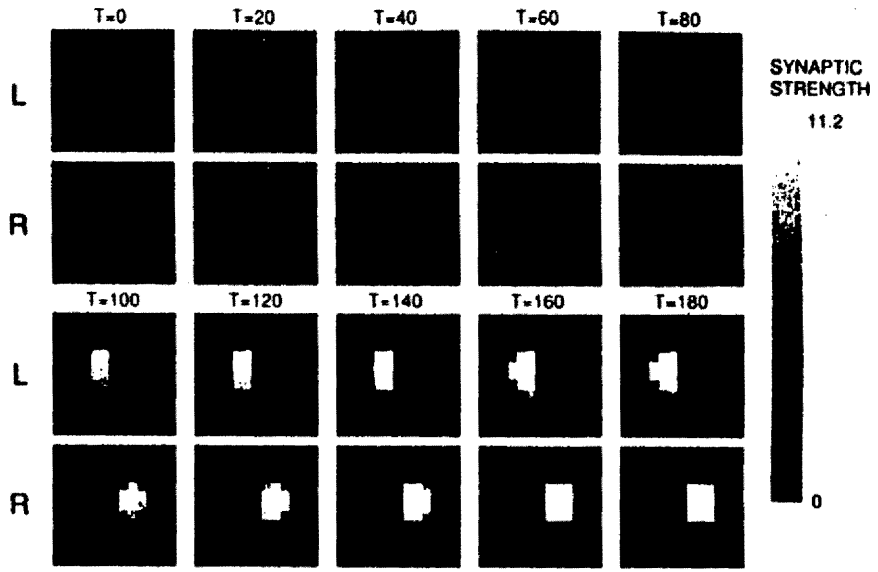

FIG. 7.13. Development of two geniculate cells, one serving each eye, innervating a cortical layer. The inputs segregate to innervate separate patches of cortex. The activities of the two geniculate cells are assumed to be negatively correlated with one another, as described in the text. Cortical interaction function was that shown in Fig. 7.9. Inputs serving each eye were constrained to keep a constant total synaptic strength, by subtraction of $\epsilon^L(t)A(\alpha)$ from each left-eye total synaptic strength after each iteration, where $\epsilon^L(t) = \frac{\Sigma_\alpha \frac{d}{dt} S^L(\alpha,t)}{\Sigma_\alpha A(\alpha)}$, and similarly for the right eye. Conventions, initial conditions, and parameters otherwise as in Fig. 7.8.

FIG 7.13

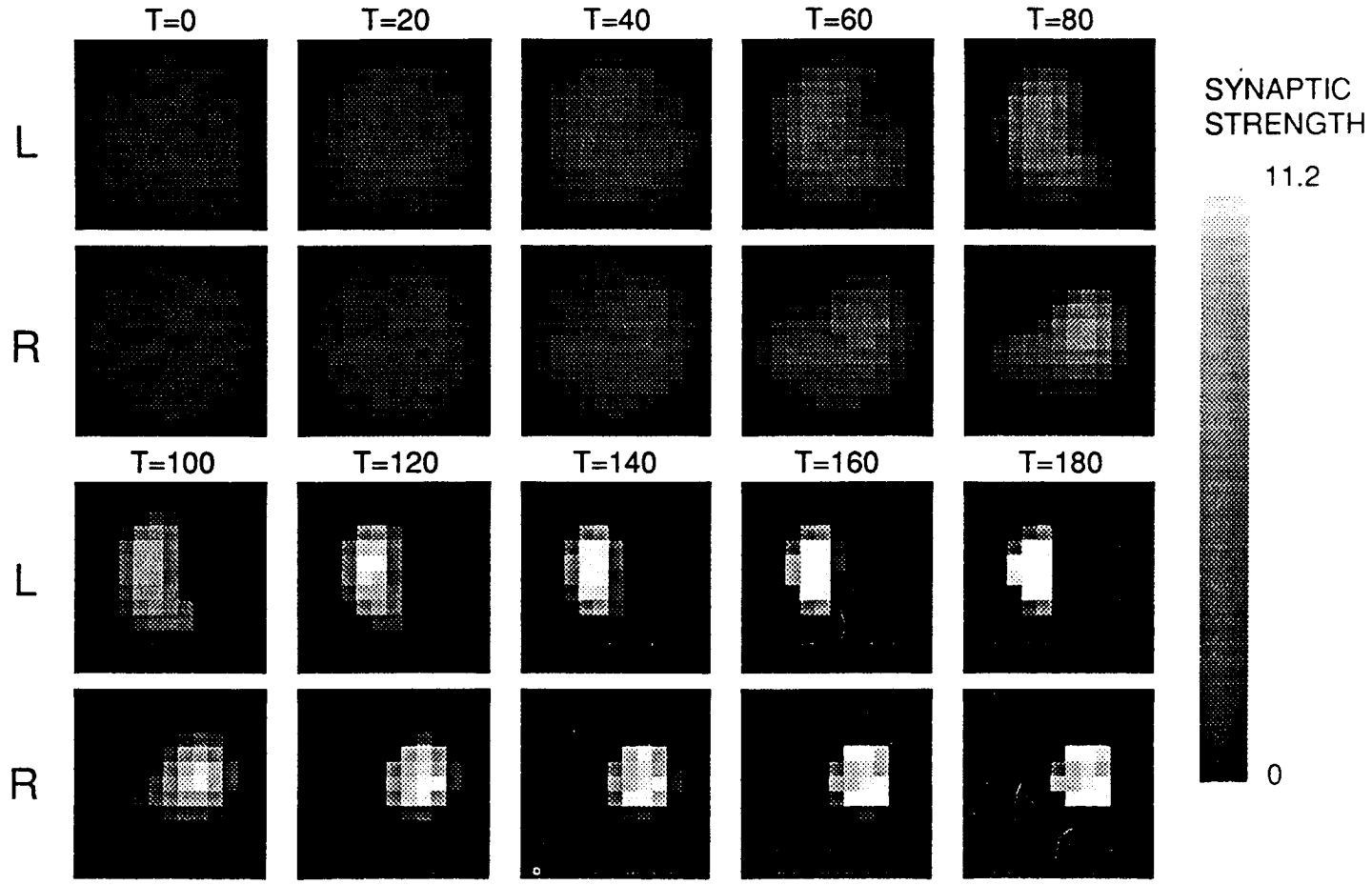
T=0
T=20
T=40
T=60
T=80
L
R
T=100
T=120
T=140
T=160
T=180
L
R
SYNAPTIC STRENGTH
11.2
0

terms of growth of their synapses, if cells with inputs from the left eye are surrounded by left-eye cells over distances at which the cortical interaction function is positive, and by right-eye cells over distances at which the cortical interaction function is negative. It is not possible for each cell to be at the center of its own such "bulls-eye"; but interactions will be most favorable over all cortical cells, if the segregation is into patches whose widths are given by the dominant oscillation in the cortical interaction function.

A simulation illustrating cortical development with positive same-eye correlations and a Mexican hat cortical interaction function is shown in Fig. 7.14. The functions used in this and other simulations of the geniculocortical innervation are shown in Fig. 7.15. For this simulation three 25 by 25 grids of cells were used to represent one cortical layer and two geniculate layers, one for each eye. Each geniculate cell was connected to a 7 by 7 square of cortical cells centered at the retinotopically corresponding point in the cortical grid, resulting in a total of $2 \times 25 \times 25 \times 7 \times 7 = 61{,}250$ connections. A simple "flat" arbor function was used, equal to 1 over the 7 by 7 arbor and zero outside.[15] Synapses were initially assigned a random strength near 1, and allowed to grow until they reached a strength of 8 or 0. Constraints were used to conserve total synaptic strength over each cortical cell, and to maintain total synaptic strength over each input cell within a range between 0.5 and 1.5 times the initial total. To eliminate boundary effects, periodic boundary conditions were used on the grids, so that left and right edges of the grids were taken to be adjacent, as were top and bottom edges.[16]

The cortex initially receives innervations of uniform strength from the two eyes, indicated by the intermediate grey color at time 0 (Fig. 7.14a). Gradually, the left-eye (black) and right-eye (white) inputs come to dominate alternating sets of cortical cells, yielding a pattern of ocular dominance stripes or patches. Individual cortical cells focus their input strength centrally, then become monocular as they continue to refine (Fig. 7.14b). As the inputs from the two eyes segregate and the full set of afferents from a single eye are restricted to innervate only half the cortical cells, individual

[15]A tapering arbor function effectively reduces the size of the arbor. Hence, because our arbor size was limited for computational reasons, we chose to use a flat arbor to maximize the chance to see significant internal structure in receptive fields. We have also studied the use of the tapering arbor function. Results for overall ocular dominance in that case are completely consistent with the results presented here; a smaller wavelength develops due to the effectively smaller arbor, and is correctly predicted by our analysis.

[16]The distance across visual cortex corresponds to 10 or 20 patch wavelengths, whereas interactions may be expected to be localized to at most a few wavelengths. Hence, the boundaries are likely to play little role in deciding whether patches will develop, or in determining their wavelength, though they may play a role in determining the detailed form or layout of the patches or stripes.

receptive fields become somewhat elongated. Individual geniculate cells from the two eyes focus their input and then sort into mutually exclusive, complementary right-and left-eye patches (Fig. 7.14c), much as appears to be the case in filled arbors in cats (Humphrey, Sur, Uhlrich, & Sherman, 1985a, 1985b; Levay & Stryker, 1979). The results are basically those predicted from consideration of the development of individual cortical and geniculate cells, though the meshing of the full cortical and geniculate grids leads to some alterations in details of receptive fields and afferent arborizations. These results are completely robust, being qualitatively identical for all sets of random initial conditions we have tried as well as for varying sizes of simulations (Miller, 1989a; Miller et al., 1989; Miller & Stryker, 1989).

A more complicated case to understand is one in which there are local correlations within each eye, and a purely excitatory cortical interaction function. Under these conditions, individual cortical cells will refine and become monocular, but so too will individual pairs of input cells. For these tendencies to mesh compatibly, large regions of cortex must become dominated by a single eye's inputs. There can be more than one such region, separated by fracture lines along which individual cortical cells or pairs of input cells are binocular. In simulations, one eye's inputs often take over the entire cortex. If a constraint is used conserving total synaptic strength over each input cell, isolated input cells will refine but a difference in strength between the two eyes cannot develop. For this to mesh with the tendency of isolated cortical cells to develop monocularity, each pair of input cell arbors must segregate into complementary patches of cortex, as in the case of a Mexican hat cortical interaction function. In this case, however, the purely excitatory cortical interaction provides no clue as to the size of the segregated patches. The size of the patches is selected by the arbor function: The cortex "tries" to assume its unconstrained form, in which one eye's domain spreads indefinitely over the cortex as a whole, but is limited by the need to accommodate both eyes within the breadth of a single initial arborization. Thus, a purely excitatory cortical interaction can support ocular dominance segregation, but maintenance of equality of the eyes depends on tight constraints on total synaptic strength of input cells. The results of simulations with an excitatory cortical interaction, with and without such constraints, are shown in Fig. 7.16. With tight constraints, development is essentially like that with a Mexican hat cortical interaction function, although there is a slight increase in the scale of the stripes. For comparison, results with a Mexican hat cortical interaction function with and without constraints are also shown. Constraints have essentially no effect in this case.

Dependence on the correlation function is as expected from the results for individual cells, as shown in Fig. 7.17. Broader correlations within each

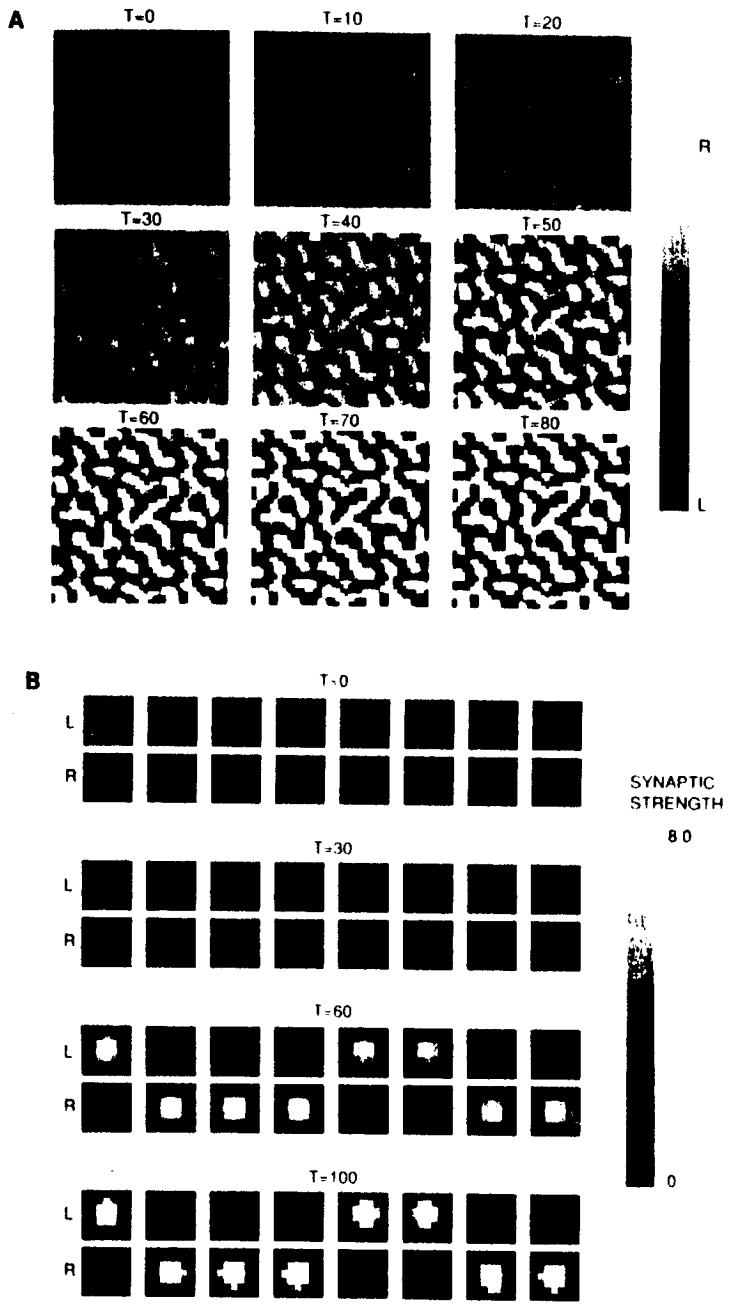

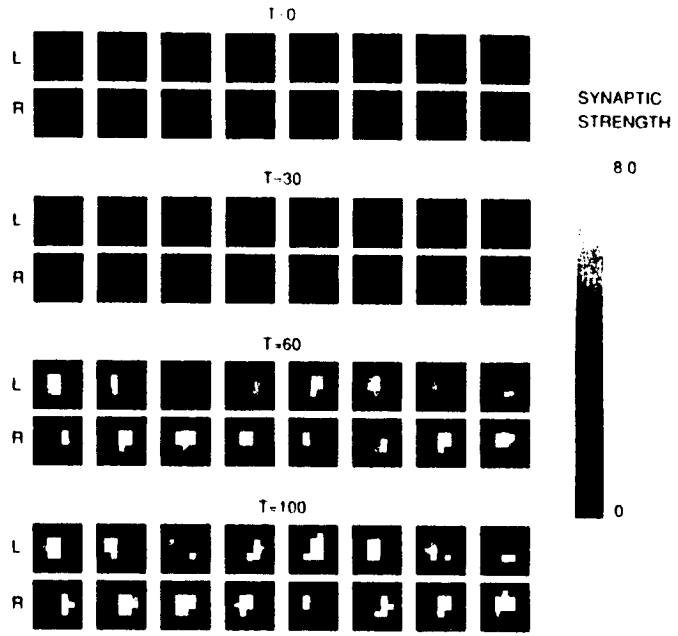

FIG. 7.14. Development of a full cortical layer innervated by two geniculate layers, one representing each eye. (a) The cortical grid, illustrated at each of nine times, from time 0 to the 80th iteration. The greyscale illustrates the ocular dominance, *OD*, of each cortical cell; $OD(x) \equiv \Sigma_{\alpha}[S^R(x,\alpha) - S^L(x,\alpha)]$, on a scale from monocular for the right eye (white) to monocular for the left eye (black). A pattern of ocular dominance segregation develops and then grows to monocularity. Each square shows 40 by 40 cortical cells, although the cortical grid was only 25 by 25, so that the pattern across the periodic boundary conditions can be seen; thus, the top 15 and bottom 15 rows within each square are identical, as are the left 15 and right 15 columns. (b) Development of receptive fields of eight cortical cells. Left- and right-eye inputs to each of eight adjacent cortical cells are illustrated at each of four times. The eight cells illustrated are the eight at the bottom left of the cortical pictures of (a). Each vertical L,R pair illustrates the left- and right-eye synaptic inputs to a single cortical cell at one time. Greyscale shows strength of synaptic input from each of the 7 by 7 geniculate positions which send input to the cortical cell. Receptive fields concentrate their strength centrally, refining in size, and become monocular. Adjacent groups of cells tend to become dominated by the same eye, providing the basis for ocular dominance segregation across the cortex as a whole. (c) Development of arbors of eight left-eye and eight right-eye geniculate cells, from eight adjacent geniculate grid positions. The eight grid positions are those in the geniculate corresponding retinotopically to the eight cortical cells illustrated in (b). Each

FIG 7.14 A

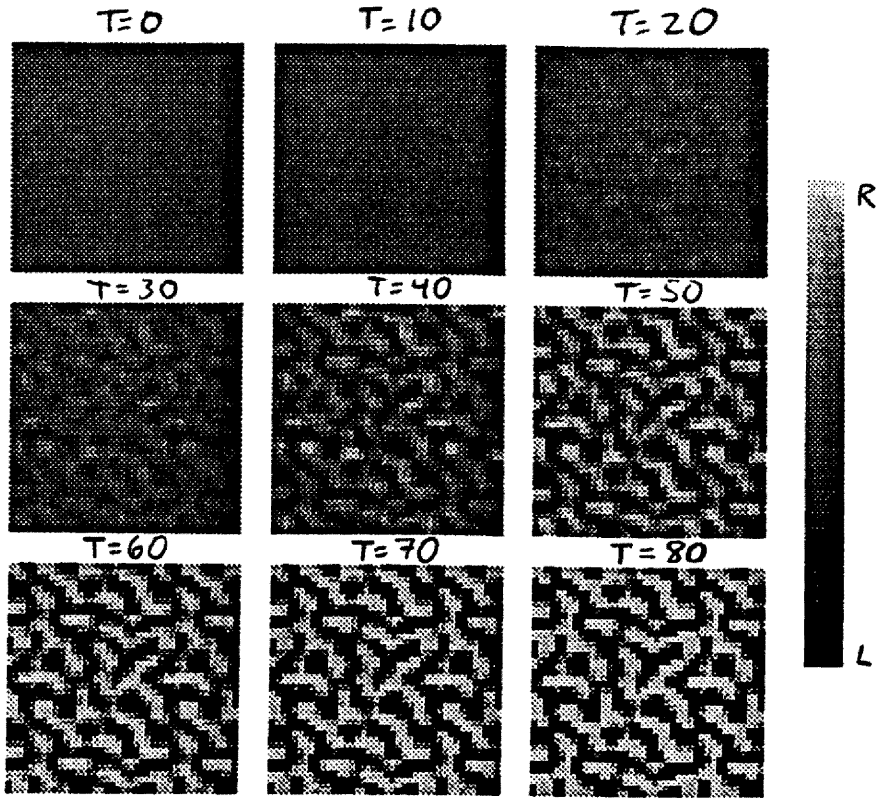

FIG 7.14 B

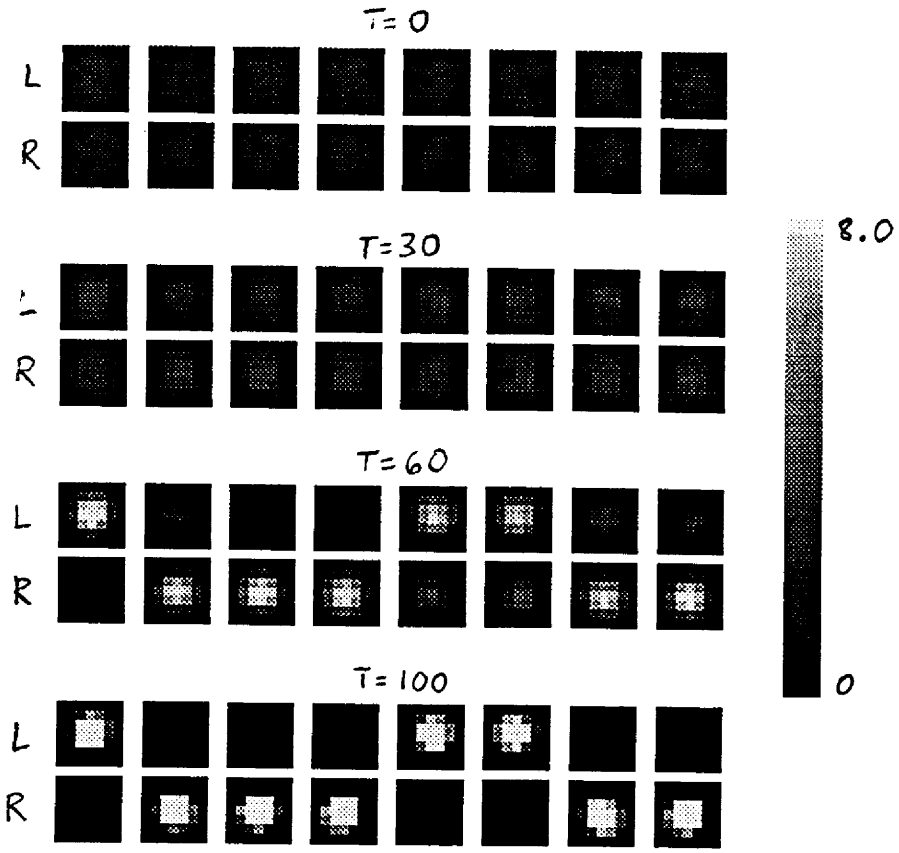

FIG 7.14 C

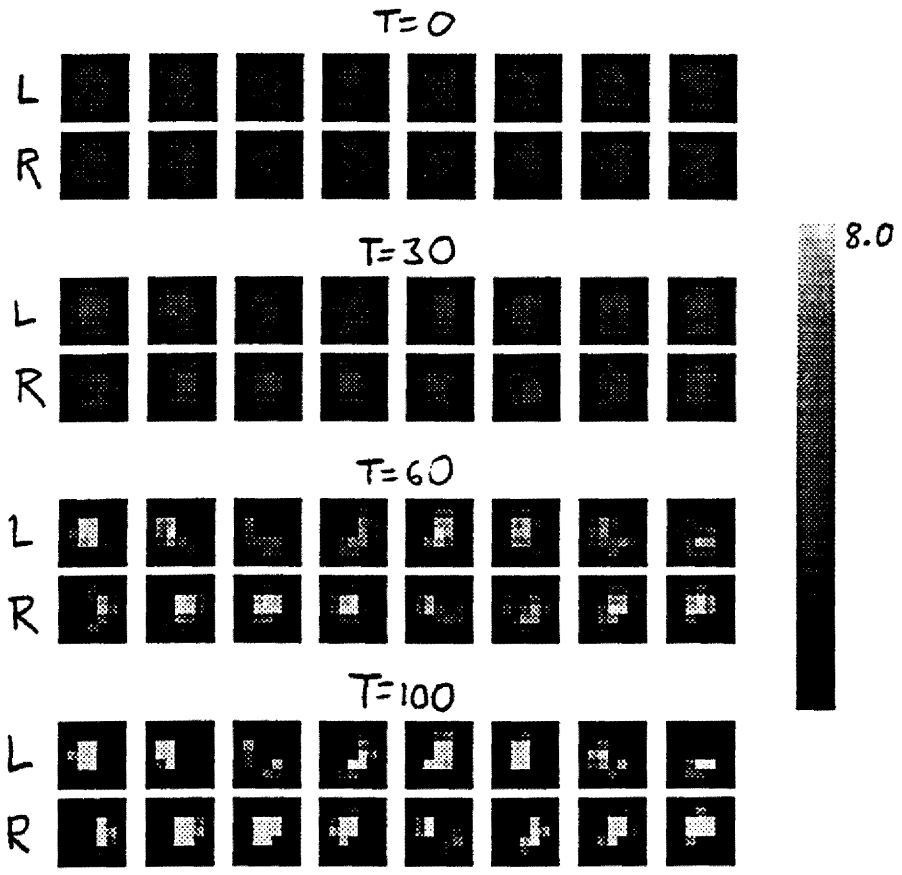

eye or addition of opposite-eye anticorrelations leads to a more completely monocular cortex. This agrees with experimental findings in which artificially induced strabismus or alternating monocular deprivation, which reduce correlations or induce anticorrelations between the eyes, lead to an increase in monocularity throughout the cortex (Hubel & Wiesel 1965). Narrower correlations within each eye lead to more binocular cells at the borders between eyestripes without otherwise altering the pattern of stripes. Same-eye anticorrelations also lead to more binocular cells at the borders between eye stripes and, if present within an arbor radius, tend to destroy monocularity and to destroy the regular cortical organization of ocular dominance.

Monocular deprivation within a critical period results in the open eye taking over many more cells and thus a much larger percentage of cortex, as seen experimentally and suggested by results on individual cells. The precise results of deprivation in the model depend on the time of onset, duration, and strength of deprivation, and the constraints which limit the degree to which afferent arbors can shrink in total synaptic strength. When deprivation is initiated early and maintained through development, the open eye takes over all cortical cells to the limits allowed by constraints. If constraints prevent the deprived eye from losing all cortical inputs, or if deprivation is initiated somewhat later in development, islands of cells dominated by the closed eye develop in the midst of a sea of open-eye cells,

vertical L,R pair illustrates the arbors of a left- and a right-eye geniculate cell from identical geniculate grid positions at one time. Greyscale shows synaptic strength of connection to each of the 7 by 7 cortical cells contacted by the arbor. Arbors focus their strength centrally, but then sort into complementary patches of cortex. The functions used for this simulation, illustrated in Fig. 7.15, were the "same-eye correlations" correlation function with parameter 0.3, and the Mexican hat cortical interaction function. The arbor function, as described in the text, was equal to one over a 7 by 7 square arbor and zero outside. ϵ^L ϵ^R, and γ were set to zero. $\lambda = 0.0069$. In cortical simulations in general, λ is set for each choice of functions so that average change in S^D per iteration should initially be about 0.003. This yields $0.003 < \lambda < 0.015$. Cortical cells were constrained to conserve total synaptic strength as described in legend to Fig. 7.8. Afferent arbors were then constrained as described in legend to Fig. 7.13, except that the factor subtracted from each synapse in an arbor was multipled by minimum $\left[[(1 - \frac{S_{tot}}{49})/0.5]^2, 1.0\right]$ where S_{tot} is the total synaptic strength over the arbor. This has the effect of allowing total synaptic strength to vary between 0.5 and 1.5 of the average initial value of 49. Synaptic strengths were frozen if their value reached either zero or 8: they were no longer allowed to change, assigned derivatives of zero and omitted from the constraint.

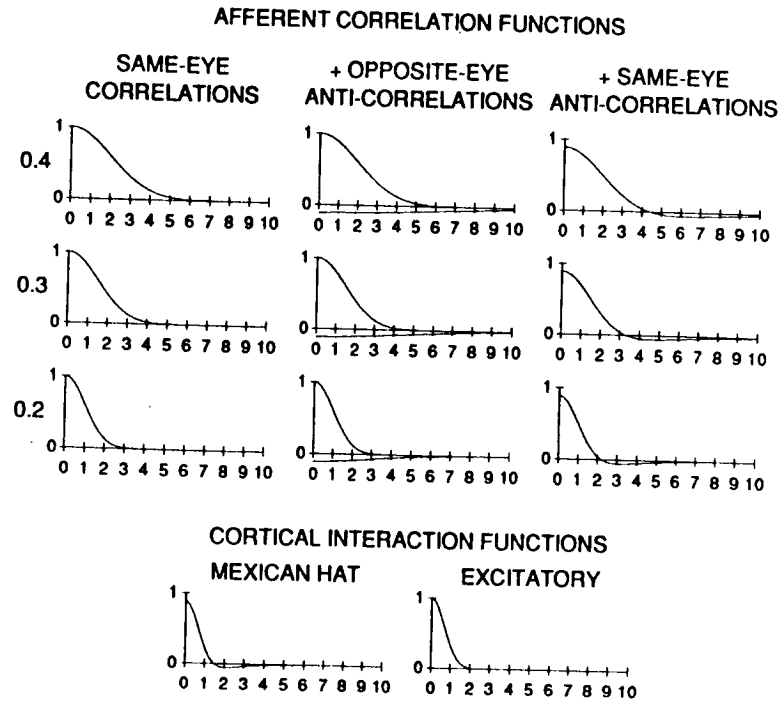

FIG. 7.15. Functions used for simulations of full geniculocortical innervation. Function value, vertical axis, versus distance in grid intervals, horizontal axis. Top: Correlation functions. These are identical to those shown in Fig. 7.9, with two changes: $D = 7$ rather than 13; and $x = 0.4, 0.3, 0.2$ rather than 0.45, 0.3, 0.15. Bottom: Cortical interaction functions. Left, Mexican hat function, identical to the cortical interaction function of Fig. 7.9 but with $D = 7$. Right, a purely excitatory cortical interaction function, given by just the excitatory gaussian of the Mexican hat function.

as is seen in cats following monocular deprivation (Shatz & Stryker, 1978). These islands are spaced with a periodicity equal to that of the stripes that would form in the nondeprived cortex. With later onset or briefer duration of deprivation, or stronger limits to the degree to which individual afferents can shrink in total synaptic strength, the islands are linked into thin stripes, similar to the results seen in monkeys (Hubel et al., 1977). When the deprivation begins sufficiently late, the cortex develops normally, except that cells at the border of the two eyes' stripes that would become binocular without deprivation can become dominated by the open eye, as previously discussed. This is illustrated in Fig. 7.18, which shows the results of brief deprivation initiated at varying times in development. Early onset of brief

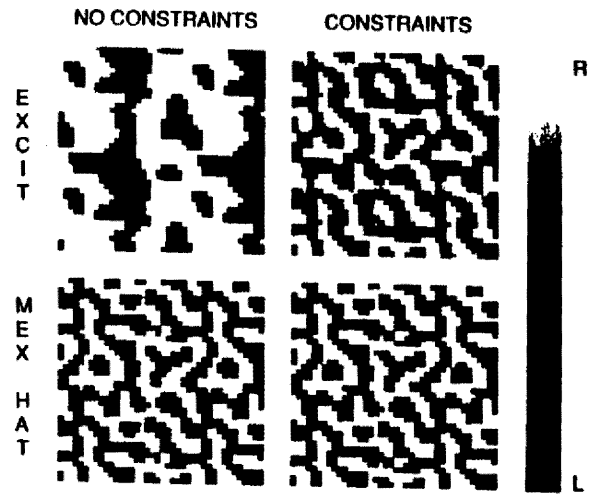

FIG. 7.16. Cortical patterns of ocular dominance resulting from development with the excitatory cortical interaction function of Fig. 7.15, with and without constraints fixing the total synaptic strength over each afferent arbor. For comparison, results using the Mexican hat cortical interaction function of Fig. 7.15, with identical constraints, are shown below. The final cortex (T=200) is shown in each case. Conventions, parameters, initial conditions, and arbor function as in Fig. 7.14. The correlation function used is "same-eye correlations" with parameter 0.4, rather than 0.3 as in Fig. 7.14. With 0.3, the excitatory cortical interaction function leads to patterns similar to those shown here, but many more cells in the final cortices are binocular.

deprivation leads deprived-eye stripes to become thin and broken. Later onset leads to progressively more equal widths of stripes, and sufficiently late onset is indistinguishable from normal development. The effects of longer durations of deprivation are illustrated in Miller et al. (1989).

To use these results to guide experiment, one would like to know how measurable features of the results, in particular the width of the stripes, depend on measurable biological parameters. We have suggested that the cortical interaction function determines the width if it is a Mexican hat function, and that if it is purely excitatory the width is determined by the arbor function. To achieve a more precise understanding, we again assume equality of the two eyes and, defining S^S, S^D, C^S, C^D as before, develop equations for S^S and S^D. Equation 1 becomes

$$\frac{d}{dt}S^S(x,\alpha,t) = \lambda A(x-\alpha)\sum_{y,\beta} I(x-y)C^S(\alpha-\beta)S^S(y,\beta,t) - \gamma S^S(x,\alpha,t) - 2\epsilon(x,\alpha)$$

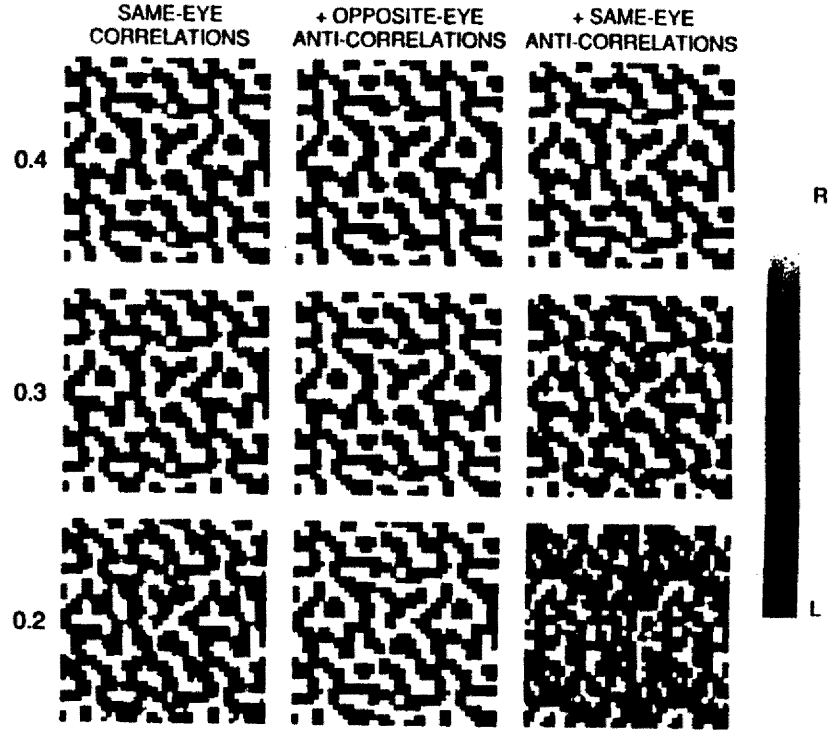

FIG. 7.17. Cortical patterns of ocular dominance resulting from development with each of the nine correlation functions of Fig. 7.15. Each development began with the same initial condition and used the same arbor and cortical interaction function, in all cases identical to those used in Fig. 7.14. The final cortex (T=200) is shown in each case. Conventions, parameters and constraints as in Fig. 7.14.

$$\frac{d}{dt}S^D(x,\alpha,t) = \lambda A(x-\alpha)\sum_{y,\beta} I(x-y)C^D(\alpha-\beta)S^D(y,\beta,t) - \gamma S^D(x,\alpha,t) \tag{6}$$

The equation for S^D controls the development of a pattern of segregation between the two eyes. We again find the characteristic patterns of ocular dominance: the patterns of S^D that evolve independently, each at its own rate, from the random initial condition near $S^D = 0$. As before, any random initial condition can be expressed as a sum of such patterns, and the patterns each grow independently and exponentially so that the fastest-growing pattern will quickly dominate.

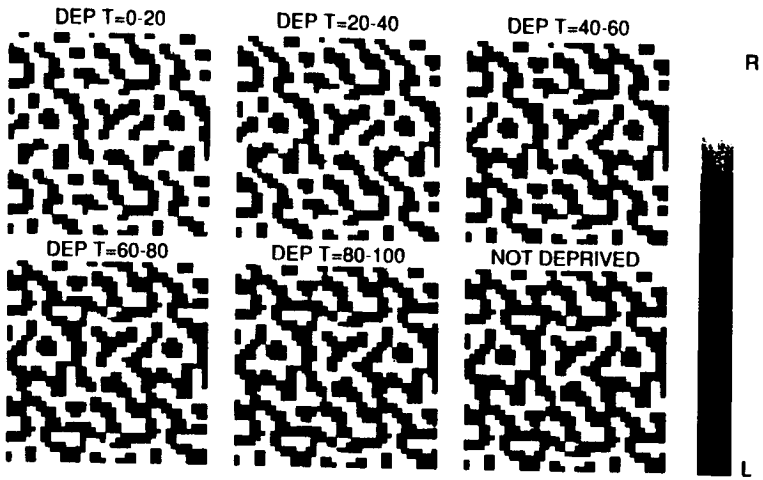

FIG. 7.18. Cortical patterns of ocular dominance resulting from brief monocular deprivation for 20 iterations during development. Results of initiating the 20 iterations of deprivation at iteration 0, 20, 40, 60, or 80 are shown, and compared to the results in the absence of deprivation. All parameters, functions, and initial conditions are identical to those used in Fig. 7.14, except that the deprived eye's correlation function was multiplied by 0.7 during the 20 iterations of deprivation. Final cortices (T=200) are shown for each case. Synaptic strengths were frozen upon reaching the limiting values of 0 or 8, as described in Fig. 7.14 legend; without such stabilization, late onset of deprivation would convert the binocular cells at the patch borders into open-eye dominated cells.

For the full geniculocortical innervation, each characteristic pattern of ocular dominance consists of a receptive field of synaptic differences, and an oscillation of ocular dominance across cortex (Fig. 7.19; appendix 2). The receptive field specifies the pattern of ocular dominance within the receptive field of a single cortical cell, whereas the oscillation specifies the change of this pattern between cortical cells. The characteristic receptive field may be monocular (Fig. 7.19a) or binocular (Fig. 7.19b). If binocular, it may involve stripes of left- and right-eye input in different portions of the receptive field, or more complicated distributions of left- and right-eye input. The oscillation of the characteristic pattern means that, across cortical cells, there is a sinusoidal change as to which eye is dominant in each portion of the receptive field. If the characteristic receptive field is monocular, cortical cells will oscillate, across cortex, between domination by one eye and domination by the other. Thus, if a characteristic pattern has a monocular receptive field, cortical cells in the pattern will be grouped into ocular dominance patches or stripes. The width of a left-eye

patch plus a right-eye patch is given by the wavelength of the pattern's oscillation.

Hence, to determine the width of ocular dominance stripes that should develop, we need to answer two questions. First, what determines whether the fastest-growing pattern has a monocular receptive field, and thus whether segregation of ocular dominance patches will occur? Second, if the fastest-growing pattern is monocular, what determines the wavelength of its oscillation?

The answer, for biologically reasonable choices of functions, is as suggested by our study of the development of isolated cells. The pattern of ocular dominance within a receptive field is largely determined by the correlation function C^D, so that the dominant oscillation in C^D (the wavelength of the peak of its fourier transform) shapes the fastest-growing receptive field. If that dominant oscillation is flat (infinite wavelength), or has a wavelength longer than the arbor diameter, the receptive field will be monocular. The oscillation in ocular dominance of geniculate arbors representing a single receptive field point is similarly largely determined by the dominant oscillation in the cortical interaction function I. The cortical oscillation is the sum of these two oscillations, that within receptive fields and that within arbors. The cortical oscillation determines the change between cortical cells of the ocular dominance of receptive fields, or the change between receptive field points of the ocular dominance of arbors. Thus, the cortical oscillation of the fastest-growing pattern is essentially determined by both C^D and the cortical interaction function I, as the sum of the dominant oscillation of each function. In the case of monocular receptive fields, for which the dominant oscillation in C^D is nearly flat, this is simply the dominant oscillation in I. Therefore, when monocular receptive fields form, they will be organized into ocular dominance patches with a width, of left- plus right-eye patch, corresponding to the peak of the fourier transform of the cortical interaction function I.

In the case of a purely excitatory cortical interaction function, the peak of the fourier transform of I corresponds to an infinite wavelength, that is dominance by a single eye everywhere. Addition of constraints on the total synaptic strength of input cells modifies the equation, forcing the left- and right-eye inputs from each retinotopic location to divide between them the cortical surface over which they initially arborize. The result is to suppress the growth of monocular patterns with wavelength longer than an arbor diameter, so that the fastest-growing monocular pattern has a wavelength of about an arbor diameter.

These results can be demonstrated by three methods. One method is to analyze the equation for S^D mathematically, and in particular to determine exact solutions in limiting cases or reasonable approximations. A second method is to numerically compute the characteristic patterns for varying

a. CHARACTERISTIC RECEPTIVE FIELDS

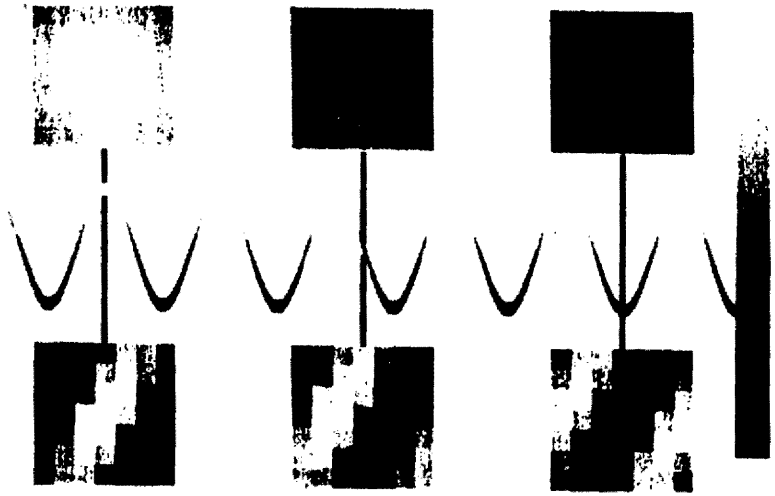

CHARACTERISTIC ARBORS

FIG. 7.19. Characteristic patterns of ocular dominance. The characteristic receptive field, and associated characteristic arbor, are illustrated at three positions for each of two characteristic patterns, one monocular (a) and one binocular (b). The sinusoids illustrate the oscillation of ocular dominance across cortex associated with each characteristic pattern, correctly scaled to the arbor and receptive field sizes. Greyscale codes S^o, the difference between the synaptic strengths of the two eyes, varying from dominance by one eye to dominance by the other. The characteristic receptive field shows the pattern of S^o within the receptive field of a cortical cell, illustrating the retinotopic positions from which the cell receives stronger left-eye or right-eye input. The characteristic arbor at the same point shows the pattern of S^o in the projections of the left- and right-eye geniculate arbors from the retinotopically corresponding point, illustrating the cortical positions to which the left eye or right eye projects more strongly from that retinotopic position. (a) A monocular characteristic pattern. At the cortical point corresponding to the leftmost receptive field, cortical cell inputs are dominated by the right eye. Afferents with the corresponding retinotopic position therefore project arbors such that the right eye afferents preferentially project to the central patch of the arbor (cortical right-eye stripe) and the left-eye afferents preferentially project to the peripheral patches (left-eye cortical stripe). Similarly, the central receptive field is at the border between left-eye and right-eye stripes, where the two eyes have equal innervation, and the rightmost receptive field is in the center of a left-eye stripe. The pattern shown here is one of the set (identical except for rotations of the direction of the oscillation) of fastest-

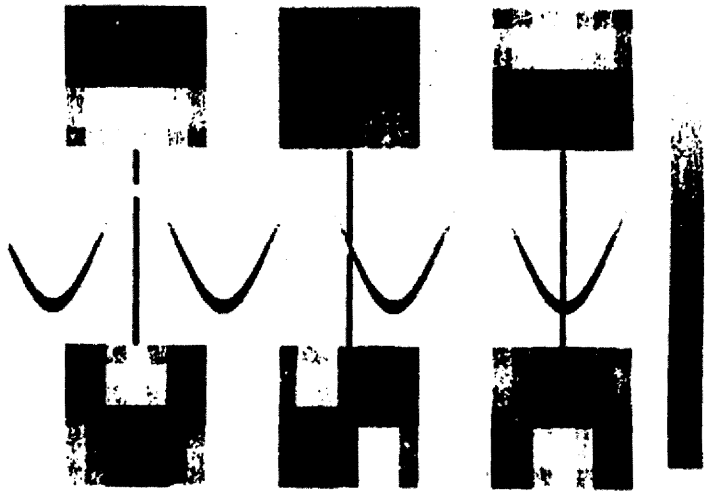

growing characteristic patterns for the correlation function "same-eye correlation 0.4," and the Mexican hat intracortical interaction, of Fig. 15. A flat 7 by 7 arbor function is used, = 1 within the 7 by 7 arbor, 0 outside. The oscillation projects in a direction perpendicular to the stripes across the arbors, rather than horizontally as depicted. (b) A binocular characteristic pattern. This is one of the set (identical except for rotations of the direction of the oscillation) of fastest-growing characteristic patterns for the correlation function "+ same-eye anticorrelations 0.2" of Fig. 7.15, with a Mexican hat cortical interaction and a flat 7 by 7 arbor as in (a). The oscillation projects horizontally as depicted. Receptive fields are dominated above by one eye and below by the other; the eye that dominates each region of a receptive field varies sinusoidally across cortical cells. The arbors show the corresponding pattern of geniculate projections necessary to sustain this cortical pattern of receptive fields. Note that the central receptive field is not strictly neutral, but itself has weak dominance by opposite eyes in different regions. The basis for this is briefly described in appendix 2.

forms of the cortical interaction, correlation, and arbor functions. A third method, which will not be further discussed here, is to analyze simulations of time development across varying functions, to see if monocular cells develop when predicted and, if so, if the period of ocular dominance segregation that develops is that predicted by the cortical interaction function. Such analysis shows that the patterns of ocular dominance develop as predicted (Miller, 1989a; Miller & Stryker, 1989).

One case in which the equations are easily soluble is the case of full connectivity. Then all geniculate cells are connected with equal numbers of synapses to all cortical cells, so that the arbor function is a constant: $A(x - \alpha) \equiv A$. In this case, the solutions are precisely as we have just

FIG 7.19 A

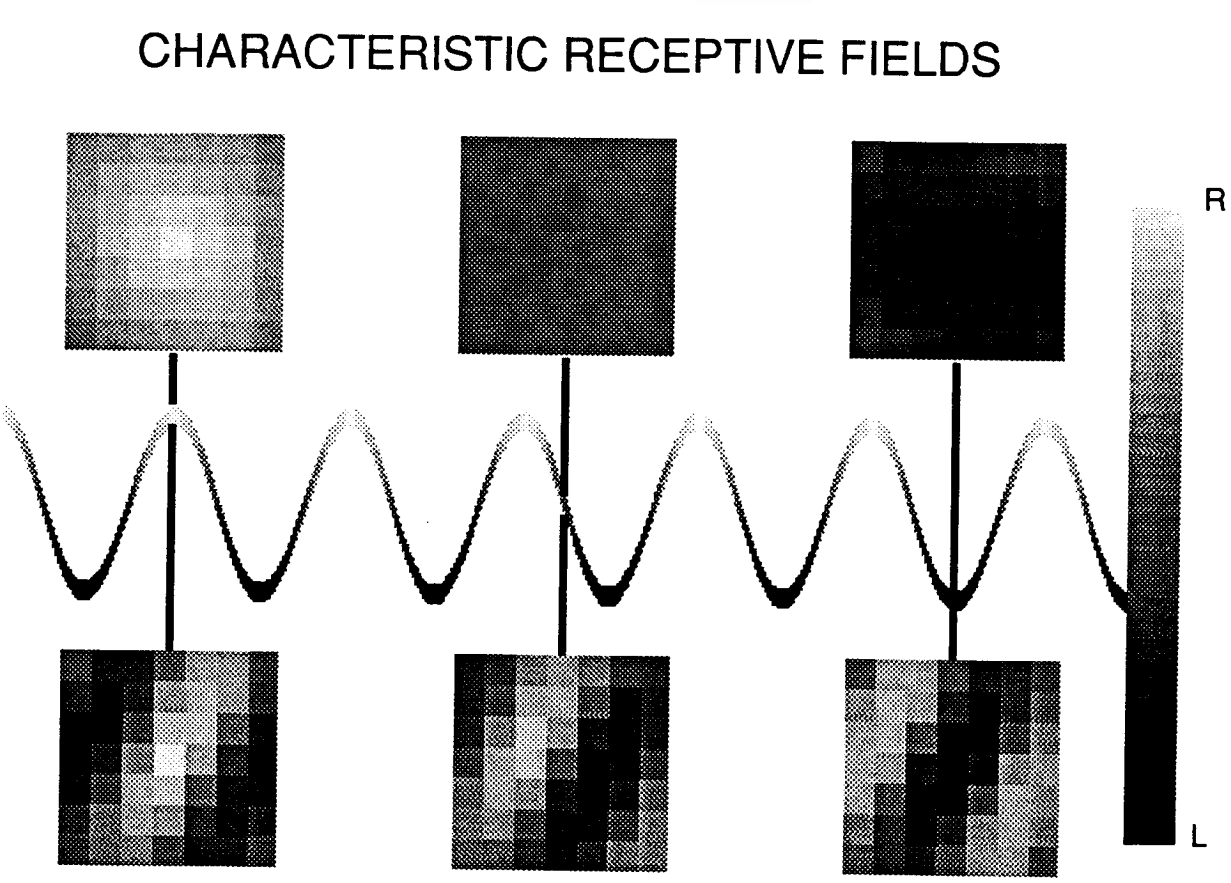
CHARACTERISTIC RECEPTIVE FIELDS
R
L
CHARACTERISTIC ARBORS

FIG 7.19 B

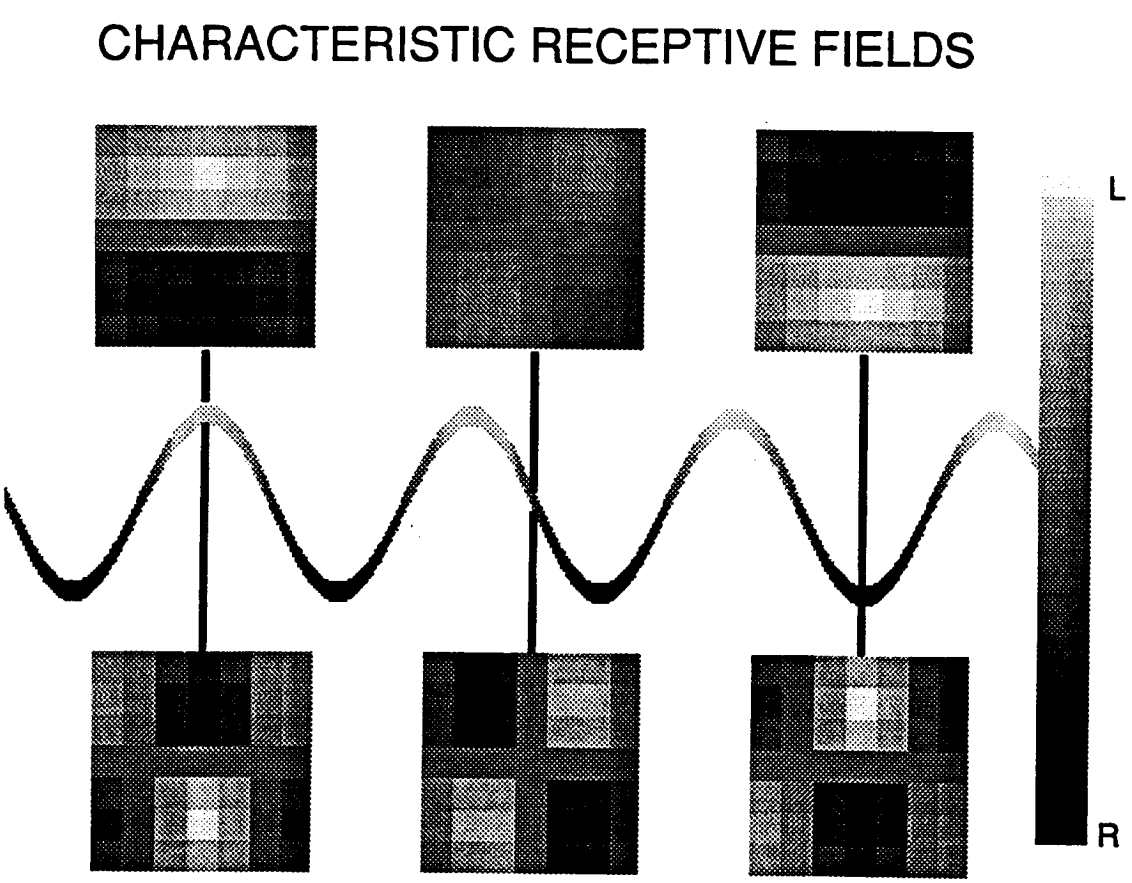
CHARACTERISTIC RECEPTIVE FIELDS
L
R
CHARACTERISTIC ARBORS

suggested: a receptive field oscillation is determined by C^D, an oscillation across afferent arbors by I, and the cortical oscillation is the sum of these two oscillations. Constraints on input cell synaptic strengths in this case suppress the growth of monocular patterns with infinite wavelength, and leave all other patterns unaffected. Two other particularly simple cases in which the equations are exactly soluble occur if correlations are constant, $C^D(\alpha - \beta) \equiv C$;[17] or if correlations are sufficiently broad compared to arbors that one can approximate the correlation between $S^D(x,\alpha)$ and $S^D(y,\beta)$ by the *average* correlation of $S^D(x,\alpha)$ to all inputs synapsing onto the cortical cell at y. Both these limits allow reduction to a simple equation studied previously by Swindale (1980). In both cases, as suggested by the essential constancy of correlations over an arbor, monocular receptive fields develop. As expected, they are organized into ocular dominance patches with width of left- plus right-eye patches given by the wavelength of the peak of the fourier transform of I. If constraints on input cells are present, monocular organization with wavelength longer than an arbor diameter is suppressed.

Numerical computation of the characteristic patterns for a variety of choices of correlation function verify these predictions. Figure 7.20 shows results of computations for the functions used in Fig. 7.16. The growth rates of the characteristic patterns are shown as a function of inverse wavelength and degree of monocularity, and compared to the predictions of the broad correlations limit. As expected, constraints suppress the growth of longer-wavelength monocular patterns. This has no effect on the fastest-growing patterns for the Mexican hat cortical interaction function, but drastically alters the expected outcome for a purely excitatory cortical interaction function. We have shown elsewhere (Miller, 1989a; Miller et al., 1989; Miller & Stryker, 1989) that the broad correlations limit accurately predicts the growth rates of monocular patterns as a function of wavelength, even when the correlation function oscillates significantly so that the fastest-growing patterns are not monocular. The infinite arbor limit predicts, at least qualitatively, the maximum growth rate as a function of wavelength over all patterns, without concern for monocularity.

DISCUSSION

Biological Interpretation of the Results

The model we have developed predicts the development and width of periodic ocular dominance segregation in terms of functions describing input correlations, geniculocortical arbors and cortical interactions. We can compare the model results to experimental measurements.

[17]The correlations need only be constant over distances $\alpha - \beta$ less than the maximum diameter of an arbor plus the maximum distance over which the cortical interaction function $I(x)$ is nonzero; more widely separated inputs never interact.

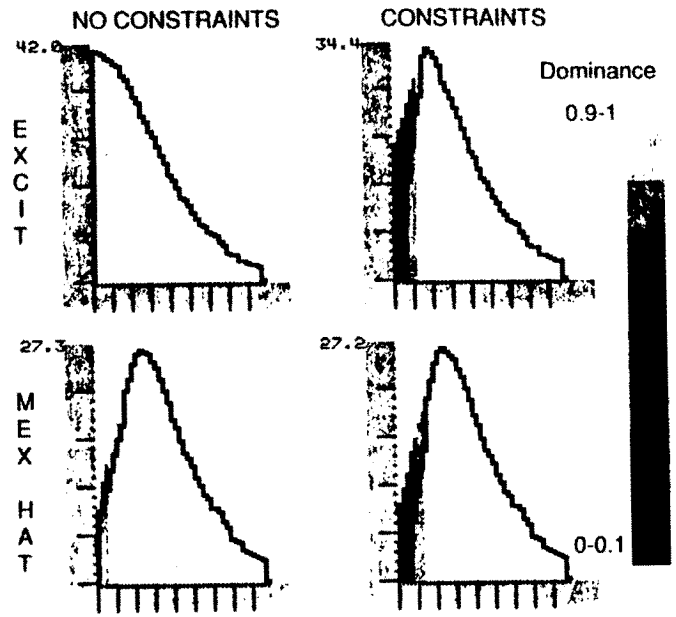

FIG. 7.20. Computed growth rate (vertical axes) of characteristic patterns of ocular dominance, as a function of inverse wavelength of the pattern (horizontal axes), for the two cortical interactions and the two choices of constraints on afferent arbors of Fig. 7.16. Black lines indicate predictions of the broad correlations limit, described in the text. Greyscale indicates maximum dominance of any characteristic pattern with the given wavelength and growth rate. Dominance is a measure of the degree of monocularity of the pattern's characteristic receptive field, on a scale from 0 for complete binocularity to 1 for complete monocularity. The constraints suppress the growth of monocular patterns with wavelength longer than an arbor diameter. This has a profound effect on the outcome when the excitatory cortical interaction function is used, selecting a wavelength of about an arbor diameter. There is little effect when the mixed excitatory/inhibitory interaction function is used, because that function normally selects a wavelength shorter than an arbor diameter. Maximum growth rates are at wavelengths of 7.3-8.3 grid intervals (excitatory function, with constraints) or 5.4-5.9 grid intervals (Mexican hat function). The number beside the vertical axis indicates the maximum growth rate of any pattern. The horizontal axis represents wavenumber; the wavelength in units of grid intervals is 25 divided by the wavenumber. The first bin on the horizontal axis represents wavenumbers 0-0.23; subsequent bins represent increments of 0.4 in wavenumber, so that the second bin represents wavenumbers 0.23-0.63, etc. The arbor and correlation functions are as in Fig. 7.16. From Miller, Keller, and Stryker, 1989. © 1989 by the AAAS.

In the visual cortex of adult cats, the final patches have a period (width of left- plus right-eye patch) of about 850 μm (Anderson, Olavarria, & Van Sluyters, 1988; Shatz, Lindstrom, & Wiesel, 1977; Swindale, 1988). Judging largely by the patchy extent of the final adult arbors, initial arbors in cats may fill a region with diameter 1-1.5 mm (X-cells) or larger than 2 mm (Y-cells) (Humphrey et al., 1985a, 1985b; LeVay & Stryker, 1979). To estimate the correlation function, we use measurements of correlations in maintained activities in darkness of retinal ganglion cells in adult cats (Mastronarde, 1983a, 1983b), and measurements of the retinotopic map onto the cortex (Tusa, Palmer, & Rosenquist, 1978). Together, these indicate that inputs representing a single eye are positively correlated at retinotopic separations corresponding to cortical distances of from $\frac{1}{2}$ (X-cells) to $\frac{3}{2}$ (Y-cells) of a geniculocortical arbor radius (Miller et al., 1989). Horizontal corticocortical synaptic interactions may be excitatory at short range, and appear to be inhibitory to distances of perhaps 400-500 μm (Hata, Tsumoto, Sato, Hagihara, & Tamura, 1988; Hess, Negishi, & Creutzfeldt, 1975; Toyama, Kimura, & Tanaka, 1981a, 1981b; Worgotter & Eysel, 1989). In addition, long-range synaptic interactions exist over distances of 1 mm or more (Gilbert & Wiesel, 1983). These interactions connect only discrete patches of cortex and so may quantitatively have less impact than the shorter-range interactions. In the adult, these long-range connections may connect cells of like orientation specificity by excitatory connections, and may also make inhibitory contributions to direction-selectivity (Tso, Gilbert, & Wiesel, 1986; Worgotter & Eysel, 1989). In the kitten, even before patch development but after the development of orientation selectivity, the long-range connections appear to connect many more patches than in the adult, with a periodicity consistent with the period of orientation columns as well as of the subsequent ocular dominance columns (Luhmann, Martinez Millan, & Singer, 1986).

The results of our analysis are consistent with the sizes suggested by these measurements. The observed patch period of about 850μm can be produced by a variety of short-range intracortical interactions including focal excitation with lateral inhibition over the range observed, ranging from excitation over a radius of 200μm or more surrounded by strong inhibition, to excitation over 50μm or less surrounded by weak inhibition. The longer-range intracortical interactions might be quantitatively negligible in comparison, but if not their periodicity (presumably due to the early periodicity of orientation columns) might also contribute to the period of ocular dominance patches. Similarly, a variety of arbor sizes, ranging from arbors uniform over a diameter of about 850μm to larger, tapering arbors, would yield 850μm patch periods by an arbor-driven mechanism. Such a mechanism seems consistent with X-cell, though not with Y-cell, initial arbor sizes. X-cells mature earlier and might therefore determine patch size (Garraghty, Sur, & Sherman, 1986).

In the model, correlations that are narrow relative to a geniculocortical arbor radius lead to increased binocularity at the borders between patches. In the cat, layer 4 does not consist entirely of monocular cells. Rather, there is a substantial overlap of left- and right-eye input at the borders between ocular dominance patches (Shatz & Stryker, 1978). If X-cells determine patch organization, this overlap is consistent with the fact that X-cells appear correlated over separations of only about $\frac{1}{2}$ of a geniculocortical arbor radius. The increase in monocularity seen with strabismus or alternating monocular deprivation is consistent with the increase in monocularity seen in the model when opposite eyes have decreased correlations or are anticorrelated.

Not all higher mammals develop ocular dominance segregation. Many New World monkeys show no segregation, although there are signs of periodicity in the innervation to cortex representing each eye (reviewed in LeVay & Nelson, 1989). The model suggests a possible explanation for this result. The development of a periodic difference in the synaptic strengths serving the two eyes follows robustly from the choice of correlation function and cortical interactions. However, whether this development of periodicity leads to monocularity and thus to segregation depends on the constraints. If the total synaptic strength over a cortical cell is limited, for example, then the synapses representing the weaker eye in a patch must decrease in strength as the synapses representing the stronger eye grow; this will lead to segregation. If synapses serving both eyes are increasing in strength everywhere, however, then the synapses representing the weaker eye will simply grow more slowly than those representing the dominant eye. In the absence of such constraints, then, one may see periodicity in each eye's innervation without seeing organization of monocular patches.

The model accounts simply for a number of other phenomena seen in development, including refinement of receptive fields, development of patchy geniculocortical arbors, and the effects of monocular deprivation including many elements of a critical period. In summary, a simple correlation-based plasticity rule, combined with a very simple model of geniculate correlations, geniculocortical connectivity, and cortical connectivity or interactions, is sufficient to account for a large part of the observed phenomenology of ocular dominance segregation. This lends plausibility to the notion that these phenomena depend largely on such simple elements, which many more detailed mechanisms would have in common.

Experiments Suggested by the Model

The most fundamental experiments suggested by the model are to characterize the correlations, arbors, and cortical interactions early in development when patch formation begins. Such measurements are quite difficult

technically. These measurements, if made in differing brain regions or species, can be used to test a proposed developmental mechanism by determining whether the periodicity that emerges in each case is consistent with the measurements of the functions defined by the proposed mechanism. For example, area 18 of the cat has patches 1.5 to 2 times wider than those in area 17; arbors are also more widespread, as are correlations since area 18 is Y-cell dominated (Anderson et al., 1988; Humphrey et al., 1985a, 1985b; Swindale, 1988). If a Hebb mechanism is responsible, young kittens should show either a difference between the two regions in intracortical connectivities sufficient to account for the difference in patch width, or predominantly excitatory intracortical connections resulting in arbor-limited patch widths.

Perturbation of the three functions in an experimental preparation before the onset of segregation, and comparison of the resulting periodicity to the unperturbed case, can also test mechanisms. The model predicts that broader correlations within each eye will increase monocularity of layer 4 for mechanisms of the type we study. This could be tested by inducing broader correlations through pharmacological interventions in the retinas. One could also measure whether retinal correlations are broadened in animals deprived of pattern vision. Such animals have increased numbers of monocular cortical neurons (reviewed in Sherman & Spear, 1982). Measurement could also determine whether retinal correlations are broader relative to geniculocortical arbors in monkeys, which have almost completely segregated inputs to layer 4, than in cats, which have a more overlapping innervation.

If a Hebb mechanism underlies ocular dominance plasticity, periodic ocular dominance segregation depends on intracortical synaptic connections. Inhibition of all postsynaptic cells will eliminate activation of such connections. Such inhibition can be achieved by local infusion into cortex of muscimol, which mimics the inhibitory neurotransmitter GABA. If a Hebb mechanism is responsible for column development, one would not expect a periodic pattern of ocular dominance organization to occur in a muscimol-infused region, although individual cells might become monocular. Alternatively, one can attempt to modify rather than eliminate the intracortical interactions. Local infusion of bicuculline, which blocks the receptors for GABA, will selectively eliminate inhibitory intracortical connections. If the resulting purely excitatory intracortical synaptic connections yields patches with an increased period, this would be consistent with a Hebb mechanism whose period is determined by the intracortical interactions. If patch period were unchanged by bicuculline, one would conclude either that the period was normally arbor-limited (which could be tested by measuring whether intracortical interactions were predominantly excitatory during initial column development) or that a non-Hebb mechanism was involved.

Comparison to Other Models

Models of Ocular Dominance Segregation

A variety of related models of ocular dominance column formation have been developed. In a series of papers in the 1970s, Willshaw and von der Malsburg (1976, 1979; von der Malsburg & Willshaw, 1976, 1977; von der Malsburg, 1979) demonstrated that mechanisms like those described here, as well as mathematically similar mechanisms involving exchange of biochemical markers, could give rise to the development of ocular dominance stripes and to the development of topographic mappings. Fraser (1980, 1985) developed a model of development of the retinal projection to optic tectum incorporating a series of activity-independent interactions of varying strengths. When a weak activity-dependent competitive interaction is added and two eyes innervate a single tectum, ocular dominance stripes can form (Fraser, 1985). The model as implemented on a computer did not involve change of strength of individual synapses, but rather movements of whole terminal arbors of individual retinal cells; hence the width of stripes was determined by the arbor size, and was equal to either one or two terminal arbor widths.

Swindale (1980) assumed that synapses exert influences on one another's growth as a function of their eye of origin and the distance across cortex between them. He showed that if synapses facilitate synapses of the same eye at short distance and inhibit them at longer distances, and conversely inhibit synapses of the opposite eye at short distance and facilitate them at longer distances, many phenomena of ocular dominance stripes could be reproduced. The width of the stripes could be simply determined from these influences. Synapses were identified only by eye of origin without regard to retinotopic position of origin, and hence receptive field and arbor structures were not addressed. In the limit in which correlations within an eye extend very broadly compared to an arbor radius, our model yields an equation like Swindale's for cortical ocular dominance, but the influence between synapses becomes expressed in terms of measurable quantities, namely the correlation, arbor, and cortical interaction functions. Hence our model generalizes Swindale's to more complex correlation structures, while providing specific biological underpinnings to Swindale's postulated influence in the limit in which correlations extend broadly within each eye. Our model also allows understanding of receptive field and arbor as well as cortical structure, and demonstrates and analyzes much more generally the conditions under which columns may form.

Cooper and colleagues have studied development of monocularity in single cortical cells, using a Hebb rule whose postsynaptic threshold

for synaptic modification depends nonlinearly on postsynaptic activity[18] (Bienenstock, Cooper, & Munro, 1982; Bear & Cooper, chap. 2 in this volume). The sliding threshold is an alternative method of stabilizing a Hebb synapse rule, that is of ensuring that total synaptic strengths stay within a reasonable range. The effect of this sliding threshold is to subtract a time-varying amount $\epsilon(t)$ from all synapses on a cortical cell at each timestep (see definition of ϵ^L in appendix 1), and thus to subtract $A(\delta)\epsilon(t)$ from the total synaptic strength $S(\delta)$.[19] When the mean output of the cortical cell is low compared to the desired level, less is subtracted from each synapse, raising the total synaptic strength over the cortical cell. This occurs when either the activity input to the cell, or the synaptic strength over the cell, or both, are low. When the mean output of the cortical cell is high, the cortical cell's total synaptic strength is lowered in a similar manner.

In contrast, we stabilized the Hebb synapse rule with constraints on total synaptic strength over a cortical cell. The effect of this constraint is also to subtract a time-varying amount $\epsilon(t)$ from all synapses on a cortical cell at each timestep. For a fixed level of mean input activity, the two rules are essentially identical. If mean input activity changes, the nonlinear sliding threshold causes an increase or decrease in total synaptic strength that returns mean cortical activity to the desired baseline, whereas constraints on total synaptic strength keep total synaptic strength fixed and allow the change in mean cortical activity to persist. The biological truth is likely not to be as simple as either of these rules. The changes in cortical cells in response to deprivation or saturation of input activity are likely to be complex. Nonetheless, it is of interest to contrast the behavior of the two rules in such situations (see also discussion in Bear & Cooper, chap. 2 in this volume):

1. The most obvious prediction of the nonlinear sliding threshold model is that, in response to a period of reduced activation, cortical cells should develop increased total synaptic strength and thus become hyperreactive to normal stimulation.[20] In fact, binocular deprivation during the critical period never results in a subsequent increase in cortical responsiveness. Rather, such deprivation either leaves subsequent cortical responsiveness unchanged, as would be predicted by conservation of synaptic strength, or else decreases cortical responsiveness.[21]

2. When cortex is totally inhibited by infusion of muscimol, each synapse decays proportionally to its mean activity, without interaction between synapses. Using conservation of synaptic strength, monocular deprivation then leads to an ocular dominance shift to the closed eye, as observed experimentally. Using the nonlinear sliding threshold, one must assume that the threshold cannot slide sufficiently low to allow the more active eye's inputs to be rewarded. In this case, there is nothing to stabilize the synaptic strengths: All synaptic strengths will decrease to zero, although the open eye's strengths will decrease faster than the closed eye's.

3. After monocular deprivation, reverse suture (opening the previously deprived eye while simultaneously suturing closed the previously open eye) if initiated sufficiently early leads to an ocular dominance shift in favor of the newly opened eye. To model reverse suture, both models must assume some small ability of the newly opened eye to activate the postsynaptic cell in spite of the fact that it has just suffered from monocular deprivation. The newly opened eye then gains more than the closed eye from synaptic interactions, because the opened eye's activity is more effective in activating the postsynaptic cell. Yet the newly opened eye also loses more through decay, by virtue of having a greater quantity of activity while the cortical cell is often inactive. Both eyes are likely to have decreasing

[18]The idea of a linear sliding threshold for synaptic modification is virtually as old as the Hebb synapse itself (Rochester & Holland, 1956; see also Sejnowski, 1977). Previously the sliding threshold was often taken to be the mean activity of the postsynaptic cell, so that activity greater than the mean led to strengthening of correlated synapses, while activity less than the mean led to weakening of correlated synapses. Such a sliding threshold need not alter the mean activity itself. Bienenstock, Cooper, and Munro added the idea of a nonlinear dependence of the threshold on the mean postsynaptic activity, designed to return mean cortical activity to a fixed prespecified level despite lowering or raising of input activity.

[19]If different populations of inputs have different mean activity levels, as in monocular deprivation, the $\epsilon(t)$ subtracted from the less active inputs is proportionally smaller, as the definition of ϵ^L indicates. Less active inputs still lose strength relative to more active inputs, however, because more active inputs gain far more through synaptic interactions resulting from coactivation of the postsynaptic cell. If all inputs have the same mean activity level, $\epsilon(t)$ is identical for all synapses on the cortical cell.

[20]Bear and Cooper argue that binocular deprivation corresponds to an input of noise, and define this to mean that average input activity is 0. In this case, the cortical threshold has no effect, on the average, on synaptic strength (see definition of ϵ^L in appendix 1 for the case when $\langle f_1[a^L(\alpha,t)]\rangle = 0$; Bear and Cooper use $f_1(a) = a$). However, the basis of this proposal is unclear, as ocular dominance segregation begins in utero in monkeys, and occurs in dark-reared animals. The proposal, even if accepted, does not provide a robust explanation of binocular deprivation. If average input activity were ϵ where $\epsilon > 0$, then hyperreactiveness would develop. Many forms of deprivation, yielding many different input activity levels, have been studied experimentally and none lead to subsequent hyperresponsiveness.

[21]Loss of responsiveness, as well as loss of selectivity of responses, occurs in a significant percentage of cortical cells after longer times of binocular deprivation in kittens. However, these effects do not appear to occur over short times of a few days to a week of binocular deprivation (Sherk & Stryker, 1976; see review in Movshon & Van Sluyters, 1981). In contrast, monocular deprivation over such short time causes strong shifts of ocular dominance. Therefore, these two effects of longer-term binocular deprivation may simply reflect atrophy due to disuse, which may occur through mechanisms different than the competitive mechanisms studied by the models. Alternatively, these effects might be explicable within the context of the models by postulating that inputs become uncorrelated, or that cortical cells fail to reach the threshold for synaptic reward.

input strength in the absense of conservation of synaptic strength, but it is not clear which eye will decrease faster. The nonlinear sliding threshold model assumes that the threshold slides faster than synaptic strengths decrease, so that eventually the average activation in response to the newly opened eye is suprathreshold and that eye can gain strength. Using conservation of total synaptic strength, one assumes that the input strength of the newly opened eye decreases relatively more slowly than that of the newly closed eye.[22]

4. Finally, when the cortex is disinhibited by application of bicuculline, there is significant reduction in the ocular dominance shift in response to subsequent monocular deprivation (Ramoa, Paradiso, & Freeman, 1988). Stimulus selectivity of cortical neurons was strongly reduced during bicuculline infusion: Cortical neurons responded to a much broader range of stimuli than normal, and to stimulation in a much larger portion of the visual field than normal. The investigators suggested that this may lead to an increase in the correlation between the spontaneous activity from the closed eye and the visually-driven responses of the open eye. They propose that such correlation accounts for the decreased effect of monocular deprivation. If this is the correct explanation of the reduced ocular dominance shift, the form of stabilization is irrelevant to the outcome.

To summarize, both methods are equivalent in normal circumstances. Neither method is perfect under conditions of deprivation or overstimulation of cortex. The robust features of a Hebb-type model, such as refinement of receptive fields and development of ocular dominance, depend on differentials in the relative rates of growth of different synaptic populations. These robust effects occur in most cases due to the synaptic interactions rather than to decay. The methods of stabilization of synaptic strengths determine the absolute values of the growth rates. These methods are motivated by mathematical convenience as much as or more than by biological knowledge. The important point in understanding a correlation-based model is to understand the reliable conclusions that can be drawn, and by and large this means understanding the results of the synaptic interactions that such models have in common.

[22]There is a critical period for reverse suture, as for monocular deprivation, experimentally as well as in both models. For a reverse shift to occur in the models, just as for ordinary monocular deprivation, the newly opened eye must more effectively activate the cell than the newly closed eye. This depends both on the differential in their activities, and on the differential in their synaptic strengths on the cell at the time of reversal. For any given differential in activity, there will be some "point of no return", a differential of synaptic strength which the activity difference can no longer reverse.

Some Related Correlation-Based Models

Linsker (1986, 1988) developed a model of plasticity that is formally nearly identical to ours. However, the implementation of the model is quite different. Linsker considered inputs from only a single eye. Arbors were assumed to be gaussian. Synapses were allowed to have either positive or negative strength, which was achieved in one of two ways. First, each individual synapse might be capable of being both positive and negative. In contrast, biological synapses are exclusively excitatory or exclusively inhibitory. Equivalently, there might be two populations, one exclusively positive, one exclusively negative, subject to conditions that render them the positive and negative halves of a single, statistically indivisible population. The two populations must have approximately identical distributions of locations and initial arborizations, and the correlation between the activities of two inputs must depend only on the distance between them, without regard for whether either is inhibitory or excitatory. This is biologically implausible, because an excitatory and an inhibitory population would be expected to have different inputs and different connectivities, and because inhibitory cells are often interneurons which, when active, inhibit nearby excitatory cells; but it is not impossible.

Linsker applied his model to study the development of orientation selectivity in a visual cortical layer from a non-oriented input layer. In cats, all cortical cells are oriented, so the non-oriented input layer must represent the LGN. Inputs from LGN to cortex are exclusively excitatory. This represents an additional problem for the use of negative synapses. In monkeys, the cortical layer 4 cells receiving geniculate input are not oriented. Hence orientation selectivity in monkeys might be regarded as emerging from projections from layer 4 of cortex to the upper layers, in which case both excitatory and inhibitory projections could be involved.

Because synapses from each location in Linsker's model can be either positive or negative, the initial condition is a random perturbation from all synapses having zero strength. Thus, formally, his model of a single eye's inputs with synapses of either sign, is equivalent to our model of S^D, the difference between the strength of two eyes.

His model involves four essential steps. First, with an input layer of random noise, all synapses are made to grow until saturation, without synaptic interactions (formally, the $-\epsilon$ decay term is made large and positive). Because arbors overlap, input cells at the next layer becomecorrelated in their activity by virtue of receiving common inputs. These correlations decrease with distance in proportion to the corresponding decrease in the overlap of arbors. Second, when a layer with such correlations projects to a cell in a third layer, the fastest-growing pattern is

one that grows faster in the center than in the periphery of that cell's receptive field, as we have seen. The cell is stabilized by fixing the final summed synaptic strength over the cell (excitatory strength minus inhibitory strength).[23] This has the effect of fixing the final percentage of positive and negative synapses, because all synapses saturate at either the maximum positive or the maximum negative strength. When 30% of final synapses are forced to be negative, the result is a center of positive synapses surrounded by a ring of negative synapses. Hence, formation of these "center-surround" cells depends critically on the negative synapses and the stabilization condition. The robust feature is that central synapses grow faster than peripheral ones. In a layer of such "center-surround" cells, cells separated by short distances, whose centers overlap, have correlated activities, whereas cells separated by longer distances, such that one cell's center overlaps the other's surround, have anticorrelated activities. This yields a Mexican hat correlation function.

Third, suppose a layer with a Mexican hat correlation function, whether derived as just described or otherwise, projects to a cell in a further layer. We have seen that if such a correlation function is sufficiently narrow with respect to the arbor function, the fastest-growing receptive field pattern has a positive stripe adjacent to a negative stripe. Linsker used such a correlation function but with additional oscillations in sign with increasing distance, and found that oriented cells can result. I am told that oriented cells can also result from such a correlation function when synapses are required to remain positive (Linsker, private communication), though in my own experience special constraints seem necessary to avoid circularly symmetric results. Finally, Linsker showed that if these oriented cortical cells develop while connected by weak excitatory corticocortical synaptic connections, an interesting cortical organization of orientation modules can arise. Note that our eigenfunction analysis of S^D suggests that cortical organization should include an oscillation in phase, between positive and negative synapses, as one moves across cortex. Linsker's constraints, which force a majority of synapses on each cell to be positive, suppress the growth of oscillating modes in favor of modes with frequency zero. These points are discussed in greater detail elsewhere (Miller & Stryker, 1989).

In sum, Linsker developed a very similar model, and pointed out that Hebbian mechanisms can determine the structure of individual receptive

[23] Linsker's constraint consists of subtracting a term $-|k_2|(\bar{s} - \text{TARGET})$ from the expression for $\frac{d}{dt}s(\alpha)$, where $s(\alpha)$ is the strength of an individual synapse and $\bar{s}$ is the average value of s over the cortical cell. $|k_2|$ is large so that this term dominates $\frac{d}{dt}s(\alpha)$ for all α if the average synaptic strength is not approximately equal to TARGET, and thus drives s back toward TARGET. TARGET, in Linsker's notation, is $-k_1/k_2$.

fields and their cortical organization in very interesting ways. The value may be more as an important example of the capacities of Hebbian mechanisms than as a specific model of biological phenomena. Linsker's results can be simply understood on the basis of the eigenfunction analysis of the development of S^D.

A number of authors have recently explored similar models of Hebb-type development in a single postsynaptic cell, in which synapses may be positive or negative, in terms of an eigenfunction analysis and its relation to methods of statistical analysis or information theory (Baldi & Hornik, 1989; Linsker, 1988; Oja, 1982; Sanger, 1989). Our analysis contains two important features not seen in the other work. First, we have shown that as a model of S^D, that is of the development of ocular dominance, such models are biologically realistic and resilient against nonlinearities. In contrast, model outcomes that are dependent on the existence of both positive and negative synapses, on an initial condition which is a small random perturbation of synaptic strengths on both sides of zero, or on linearity cannot be regarded as applicable to biological systems. In addition, we have developed the eigenfunction analysis for a model with a layer of postsynaptic cells interconnected by synaptic interactions. In this context, two novel features arise. First, characteristic receptive fields (the eigenfunctions of the isolated cell) acquire a phase shift or characteristic oscillation between cortical cells to form the characteristic patterns or eigenfunctions of the system as a whole. Second, the characteristic receptive fields themselves are altered by the cortical interactions. In particular, monocular characteristic fields have both their growth rate and their degree of monocularity enhanced at the dominant frequency of the cortical interaction.

There is an interesting connection between the case of "identity mapping" in backpropagation networks, discussed by Zipser (chap. 8 in this volume), and simple Hebb-type models (Baldi & Hornik, 1989). Identity mapping is a form of unsupervised learning in which the input is also the desired output, and a layer of some number N of intermediate or hidden units are trained by backpropagation of error to produce this desired identity mapping. If the backpropagation network is linear, the hidden units extract the N fastest-growing eigenvectors of the input correlation matrix. An isolated Hebb-type cell is similarly predominantly shaped by the fastest-growing eigenvector of the input correlation matrix.

Outstanding Theoretical Questions

Many theoretical questions are raised by the problems we have addressed. We may roughly subdivide these as questions involving the application of

simple correlation-based models to other problems, and questions about the effects of incorporating greater biological complexity into the models.

In the first category, one outstanding question involves application of simple models to a three-dimensional output structure. Under what conditions will two inputs segregate into stripes, that is a breakup of the retinotopic map into alternating patches, and under what conditions will they instead segregate into laminae, that is two complete retinotopic maps one above the other? The visual cortex in most species that show segregation, and the amphibia and fish optic tecta, form stripes, while the visual cortex in tree shrew (Kretz, Rager, & Norton, 1986), and the lateral geniculate nucleus, segregate into laminae. A simple proposal motivated by the model presented here is that inputs from a single eye extend in a plane with more excitatory connections, while the two eyes segregate from one another in a plane with more inhibitory connections. Alternatively, Schmidt (1985) suggested that inputs from a single eye may extend in a plan determined by a bias in the plane of extension of dendrites of receiving cells. A related, more specific, outstanding problem, is to study the conditions under which simple models will reproduce the variety of laminar segregation processes seen in the LGN. Both for studies of LGN and of cortex, one would like to understand the effects of having four statistical classes of inputs (ON- and OFF-cells from each eye), or even eight classes (X- and Y-cells of each of the four previous types). To pursue such models very far, one must have reasonable biological ideas of the correlations within and between the classes of inputs (Mastronarde, 1989).

Another problem is to understand the determinates of the form of ocular dominance stripes or patches. For example, in the monkey the stripes tend to be long and straight and to run perpendicular to the borders of primary visual cortex (LeVay, Connolly, Houde, & Van Essen, 1985). In the cat, the segregation is more patchy, irregular, and rarely straight, and does not run at any special angle with respect to the borders (Anderson et al., 1988). Our simple linear theory predicts the wavelength of periodicity, but the final form depends on a nonlinear interaction between all the characteristic patterns with that wavelength and hence cannot be predicted by the theory. Swindale (1980) showed that ocular dominance stripes resulting from the simple dynamics he proposed and a simple nonlinearity tend to run perpendicular to the borders. He also showed that a bias in the direction of cortical growth during column formation could lead to extension of the stripes in the direction of preferred cortical growth. Because his dynamics result as a simple limiting case from our model, similar results can be obtained with our model, but one would like to understand more generally when these results will or will not occur. A recent theory assumes the existence of patches or stripes of a fixed width, and proposes that their arrangement is determined by the need to optimize retinotopic match

between inputs and cortex (Anderson et al., 1988; Jones, Van Sluyters, & Murphy, 1988). This theory can explain the variation of form across species by examining the diverging shapes of cortex or tectum and layouts of the overall retinotopic map in the various species considered. One would like to understand if correlation-based mechanisms would robustly tend to cause such optimization to occur.

Understanding the conditions under which simple correlation-based models will yield orientation selectivity with nonnegative synapses remains an important problem. Under such conditions, one would also like to understand the relationship of orientation to ocular dominance, both on individual cells and across the cortex as a whole. For example, if C^S is Mexican hat, like the function Linsker used to obtain oriented receptive fields, while C^D is purely positive, to produce monocularity, the eigenfunction analysis suggests that a monocular and oriented cell could develop even when all synapses remain positive. C^S and C^D can have the required form if C^{SameEye} is Mexican hat and opposite eyes are anticorrelated. Monocular and at least somewhat oriented cells do develop in this case, provided that synapses are constrained by multiplication of all synapses by a constant after each timestep to preserve the sum of total synaptic strength, rather than by subtraction of a constant from all synapses. With subtractive constraints, monocularity may develop but the receptive field tends to refine to a circularly symmetric structure. However, multiplicative constraints will never allow monocularity to develop without opposite-eye anticorrelations, which seems overly restrictive.[24] One would like to understand more generally the classes of methods of stabilization and saturation that can yield the oriented result. More recently, I have proposed that interactions between ON-center and OFF-center inputs may yield oriented cells using positive synapses in a manner robust with respect to methods of stabilization (Miller, 1989b). ON- and OFF-center inputs are known to be anticorrelated with one another at retinotopic separations over which their centers overlap (Mastronarde, 1983a, 1983b). Orientation selectivity would

[24]Let the equations, before multiplicative constraints, be written $\frac{d}{dt} S^S = L^S S^S$, $\frac{d}{dt} S^D = L^D S^D$. Then, in the absence of the nonlinear cutoff of synaptic strengths at zero, it is easy to show that S^S will develop under multiplicative constraints into the principal eigenfunction of L^S (first noted in Oja, 1982; intuitively, S^S is really growing linearly because the multiplicative renormalization is only a change of scale, hence the principal eigenfunction will exponentially dominate). Given the nonlinear cutoff, it is plausible to think that the oriented structure would persist. The development of S^D, in the absence of the cutoff, involves the growth of all eigenfunctions of L^D but with growth rates equal to the corresponding eigenvalue minus the principle eigenvalue of L^S; that is, patterns of S^D must grow faster than the fastest pattern in S^S, or the multiplicative renormalization that keeps the sum constant will cause the difference to shrink. Hence, monocularity should develop if and only if the principal eigenfunction of L^D is monocular and has a larger eigenvalue than that of L^S. Note that this requires opposite-eye anticorrelations.

develop if these inputs were correlated with one another at greater distances of retinotopic separation; receptive fields like those of Fig. 7.19b would develop, where now black and white are to be interpreted as dominance by ON- versus OFF-center cells rather than by left- versus right-eye cells.

Many important problems are raised by the plasticity of somatotopic maps in adult somatosensory cortex. Monocular deprivation shifts are a crude form of the result that more active synapses gain more territory at the expense of less active synapses, but in that case a critical period arises due to the disconnection of one eye's inputs. One would like to understand the conditions under which a cortical map can be dynamically and reversibly maintained so that the amount of cortical territory controlled by a portion of the periphery is roughly porportional to the level of activity of that portion of the periphery, up to limits imposed by the finite extent of terminal arborizations. This might be achieved by the use of multiplicative constraints. An important feature of somatosensory plasticity appears to be the overlap rule: The degree of overlap of two receptive fields a fixed distance apart across cortex remains roughly constant (Allard, 1989; Merzenich et al., 1988; Sur, Merzenich, & Kaas, 1980). This is equivalent to the statement that receptive field size varies inversely with cortical magnification, or to the statement that point image size (the size of the cortical area activated by a given peripheral location) remains constant. Understanding the conditions under which a correlation-based rule will yield this result remains an outstanding problem.

The second type of question, as suggested, concerns the effects of incorporating greater biological complexity into the model. A more complex model might consider the possibility that intracortical connections, geniculocortical anatomical connectivity or input correlations are modifiable during development. Both excitatory and inhibitory intracortical synapses show modifications by early experience in cat visual cortex (Beaulieu & Colonnier, 1987), though it is not clear if such changes occur as early as patch formation. The final structure of ocular dominance patches develops through anatomical removal of geniculate input terminals from patches of opposite-eye input. Many postsynaptic cells in layer 4 of monkey visual cortex and in frog optic tectum similarly remove their dendrites from patches of inappropriate eye input (Katz & Constantine-Paton, 1988; Katz, Gilbert, & Wiesel, 1989). We have assumed that these anatomical changes in geniculocortical connectivity occur subsequent to the development of an initial physiological pattern of ocular dominance. Finally, both dendrites and retinogeniculate arbors of retinal ganglion cells are undergoing extensive modifications during the time of patch development (Ramoa, Campbell, & Shatz, 1988), and it is quite possible that geniculate circuitry is also developing at that time, so correlations among geniculate inputs may be changing during patch formation.

Many other factors might also contribute to the final developmental outcome under correlation-based models. For example, the details both of the arrangement of the grid of inputs, and of the retinotopic map of that grid onto cortex, might play important roles in the development of receptive field structure (Mallot, 1985; Soodak, 1987); so too may interactions among the many statistical subtypes of inputs serving each eye. Activity-independent interactions, among inputs and between inputs and postsynaptic cells, must be considered (Fraser, 1980, 1985). We have assumed that only pairwise correlations among inputs are significant to the activity-dependent interactions, but higher-order correlations may also play a role (see footnote 2, appendix 1). Details of the temporal structure of the plasticity mechanism, and in general greater biophysical detail, may contribute new features to development. In studying each potentially complicating factor, one would like to understand whether, and in what ways, they can lead to qualitatively new developmental outcomes or to significant quantitative alterations in development, in comparison to the outcomes already inherent in simple correlation-based interactions.

CONCLUSION

A variety of biophysical and biochemical mechanisms may underlie the plasticity associated with correlation-based mechanisms of neural development. In this chapter I have attempted to demonstrate that many features of development under such mechanisms can be studied and understood in terms of a few simple features that are largely independent of the underlying details. These features include the correlations in activity among input neurons; the connectivity between the input neurons and the receiving neurons; interactions by which coactive synapses influence one another's development; and the constraints or limits that stabilize synaptic strengths.

A simple model, in which correlations, connectivity, and interactions depend only on the distances between neurons and, in the case of correlations, on the eye represented, is sufficient to explain a wide variety of features of the development of ocular dominance patches in mammalian visual cortex. These features include the development of patches and the determination of their width; the refinement of individual cortical receptive fields; the refinement and confinement to patches of the terminal arbors of geniculate cells; the effects of the breadth of correlation or of opposite-eye anticorrelations on the degree of segregation that develops; and the effects on development of abnormal experience such as monocular deprivation, including elements of a critical period.

A critical feature characterizing a proposed mechanism of ocular dominance plasticity is the type of cortical interaction function it predicts. If a

mechanism predicts a purely excitatory cortical interaction, it predicts ocular dominance periodicity determined by the arbor diameter and dependent on constraints that tightly conserve total synaptic strength over each geniculate terminal arbor. If a mechanism predicts a mixed excitatory and inhibitory cortical interaction, whose dominant oscillation is smaller than an arbor diameter, it predicts ocular dominance periodicity determined by the cortical interaction and not dependent on constraints on geniculate arbors. This provides a basis for experimental distinction between proposed mechanisms.

By understanding the features in a model that are responsible for the developmental outcome, one can gain insight into the elements of a proposed biological mechanism that may be critical to the observed biological outcomes. At the same time, one can learn which elements of the model's outcome are likely to be robust, and which are likely to depend on the probably unbiological details of implementation. In the model of visual development, the influences of synapses on one another through correlations lead to robust tendencies to development of receptive field refinement and monocularity. If individual cortical cells do tend to become monocular, the extension of influences across cortex by intracortical interactions leads robustly to an oscillation of ocular dominance with a period selected by the intracortical interactions. Other features of the model, such as the method of stabilization, may suppress or enhance the expression of these tendencies, but are not fundamentally responsible for them.

In conclusion, even a simple neural model can serve to unify a large group of phenomena in terms of measurable biological elements. At the same time, a model can point out new lines of distinction between mechanisms. In this way, neural modeling may play an important part in the effort to understand the mechanisms underlying neural development and function.

ACKNOWLEDGMENTS

I would like to acknowledge the advice, support, and collaboration of my graduate advisors, Michael P. Stryker and Joseph B. Keller, in the modeling work described in this chapter. I thank Barbara Chapman, Michael Stryker, and Kathleen Zahs for helpful comments on this chapter. I was supported while writing this chapter by National Science Foundation grant BNS-8820406, a Bioscience Grant for an International Joint Research Project from the NEDO, Japan, and a grant from the System Development Foundation, all awarded to Dr. Michael P. Stryker.

APPENDIX 1: FORMULATION OF THE MODEL EQUATIONS

We use the following notation in addition to that defined in the text. $c(x,t)$ is the activity (membrane potential, or spike frequency) of the cortical cell at x at time t. $a^L(\alpha,t),a^R(\alpha,t)$ is the activity of the geniculate input representing the left or right eye, respectively, from position α at time t. We formulate equations for S^L. Equations for S^R are identical if L and R are exchanged throughout.

For a Hebb rule, the model equations may be formulated as follows. First, we formulate the equation for the Hebb plasticity rule itself. For an individual left-eye synapse from α to x, the change at a given time is proportional to a product of some function of postsynaptic activity times some function of presynaptic activity, that is to $[c(x,t) - c_{\text{thres}}(x)]f_1[a^L(\alpha,t)]$. For convenience, we have assumed the postsynaptic function is linear, but as discussed in the text and in appendix 2 this is not necessary to our analysis. $c_{\text{thres}}(x)$ is a fixed threshold; this could also be taken to be a function of mean cortical activity at x [Sejnowski, 1977; Bear and Cooper, chap. 2 in this volume]. f_1 is an arbitrary function, presumably monotonic and incorporating threshold and saturation effects. There are $A(x - \alpha)$ such synapses, all undergoing identical change, hence the total change must be multiplied by $A(x - \alpha)$. Finally we subtract terms representing possible activity-independent synaptic decays (or growths) to obtain the following equation for a Hebb rule:

$$\frac{d}{dt}S^L(X,\alpha,t) = \lambda A(x-\alpha)[c(x,t) - c_{\text{thres}}(x)]f_1[a^L(\alpha,t)] - \gamma S^L(x,\alpha,t) - \epsilon' A(x-\alpha). \quad \text{(A1)}$$

Here λ, γ and ϵ' are constants.

Second, we formulate an equation for cortical activity as a function of input activity. We take the net LGN input to the cortical cell at x at time t to be

$$\text{net}_{\text{LGN}}(x,t) = \sum_{\alpha}\left\{S^L(x,\alpha,t)f_2[a^L(\alpha,t)] + S^R(x,\alpha,t)f_2[a^R(\alpha,t)]\right\}.$$

f_2 incorporates threshold and saturation effects. We assume there is also cortical input given by $\Sigma_y B(x - y)c(y,t)$. $B(x - y)$ is a function describing intracortical synaptic connectivity, taken for simplicity to be fixed. We assume that cortical activity depends linearly on the net input, though again

a nonlinear activation function can be accommodated. Finally, we assume there is some intrinsic cortical activity $c'(x)$. Thus,

$$c(x,t) = \text{net}_{LGN}(x,t) + \sum_y B(x-y)c(y,t) + c'(x).$$

In matrix notation, this is $(\mathbf{1} - \mathbf{B})\mathbf{c}(t) = \mathbf{net}_{LGN}(t) + \mathbf{c}'$ where $\mathbf{1}$ is the identity matrix and $\mathbf{B}$ is the matrix with elements $\mathbf{B}_{xy} = B(x-y)$. Defining the intracortical interaction function $I(x-y)$ by the matrix equation[1] $\mathbf{I} = (\mathbf{1} - \mathbf{B})^{-1}$ yields

$$c(x,t) = \sum_y I(x-y)\text{net}_{LGN}(y,t) + c_{int}(x) \qquad \text{(A2)}$$

where $\mathbf{c}_{int} = \mathbf{I}\mathbf{c}'$ is the intrinsic cortical activity in the absence of input activation.

Substituting equation *A2* for $c(x)$ into equation *A1* yields an equation for the change in synaptic strengths as a function of input activities. Averaging this equation over input patterns yields an equation in terms of the measurable statistical properties of the inputs.[2] Let correlation functions C^{LL}, C^{LR}, describing the correlation in firing between two left-eye inputs or between a left-eye and a right-eye input, respectively, be defined by[3]

$$C^{LL}(\alpha-\beta) = \langle f_1[a^L(\alpha,t)] f_2[a^L(\beta,t)]\rangle,$$

$$C^{LR}(\alpha-\beta) = \langle f_1[a^L(\alpha,t)] f_2[a^R(\beta,t)]\rangle,$$

[1]This inverse will exist if **B** is sufficiently small, mathematically, or biologically if we assume cortical activity is determined by input activity.

[2]The equation obtained is actually an infinite series. The lowest order term involves two-point correlations of the input activities, and is the term we present. The higher order terms include the three-point, four-point, . . . structure of the inputs, that is the tendency of three or more inputs to fluctuate together in their activities beyond what would be predicted from knowledge of their pairwise correlations. We discard these terms for simplicity, but note that they are small either if λ is small or if fluctuations are small. It is of interest to establish theoretically what nontrivial dynamics might arise from such higher order correlational structure. The averaging is done using the smoothing procedure which is described by Keller (1977).

[3]We assume here for simplicity that $\langle f_1[a^L(\alpha,t)]\rangle = 0$. If this is not the case, C^{LL} should be defined as $\langle f_1[a^L(\alpha,t)] f_2[a^L(\beta,t)]\rangle - \langle f_1[a^L(\alpha,t)]\rangle\langle f_2[a^L(\beta,t)]\rangle$ (and similarly for C^{LR}), so that $\lim_{\alpha-\beta\to\infty} C^{LL}(\alpha) = \lim_{\alpha-\beta\to\infty} C^{LR}(\alpha) = 0$. Then our equations are identical except that C^{LL}, C^{LR} are replaced everywhere by $C^{LL} + \theta$, $C^{LR} + \theta$ where $\theta = \langle f_1[a^L(\alpha,t)]\rangle\langle f_2[a^L(\beta,t)]\rangle$. Note that θ does not depend on L, R, α, or β if we assume that all inputs are statistically equivalent. This θ is the same as the parameter k_2 in Linsker (1986). θ would not appear in the equation obtained in the text for S^D, and hence its presence would not affect the analysis of the development of ocular dominance segregation.

where $<>$ signifies an average over input patterns. Then the equation obtained is

$$\frac{d}{dt}S^L(x,\alpha,t) = \lambda A(x-\alpha)\sum_{y,\beta} I(x-y)[C^{LL}(\alpha-\beta)S^L(y,\beta,t) + C^{LR}(\alpha-\beta)S^R(y,\beta,t)] - \gamma S^L(x,\alpha,t) - \epsilon^L A(x-\alpha) \qquad \text{(A3)}$$

where $\epsilon^L = \epsilon' - \lambda[c_{int}(x) - c_{thres}(x)]\langle f_1[a^L(\alpha,t)]\rangle$. This is Eq. 1 in the text.

This equation is not unique to a Hebb synapse mechanism, but can be derived from a variety of biological mechanisms. For example, in a mechanism relying on trophic factors, cortical cells release diffusible or actively transported substances, in proportion to their activity. The substances in turn are taken up by synaptic terminals in proportion to presynaptic activity, as would be expected if uptake occurs in conjunction with vesicle reuptake. If we assume synapses gain strength in proportion to the amount of substance they take up, then we can replace Eq. A1 by

$$\frac{d}{dt}S^L(x,\alpha,t) = \lambda A(x-\alpha)\sum_l E(x-l)[c(l,t) - c_{thres}(l)]f_1[a^L(\alpha,t)] - \gamma S^L(x,\alpha,t) - \epsilon^L A(x-\alpha). \qquad \text{(A4)}$$

Here $\lambda E(x-l)$ expresses the influence of site l upon site x over the relevant times due to diffusion or transport. After substituting Eq. A2 for $c(l,t)$ into Eq. A4 and averaging, we again obtain Eq. A3, with $\Sigma_l E(x-l)I(l-y)$ in place of $I(x-y)$. If the diffusible or transported substances are released in an activity-dependent manner by the presynaptic terminals themselves, rather than by the cortical cells, Eq. A3 is obtained but now with $E(x-y)$ in place of $I(x-y)$. In this case the activity of the postsynaptic cell is of no importance to plasticity.

In addition to modifiable synapses represented by any of the mechanisms presented so far, we can consider chemospecific adhesion between input terminals and cortical cells. Such retinotopic adhesion is considered important in many models of retinotectal connections (Fraser, 1980, 1985; Whitelaw & Cowan, 1981). Suppose the degree of chemospecific adhesion between the input from α and the cortical cell at x depends only on $x-\alpha$. In this case, the retinotopic adhesion can be represented by a factor $R(x-\alpha)$ multiplying the terms in $\frac{d}{dt}S(x,\alpha,t)$. This is, formally, the role played by the arbor function. Hence, by letting $A(x-\alpha)$ represent the product of the chemospecific adhesion times the arbor strength, we can take account of retinotopic adhesion as well.

APPENDIX 2: THE CHARACTERISTIC PATTERNS OF OCULAR DOMINANCE

Eq. 3 or Eq. 6 for S^D in the text can be written

$$\frac{d}{dt}\mathbf{S}^D + \gamma\mathbf{S}^D = \mathbf{L}\mathbf{S}^D \tag{A5}$$

Here, $\mathbf{S}^D$ is the vector of synaptic weights, and $\mathbf{L}$ is a linear operator defined by the right side of Eq. 3 or 6. In Eq. 3, $\mathbf{S}^D$ is the vector with components $S^D_\alpha = S^D(\alpha)$, $\mathbf{L}$ is a matrix with entries $L_{\alpha\beta} = \lambda A(\alpha)C^D(\alpha - \beta)$, and $\mathbf{L}\mathbf{S}^D = \Sigma_\beta L_{\alpha\beta}S_\beta$. In Eq. 6, $\mathbf{S}^D$ has components $S^D_{(x,\alpha)} = S^D(x,\alpha)$, $\mathbf{L}$ has elements $L_{(x,\alpha);(y,\beta)} = A(x - \alpha)I(x - y)C^D(\alpha - \beta)$, and $\mathbf{L}\mathbf{S}^D = \Sigma_{(y,\beta)}L_{(x,\alpha);(y,\beta)}S^D(y,\beta)$.

The characteristic patterns of ocular dominance are the *eigenvectors* or *eigenfunctions* of the linear operator $\mathbf{L}$ in Eq. A5. The eigenvectors of any operator $\mathbf{L}$ are defined as those vectors $\mathbf{S}_i$ satisfying $\mathbf{L}\mathbf{S}_i = \omega_i\mathbf{S}_i$ for some constant ω_i. ω_i is the *eigenvalue* of the eigenvector $\mathbf{S}_i$, while i is an index enumerating the different eigenvectors.

For simplicity, it will be assumed that $C^D(\alpha) = C^D(-\alpha)$ and $I(x) = I(-x)$. Then the operator $\mathbf{L}$ of Eq. 3 or 6 has a complete basis of eigenvectors: That is, any vector $\mathbf{L}^D$ can be written as a weighted sum of eigenvectors $\Sigma_i c_i\mathbf{S}_i$ for some unique set of coefficients c_i.[1] In addition, all eigenvalues are real numbers.

Let the synaptic strengths at time 0 be given by the vector $\Sigma_i c_i^0\mathbf{S}_i$. Then the unique solution to Eq. A5 at any time t is given by

$$\mathbf{S}^D(t) = \sum_i c_i^0\mathbf{S}_i e^{(\omega_i - \gamma)t} \tag{A6}$$

This can be seen by applying $(\frac{d}{dt} + \gamma)$ to the right side of Eq. A6: the result is to multiply each $\mathbf{S}_i$ by ω^i. But applying $\mathbf{L}$ to the right side also results in multiplying each $\mathbf{S}_i$ by ω_i. Hence, the solution in Eq. A6 satisfies Eq. A5.

Eq. A6 shows that the eigenvectors of $\mathbf{L}$ each grow independently and exponentially. The eigenvector S_i grows with rate $\omega_i - \gamma$. The initial condition is a small perturbation of $S^D = 0$, and it can be assumed that every eigenvector is present in small amounts in that perturbation, so that no c_i^0 is equal to zero. Thus, if at least one growth rate $\omega_i - \gamma$ is positive, then the corresponding pattern of ocular dominance S_i will grow. In this case, the condition $S^D = 0$ is unstable to small perturbations, and the fastest-growing eigenvector will quickly dominate. It was assumed in the discussion of characteristic patterns in the text that there is at least one such positive growth rate.

[1] We restrict ourselves to vectors S^D which are nonzero only within an arbor, that is such that $A(\alpha) = 0$ implies $S^D(\alpha) = 0$. Define $T(x,\alpha) = S^D(x,\alpha)/\sqrt{A(x - \alpha)}$ for $A(x - \alpha) \neq 0$, $T(x,\alpha) = 0$ otherwise. Then the matrix operation on $\mathbf{T}$, $\mathbf{L}^\mathbf{T}$, has components $L^\mathbf{T}_{(x,\alpha);(y,\beta)} = \sqrt{A(x - \alpha)}I(x - y)C(\alpha - \beta)\sqrt{A(y - \beta)}$. This matrix is symmetric, $L^\mathbf{T}_{(x,\alpha);(y,\beta)} = L^\mathbf{T}_{(y,\beta);(x,\alpha)}$, which implies it has a complete basis of eigenvectors, with real eigenvalues. This in turn implies that $\mathbf{L}$ does.

In considering Eq. 6 in the text, it is useful to transform variables from cortical and geniculate variables, (x,α), to cortical and receptive field variables, (x,r) where $r = x - \alpha$. Letting $r' = y - \beta$, the operator $\mathbf{L}$ becomes $L_{(x,r);(y,r')} = A(r)I(x - y)C^D(x - y - (r - r'))$. This operator is a convolution in the cortical variables, depending only on $x - y$ and not on x or y separately. Ignoring the cortical boundaries, this means, by fourier transform of the cortical variables, that the eigenfunctions of L must be of the form $e^{ik\cdot x}R(r)$, where k is a two-vector of real numbers defining a wavelength and direction of oscillation of ocular dominance across cortex. R is a function defining a characteristic receptive field of synaptic differences S^D. Assuming as before that $C^D(\alpha) = C^D(-\alpha)$ and $I(x) = I(-x)$, the real part and imaginary part of each such complex eigenfunction are both real eigenfunctions, with the same eigenvalue. These real eigenfunctions can be chosen of the form $\cos k\cdot x\, R^+(r) + \sin k\cdot x\, R^0(r)$, where R^0 has zero net ocular dominance ($\Sigma_r R^0(r) = 0$) and R^+ may have net ocular dominance. R^+ is the leftmost receptive field of the patterns of Fig. 7.19, while R^0 is the central receptive field. If, as for the eigenfunction of Fig. 7.19a, $R^0 = 0$, then the eigenfunction is simply $\cos k\cdot x\, R^+(r)$, the product of a cortical oscillation and a receptive field function R^+.

More information on analysis of these equations can be found in Miller (1989a) and in Miller and Stryker (1989). For an introduction to the mathematics, see Hirsch and Smale (1974).

REFERENCES

Allard, T. (1989). Biological constraints on a dynamical network: The somatosensory nervous system. In S. J. Hanson & C. R. Olson (Eds.), *Connectionist modeling and brain function: The developing interface*. Cambridge, MA: MIT Press/Bradford.

Anderson, P. A., Olavarria, J., & Van Sluyters, R. C. (1988). The overall pattern of ocular dominance bands in cat visual cortex. *Journal of Neuroscience, 8,* 2183-2200.

Arikuni, T., Sakai, M., & Kubota, K. (1983). Columnar aggregation of prefrontal and anterior cingulate cortical cells projecting to the thalamic mediodorsal nucleus in the monkey. *Journal of Comparative Neurology, 220,* 116-125.

Arnett, D. W. (1978). Statistical dependence between neighboring retinal ganglion cells in goldfish. *Experimental Brain Research, 32,* 49-53.

Baldi, P., & Hornik, K. (1989). Neural networks and principal component analysis: Learning from examples without local minima. *Neural Networks, 2,* 53-58.

Beaulieu, C., & Colonnier, M. (1987). Effect of the richness of the environment on the cat visual cortex. *Journal of Comparative Neurology, 266,* 478-494.

Belford, G. R., & Killackey, H. P. (1980). The sensitive period in the development of the trigeminal system of the neonatal rat. *Journal of Comparative Neurology, 193,* 335-350.

Bienenstock, E. L., Cooper, L. N., & Munro, P. W. (1982). Theory for the development of neuron selectivity: Orientation specificity and binocular interaction in visual cortex. *Journal of Neuroscience, 2,* 32-48.

Boss, V. C., & Schmidt, J. T. (1984). Activity and the formation of ocular dominance patches in dually innervated tectum of goldfish. *Journal of Neuroscience, 4,* 2891-2905.

Bourgeois, J. P., Jastreboff, P. J., & Rakic, P. (1989). Synaptogenesis in visual cortex of normal and preterm monkeys: Evidence for intrinsic regulation of synaptic overproduction. *Proceedings of the National Academy of Sciences, 86,* 4297-4301.

Brown, M. C., Jansen, J. K. S., & Van Essen, D. (1976). Polyneuronal innervation of skeletal muscle in new-born rats and its elimination during maturation. *Journal of Physiology, 261,* 387-422.

Brown, T. H., Chapman, P. F., Kairiss, E. W., & Keenan, C. L. (1988). Long-term synaptic potentiation. *Science, 242,* 724-728.

Caminiti, R., Zeger, S., Johnson, P. B., Urbano, A., & Georgopoulos, A. P. (1985). Corticocortical efferent systems in the monkey: A quantitative spatial analysis of the tangential distribution of cells of origin. *Journal of Comparative Neurology, 241,* 405-419.

Changeux, J. P., & Danchin, A. (1976). Selective stabilization of developing synapses as a mechanism for the specification of neuronal networks. *Nature, 264,* 705-712.

Clark, S. A., Allard, T., Jenkins, W. M., & Merzenich, M. M. (1988). Receptive fields in the body-surface map in adult cortex defined by temporally correlated inputs. *Nature, 332,* 444-445.

Cline, H. T., & Constantine-Paton, M. (1988). NMDA receptor antagonist, APV, disorganizes the retinotectal map. *Society for Neuroscience Abstracts, 14,* 674.

Cline, H. T., Debski, E. A., & Constantine-Paton, M. (1987). N-methyl-d-asparate receptor antagonist desegregates eye-specific stripes. *Proceedings of the National Academy of Sciences USA, 84,* 4342-4345.

Constantine-Paton, M., & Law, M. I. (1978). Eye-specific termination bands in tecta of three-eyed frogs. *Science, 202,* 639-641.

Conway, J. L., & Schiller, P. H. (1983). Laminar organization of tree shrew dorsal lateral geniculate nucleus. *Journal of Neurophysiology, 50,* 1330-1342.

Cook, J. E. (1987). A sharp retinal image increases the topographic precision of the goldfish retinotectal projection during optic nerve regeneration in stroboscopic light. *Experimental Brain Research, 68,* 319-328.

Cook, J. E., & Rankin, E. C. (1986). Impaired refinement of the regenerated retinotectal projection of the goldfish in stroboscopic light: A quantitative WGA-HRP study. *Experimental Brain Research, 63,* 421-430.

Coss, R. G., & Perkel, D. H. (1985). The function of dendritic spines: A review of theoretical issues. *Behavioral and Neural Biology, 44,* 151-185.

Debski, E. A., & Constantine-Paton, M. (1988). The effects of glutamate receptor agonists and antagonists on the evoked tectal potential in *rana pipiens. Society for Neuroscience Abstracts, 14,* 674.

Dubin, M. W., Stark, L. A., & Archer, S. M. (1986). A role for action-potential activity in the development of neuronal connections in the kitten retinogeniculate pathway. *Journal of Neuroscience, 6,* 1021-1036.

Dumuis, A., Sebben, M., Haynes, L., Pin, J. P., & Bockaert, J. (1988). NMDA receptors activate the arachidonic acid cascade system in striatal neurons. *Nature, 336,* 68-70.

Durham, D., & Woolsey, T. A. (1984). Effects of neonatal whisker lesion on mouse central trigeminal pathways. *Journal of Comparative Neurology, 223, 424-447.*

Easter, S. S., Jr., & Stuermer, C.A.O. (1984). An evaluation of the hypothesis of shifting

terminals in goldfish optic tectum. *Journal of Neuroscience, 4,* 1052-1063.

Eisele, L. E., & Schmidt, J. T. (1988). Activity sharpens the regenerating retinotectal projection in goldfish: Sensitive period for strobe illumination and lack of effect on synaptogenesis and on ganglion cell receptive field properties. *Journal of Neurobiology, 19,* 395-411.

Fawcett, J. W., & O'Leary, D. D. M. (1985). The role of electrical activity in the formation of topographic maps in the nervous system. *Trends in Neurosciences, 8,* 201-206.

Fawcett, J. W., & Willshaw, D. J. (1982). Compound eyes project stripes on the optic tectum in *xenopus. Nature, 296,* 350-352.

Ferster, D. & LeVay, S. (1978). The axonal arborizations of lateral geniculate neurons in the striate cortex of the cat. *Journal of Comparative Neurology, 182,* 923-944.

Fladby, T., & Jansen, J. K. S. (1987). Postnatal loss of synaptic terminals in the partially denervated mouse soleus muscle. *Acta Physiologica Scandinavia, 129,* 239-246.

Fox, B. E. S., & Fraser, S. E. (1987). Excitatory amino acids in the retino-tectal system of xenopus laevis. *Society for Neuroscience Abstracts, 13,* 766.

Fraser, S. E. (1980). Differential adhesion approach to the patterning of nerve connections. *Developmental Biology, 79,* 453-464.

Fraser, S. E. (1985). Cell interactions involved in neuronal patterning: An experimental and theoretical approach. In G. M. Edelman, W. E. Gall, & W. M. Cowan (Eds.), *Molecular bases of neural development* (pp. 481-508). New York: Wiley.

Fregnac, Y., & Imbert, M. (1984). Development of neuronal selectivity in the primary visual cortex of the cat. *Physiological Review, 64,* 325-434.

Galli, L., & Maffei, L. (1988). Spontaneous impulse activity of rat retinal ganglion cells in prenatal life. *Science, 242,* 90-91.

Gamble, E., & Koch, C. (1987). The dynamics of free calcium in dendritic spines in response to repetitive synaptic input. *Science, 236,* 1311-1315.

Garraghty, P. E., Shatz, C. J., Sretavan, D. W., & Sur, M. (1988). Axon arbors of X and Y retinal ganglion cells are differentially affected by prenatal disruption of binocular inputs. *Proceedings of the National Academy of Science USA, 85,* 7361-7365.

Garraghty, P. E., Shatz, C. J., & Sur, M. (1988). Prenatal disruption of binocular interactions creates novel lamination in the cat's lateral geniculate nucleus. *Visual Neuroscience, 1,* 93-102.

Garraghty, P. E., & Sur, M. (1988). Interactions between retinal axons during development of their terminal arbors in the cat's lateral geniculate nucleus. In M. Bentivoglio & R. Spreafico (Eds.), *Cellular thalamic mechanisms* (pp. 465-477). Amsterdam: Elsevier Science BV.

Garraghty, P. E., Sur, M., & Sherman, S. M. (1986). Role of competitive interactions in the postnatal development of X and Y retinogeniculate axons. *Journal of Comparative Neurology, 251,* 216-239.

Garthwaite, J., Charles, S. L., & Chess-Williams, R. (1988). Endothelium-derived relaxing factor release on activation of NMDA receptors suggests role as intercellular messenger in the brain. *Nature, 336,* 385-387.

Gilbert, C. D., & Wiesel, T. N. (1983). Clustered intrinsic connections in cat visual cortex. *Journal of Neuroscience, 3,* 1116-1133.

Ginsburg, K. S., Johnsen, J. A., & Levine, M. W. (1984). Common noise in the firing of neighboring ganglion cells in gold fish retina. *Journal of Physiology, 351,* 433-451.

Goldman, P. S., & Nauta, W. J. H. (1977). Columnar distribution of cortico-cortical fibers in the frontal association, limbic, and motor cortex of the developing rhesus monkey. *Brain Research, 122,* 393-413.

Goldman-Rakic, P. S. (1984). Modular organization of prefrontal cortex. *Trends in Neurosciences, 7,* 419-424.

Goldman-Rakic, P. S., & Schwartz, M. L. (1982). Interdigitation of contralateral and

ipsilateral columnar projections to frontal association cortex in primates. *Science, 216,* 755-757.

Guillery, R. W. (1972). Binocular competition in the control of geniculate cell growth. *Journal of Comparative Neurology, 144,* 117-130.

Guillery, R. W. (1974). Visual pathways in albinos. *Scientific American, 230,* (5), 44-54.

Guillery, R. W., & Stelzner, D. J. (1970). The differential effects of unilateral lid closure upon the monocular and binocular segments of the dorsal lateral geniculate nucleus in the cat. *Journal of Comparative Neurology, 139,* 413-422.

Harris, W. A. (1981). Neural activity and development. *Annual Reviews of Physiology, 43,* 689-710.

Hata, Y., Tsumoto, T., Sato, H., Hagihara, K., & Tamura, H. (1988). Inhibition contributes to orientation selectivity in visual cortex of cat. *Nature, 335,* 815-817.

Hayes, W. P., & Meyer, R. L. (1988a). Retinotopically inappropriate synapses of subnormal density formed by misdirected optic fibers in goldfish tectum. *Developmental Brain Research, 38,* 304-312.

Hayes, W. P., & Meyer, R. L. (1988b). Optic synapse number but not density is constrained during regeneration onto surgically halved tectum in goldfish: HRP-EM evidence that optic fibers compete for fixed numbers of postsynaptic sites on the tectum. *Journal of Comparative Neurology, 274,* 539-559.

Hayes, W. P., & Meyer, R. L. (1989a). Normal numbers of retinotectal synapses during the activity-sensitive period of optic regeneration in goldfish: HRP-EM evidence implicating synapse rearrangement and collateral elimination during map refinement. *Journal of Neuroscience, 9,* 1400-1413.

Hayes, W. P., & Meyer, R. L. (1989b). Impulse blockade by intraocular tetrodoxin during optic regeneration in goldfish: HRP-EM evidence that the formation of normal numbers of optic synapses and the elimination of exuberant optic fibers is activity independent. *Journal of Neuroscience, 9,* 1414-1423.

Hebb, D. O. (1949). *The organization of behavior.* New York: Wiley.

Hess, R., Negishi, K., & Creutzfeldt, O. (1975). The horizontal spread of intracortical inhibition in the visual cortex. *Experimental Brain Research, 22,* 415-419.

Hirsch, M. W. & Smale, S. (1974). *Differential equations, dynamical systems and linear algebra.* New York: Academic Press.

Hubel, D. H., & Wiesel, T. N. (1962). Receptive fields, binocular interaction and functional architecture in the cat's visual cortex. *Journal of Physiology, 160,* 106-154.

Hubel, D. H., & Wiesel, T. N. (1963). Receptive fields of cells in striate cortex of very young, visually inexperienced kittens. *Journal of Neurophysiology, 26,* 994-1002.

Hubel, D. H., & Wiesel, T. N. (1965). Binocular interaction in striate cortex of kittens reared with artificial squint. *Journal of Neurophysiology, 28,* 1041-1059.

Hubel, D. H., & Wiesel, T. N. (1970). The period of susceptibility to the physiological effects of unilateral eye closure in kittens. *Journal of Physiology, 206,* 419-436.

Hubel, D. H., & Wiesel, T. N. (1977). Functional architecture of macaque monkey visual cortex. *Proceedings of the Royal Society of London Series B, 198,* 1-59.

Hubel, D. H., Wiesel, T. N., & LeVay, S. (1977). Plasticity of ocular dominance columns in monkey striate cortex. *Philosophical Transactions of the Royal Society of London Series B, 278,* 377-409.

Humphrey, A. L., Sur, M., Uhlrich, D. J., & Sherman, S. M. (1985a). Projection patterns of individual X- and Y-cell axons from the lateral geniculate nucleus to cortical area 17 in the cat. *Journal of Comparative Neurology, 233,* 159-189.

Humphrey, A. L., Sur, M., Uhlrich, D. J., & Sherman, S. M. (1985b). Termination patterns of individual X- and Y-cell axons in the visual cortex of the cat: Projections to area 18, to

the 17/18 border region, and to both areas 17 and 18. *Journal of Comparative Neurology, 233,* 190-212.

Ide, C. F., Fraser, S. E., & Meyer, R. L. (1983). Eye dominance columns from an isogenic double-nasal frog eye. *Science, 221,* 293-295.

Innocenti, G. M., & Frost, D. O. (1979). Effects of visual experience on the maturation of the efferent system to the corpus callosum. *Nature, 280,* 231-234.

Innocenti, G. M., & Frost, D. O. (1980). The postnatal development of visual callosal connections in the absence of visual experience or of the eyes. *Experimental Brain Research, 39,* 365-375.

Innocenti, G. M., Frost, D. O., & Illes, J. (1985). Maturation of visual callosal connections in visually deprived kittens: A challenging critical period. *Journal of Neuroscience, 5,* 255-267.

Jeanmonod, D., Rice, F. L., & Van der Loos, H. (1981). Mouse somatosensory cortex: Alterations in the barrelfield following receptor injury at different early postnatal ages. *Neuroscience, 6,* 1503-1535.

Jones, D. G., Van Sluyters, R. C., & Murphy, K. M. (1988). A computational model for the overall pattern of ocular dominance bands in striate cortex of cat and monkey. *Society for Neuroscience Abstracts, 14,* 1122.

Jones, E. G., Burton, H., & Porter, R. (1975). Commissural and cortico-cortical 'columns' in the somatic sensory cortex of primates. *Science, 190,* 572-574.

Jones, E. G., Coulter, J. D., & Wise, S. P. (1979). Commissural columns in the sensory-motor cortex of monkeys. *Journal of Comparative Neurology, 188,* 113-136.

Jones, E. G., & Wise, S. P. (1977). Size, laminar and columnar distribution of efferent cells in the sensory-motor cortex of monkeys. *Journal of Comparative Neurology, 175,* 391-438.

Kater, S. B., Mattson, M. P., Cohan, C., & Conner, J. (1988). Calcium regulation of the neuronal growth cone. *Trends in Neurosciences, 11,* 315-321.

Katz, L. C., & Constantine-Paton, M. (1988). Relationships between segregated afferents and postsynaptic neurons in the optic tectum of three-eyed frogs. *Journal of Neuroscience, 8,* 3160-3180.

Katz, L. C., Gilbert, C. D., & Wiesel, T. N. (1989). Local circuits and ocular dominance columns in monkey striate cortex. *Journal of Neuroscience, 9,* 1389-1399.

Kauer, J. A., Malenka, R. C., & Nicoll, R. A. (1988). NMDA application potentiates synaptic transmission in the hippocampus. *Nature, 334,* 250-252.

Keating, M. J. (1975). The time course of experience-dependent synaptic switching of visual connections in *Xenopus laevis. Proceedings of the Royal Society of London Series B, 189,* 603-610.

Keller, J. B. (1977). Effective behavior of heterogeneous media. In U. Landman (Ed.), *Statistical mechanics and statistical methods in theory and application* (pp. 631-644). New York: Plenum.

Kleinschmidt, A., Bear, M. F., & Singer, W. (1987). Blockade of 'NMDA' receptors disrupts experience-dependent plasticity of kitten striate cortex. *Science, 238,* 355-358.

Knudsen, E. I. (1985). Experience alters the spatial tuning of auditory units in the optic tectum during a sensitive period in the barn owl. *Journal of Neuroscience, 5,* 3094-3109.

Knudsen, E. I. (1988). Early blindness results in a degraded auditory map of space in the optic tectum of the barn owl. *Proceedings of the National Academy of Sciences USA, 85,* 6211-6214.

Knudsen, E. I., Du Lac, S., & Esterly, S. D. (1987). Computational maps in the brain. *Annual Reviews of Neuroscience, 10,* 41-65.

Knudsen, E. I., & Knudsen, P. F. (1985). Vision guides the adjustment of auditory localization in young barn owls. *Science, 230,* 545-548.

Kretz, G., Rager, G., & Norton, T. T. (1986). Laminar organization of on and off regions and

ocular dominance in the striate cortex of the tree shrew (*Tupaia belangeri*). *Journal of Comparative Neurology, 251,* 135-145.

LeVay, S., Connolly, M., Houde, J., & Van Essen, D. C. (1985). The complete pattern of ocular dominance stripes in the striate cortex and visual field of the macaque monkey. *Journal of Neuroscience, 5,* 486-501.

LeVay, S., & McConnell, S. K. (1982). On and off layers in the lateral geniculate nucleus of the mink. *Nature, 300,* 350-351.

LeVay, S., & Nelson, S. B. (1989). The columnar organization of visual cortex. In A. Leventhal (Ed.), *The electrophysiology of vision.* London: Macmillan Press.

LeVay, S., & Stryker, M. P. (1979). The development of ocular dominance columns in the cat. In J. A. Ferrendelli (Ed.), *Aspects of developmental neurobiology* (pp. 83-98). Bethesda: Society for Neuroscience.

LeVay, S., Stryker, M. P., & Shatz, C. J. (1978). Ocular dominance columns and their development in layer IV of the cat's visual cortex: A quantitative study. *Journal of Comparative Neurology, 179,* 223-244.

Levick, W. R., & Williams, W. O. (1964). Maintained activity of lateral geniculate neurones in darkness. *Journal of Physiology, 170,* 582-597.

Levine, R., & Jacobson, M. (1975). Discontinuous mapping of retina into tectum innervated by both eyes. *Brain Research, 98,* 172-176.

Lichtman, J. W., & Purves, D. (1981). Regulation of the number of axons that innervate target cells. In D. R. Garrod & J. D. Feldman (Eds.), *Development in the nervous system* (pp. 233-243). Cambridge: Cambridge University Press.

Linsker, R. (1986). From basic network principles to neural architecture. *Proceedings of the National Academy of Sciences, 83,* 7508-7512, 8390-8394, 8779-8783.

Linsker, R. (1988). Self-organization in a perceptual network. *Computer, 21,* 105-117.

Lisman, J. E., & Goldring, M. A. (1988). Feasibility of long-term storage of graded information by the calcium/calmodulin-dependent protein kinase molecules of the postsynaptic density. *Proceedings of the National Academy of Sciences USA, 85,* 5320-5324.

Luhmann, H. J., Martinez Millan, L., & Singer, W. (1986). Development of horizontal intrinsic connections in cat striate cortex. *Experimental Brain Research, 63,* 443-448.

Lynch, G., & Baudry, M. (1984). The biochemistry of memory: A new and specific hypothesis. *Science, 224,* 1057-1063.

Malinow, R., Madison, D. V., & Tsien, R. W. (1988). Persistent protein kinase activity underlying long-term potentiation. *Nature, 335,* 820-824.

Mallot, H. A. (1985). An overall description of retinotopic mapping in the cat's visual cortex areas 17, 18, and 19. *Biological Cybernetics, 52,* 45-51.

Malsburg, C. von der. (1979). Development of ocularity domains and growth behavior of axon terminals. *Biological Cybernetics, 32,* 49-62.

Malsburg, C. von der, & Willshaw, D. J. (1976). A mechanism for producing continuous neural mappings: Ocularity dominance stripes and ordered retino-tectal projections. *Experimental Brain Research, Supplement 1,* 463-469.

Malsburg, C. von der, & Willshaw, D. J. (1977). How to label nerve cells so that they can interconnect in an ordered fashion. *Proceedings of the National Academy of Sciences USA, 74,* 5176-5178.

Mastronarde, D. N. (1983a). Correlated firing of cat retinal ganglion cells. I. Spontaneously active inputs to X and Y cells. *Journal of Neurophysiology, 49,* 303-324.

Mastronarde, D. N. (1983b). Correlated firing of cat retinal ganglion cells. II. Responses of X- and Y-cells to single quantal events. *Journal of Neurophysiology, 49,* 325-349.

Mastronarde, D. N. (1989). Correlated firing of retinal ganglion cells. *Trends in Neurosciences, 12,* 75-80.

Mayer, M. L., & Westbrook, G. L. (1987). The physiology of excitatory amino acids in the

vertebrate central nervous system. *Progress in Neurobiology, 28,* 197-276.

McConnell, S. K., & LeVay, S. (1984). Segregation of ON- and OFF-center afferents in mink visual cortex. *Proceedings of the National Academy of Sciences USA, 81,* 1590-1593.

Merzenich, M. M., Allard, T., Jenkins, W. M., & Recanzone, G. (1988). Self-organizing processes in adult neo-cortex. In W. von Seelen, U. M. Leimhos, & G. Shaw (Eds.), *Organization of neural networks: Structures and models.* New York: VCH Publishers.

Merzenich, M. M., Jenkins, W. M., & Middlebrooks, J. C. (1984). Observations and hypotheses on special organizational features of the central auditory nervous system. In G. M. Edelman, W. E. Gall, & W. M. Cowan (Eds.), *Dynamic aspects of neocortical function* (pp. 397-424). New York: Wiley.

Merzenich, M. M., Kaas, J.H., Wall, J. T., Sur, M., Nelson, R. J., & Felleman, D. J. (1983). Progression of change following median nerve section in the cortical representation of the hand in areas 3b and 1 in adult owl and squirrel monkeys. *Neuroscience, 10,* 639-665.

Merzenich, M. M., Nelson, R. J., Kaas, J. H., Stryker, M. P., Jenkins, W. M., Zook, J. M., Cynader, M. S., & Schoppmann, A. (1987). Variability in hand surface representations in areas 3b and 1 in adult owl and squirrel monkeys. *Journal of Comparative Neurology, 258,* 281-296.

Meyer, R. L. (1979). "Extra" optic fibers exclude normal fibers from tectal regions in goldfish. *Journal of Comparative Neurology, 183,* 883-902.

Meyer, R. L. (1982). Tetrodotoxin blocks the formation of ocular dominance columns in goldfish. *Science, 218,* 589-591.

Meyer, R. L. (1983). Tetrodotoxin inhibits the formation of refined retinotopography in goldfish. *Developmental Brain Research, 6,* 293-298.

Miller, J. P., Rall, W., & Rinzel, J. (1985). Synaptic amplification by active membrane in dendritic spines. *Brain Research, 325,* 325-330.

Miller, K. D. (1989b). Orientation-selective cells can emerge from a Hebbian mechanism through interactions between ON- and OFF-center inputs. *Society for Neuroscience Abstracts, 15.*

Miller, K. D. (1989a). *Ph. D. Thesis, Stanford University Medical School.* University Microfilms, Ann Arbor.

Miller, K. D., Chapman, B., & Stryker, M. P. (1989). Responses of cells in cat visual cortex depend on NMDA receptors. *Proceedings of the National Academy of Sciences,* 86, 5183-5187.

Miller, K. D., Keller, J. B., & Stryker, M. P. (1986). Models for the formation of ocular dominance columns solved by linear stability analysis. *Society for Neuroscience Abstracts, 12,* 1373.

Miller, K. D., Keller, J. B., & Stryker, M. P. (1988). Network model of ocular dominance column formation: Analytical results. *Neural Networks, 1,* S266.

Miller, K. D., Keller, J. B., & Stryker, M. P. (1989). Ocular dominance column development: Analysis and simulation. *Science,* 245, 605-615.

Miller, K. D., & Stryker, M. P. (1988). Models for the formation of ocular dominance columns: Computational results. *Society for Neuroscience Abstracts, 14,* 1122.

Miller, K. D., & Stryker, M. P. (1989). The development of ocular dominance columns: Mechanisms and models. In S. J. Hanson & C. R. Olson (Eds.), *Connectionist modeling and brain function: The developing interface.* Cambridge, MA: MIT Press/Bradford.

Miller, K. D., Stryker, M. P., & Keller, J. B. (1988). Network model of ocular dominance column formation: Computational results. *Neural Networks, 1,* S267.

Moody, C. I., & Sillito, A. M. (1988). The role of the n-methyl-d-aspartate (NMDA) receptor in the transmission of visual information in the feline dorsal lateral geniculate nucleus (dlgn). *Journal of Physiology, 396,* 62P.

Mountcastle, V. B. (1978). An organizing principle for cerebral function: The unit module and

the distributed system. In G. M. Edelman & V. B. Mountcastle (Eds.), *The mindful brain* (pp. 7-50). Cambridge, MA: MIT Press.

Movshon, J. A., & Van Sluyters, R. C. (1981). Visual neural development. *Annual Reviews of Psychology, 32,* 477-522.

Muller, C. M., Engel, A. K., & Singer, W. (1988). Development of astrocytes in the cat visual cortex. *Society for Neuroscience Abstracts, 14,* 745.

Murray, M., Sharma, S., & Edwards, M. A. (1982). Target regulation of synaptic number in the compressed retinotectal projection of goldfish. *Journal of Comparative Neurology, 209,* 374-385.

Nahorski, S. R. (1988). Inositol polyphosphates and neuronal calcium homeostasis. *Trends in Neurosciences, 11,* 444-448.

Nicoll, R. A., Kauer, J. A., & Malenka, R. C. (1988). The current excitement in long-term potentiation. *Neuron, 1,* 97-103.

O'Brien, R. A. D., Ostberg, A. J., & Vrbova, G. (1980). The effect of acetylcholine on the function and structure of the developing mammalian neuromuscular junction. *Neuroscience, 5,* 1367-1379.

Oja, E. (1982). A simplified neuron model as a principal component analyzer. *Journal of Mathematical Biology, 15,* 267-273.

Piomelli, D., Volterra, A., Dale, N., Siegelbaum, S. A., Kandel, E. R., Schwartz, J. H., & Belardetti, F. (1987). Lipoxygenase metabolites of arachidonic acid as second messengers for presynaptic inhibition of *Aplysia* sensory cells. *Nature, 328,* 38-43.

Purves, D. (1988). *Body and brain: A trophic theory of neural connections.* Cambridge, MA: Harvard University Press.

Purves, D., & Lichtman, J. W. (1985). *Principles of neural development.* Sunderland, MA: Sinauer Associates, Inc.

Purves, D., Snider, W. D., & Voyvodic, J. T. (1988). Trophic regulation of nerve cell morphology and innervation in the autonomic nervous system. *Nature, 336,* 123-128.

Rakic, P. (1976). Prenatal genesis of connections subserving ocular dominance in the rhesus monkey. *Nature, 261,* 467-471.

Rakic, P. (1977). Prenatal development of the visual system in the rhesus monkey. *Philosophical Transactions of the Royal Society of London Series B, 278,* 245-260.

Ramoa, A. S., Campbell, G., & Shatz, C. J. (1988). Dendritic growth and remodeling of cat retinal ganglion cells during fetal and postnatal development. *Journal of Neuroscience, 8,* 4239-4261.

Ramoa, A. S., Paradiso, M. A., & Freeman, R. D. (1988). Blockade of intracortical inhibition in kitten striate cortex: effects on receptive field properties and associated loss of ocular dominance plasticity. *Experimental Brain Research, 73,* 285-296.

Rauschecker, J. P. (1989). Mechanisms of visual plasticity as a model for the formation of long-term memory. *Physiological Reviews.*

Reh, T. A., & Constantine-Paton, M. (1984). Retinal ganglion cell terminals change their projection sites during larval development of *rana pipiens. Journal of Neuroscience, 4,* 442-457.

Reh, T. A., & Constantine-Paton, M. (1985). Eye-specific segregation requires neural activity in three-eyed *rana pipiens. Journal of Neuroscience, 5,* 1132-1143.

Reiter, H. O., & Stryker, M. P. (1988). Neural plasticity without postsynaptic action potentials: Less-active inputs become dominant when kitten visual cortical cells are pharmacologically inhibited. *Proceedings of the National Academy of Sciences USA, 85,* 3623-3627.

Reiter, H. O., Waitzman, D. M., & Stryker, M. P. (1986). Cortical activity blockade prevents ocular dominance plasticity in the kitten visual cortex. *Experimental Brain Research, 65,* 182-188.

Rochester, N., Holland, J. H., Haibt, L. H., & Duda, W. L. (1956). Tests on a cell assembly theory of the action of the brain, using a large digital computer. *IRE Transactions on Information Theory, IT-2,* 80-93. Reprinted in J. A. Anderson & E. Rosenfeld (Eds.), *Neurocomputing: Foundations of research* (pp. 68-79). Cambridge, MA: MIT Press/Bradford, 1988.

Rodieck, R. W., & Smith, P. S. (1966). Slow dark discharge rhythms of cat retinal ganglion cells. *Journal of Neurophysiology, 29,* 942-953.

Rumelhart, D. E., & Zipser, D. (1986). Feature discovery by competitive learning. In D. E. Rumelhart & J. L. McClelland (Eds.), *Parallel distributed processing: Explorations in the microstructure of cognition* (Vol. 1, pp. 151-193). Cambridge, MA: MIT Press/Bradford.

Salt, T. E. (1986). Mediation of thalamic sensory input by both NMDA receptors and non-NMDA receptors. *Nature, 322,* 263-265.

Salt, T. E. (1987). Excitatory amino acid receptors and synaptic transmission in the rat ventrobasal thalamus. *Journal of Physiology, 391,* 499-510.

Sanes, D. H., & Constantine-Paton, M. (1985). The sharpening of frequency tuning curves requires patterned activity during development in the mouse, *Mus musculus. Journal of Neuroscience, 5,* 1152-1166.

Sanger, T. D. (1989). An optimality principle for unsupervised learning. In D. Touretzky (Ed.), *Advances in neural information processing systems* (pp. 11-19). San Mateo, CA: Morgan Kaufmann.

Scherer, W. S., & Udin, S. B. (1988). The role of NMDA receptors in the development of binocular maps in *xenopus* tectum. *Society for Neuroscience Abstracts, 14,* 675.

Schiller, P. H., & Malpeli, J. G. (1978). Functional specificity of lateral geniculate nucleus laminae of the rhesus monkey. *Journal of Neurophysiology, 41,* 788-797.

Schmidt, J. T. (1985). Formation of retinotopic connections: Selective stabilization by an activity-dependent mechanism. *Cellular and Molecular Neurobiology, 5,* 65-84.

Schmidt, J. T. (1988). NMDA blockers prevent both retinotopic sharpening and LTP in regenerating optic pathway of goldfish. *Society for Neuroscience Abstracts, 14,* 675.

Schmidt, J. T., & Edwards, D. L. (1983). Activity sharpens the map during the regeneration of the retinotectal projection in goldfish. *Brain Research, 269,* 29-39.

Schmidt, J. T., & Eisele, L. E. (1985). Stroboscopic illumination and dark rearing block the sharpening of the retinotectal map in goldfish. *Neuroscience, 14,* 535-546.

Schmidt, J. T., & Tieman, S. B. (1985). Eye-specific segregation of optic afferents in mammals, fish and frogs: The role of activity. *Cellular and Molecular Neurobiology, 5,* 5-34.

Schneider, G. E. (1973). Early lesions of superior colliculus: Factors affecting the formation of abnormal retinal projections. *Brain, Behavior and Evolution, 8,* 73-109.

Schwartz, M. L., & Goldman-Rakic, P. S. (1984). Callosal and intrahemispheric connectivity of the prefrontal association cortex in rhesus monkey: Relations between intraparietal and principal sulcal cortex. *Journal of Comparative Neurology, 226,* 403-420.

Schwartz, J. H., & Greenberg, S. M. (1987). Molecular mechanisms for memory: Second-messenger induced modifications of protein kinases in nerve cells. *Annual Review of Neuroscience, 10,* 459-476.

Sejnowski, T. J. (1977). Storing covariance with nonlinearly interacting neurons. *Journal of Mathematical Biology, 4,* 303-321.

Selemon, L. D., & Goldman-Rakic, P. S. (1985). Longitudinal topography and interdigitation of corticostriatal projections in the rhesus monkey. *Journal of Neuroscience, 5,* 776-794.

Shatz, C. J. (1983). The prenatal development of the cat's retinogeniculate pathway. *Journal of Neuroscience, 3,* 482-499.

Shatz, C. J. (1988). The role of function in the prenatal development of retinogeniculate connections. In M. Bentivoglio & R. Spreafico (Eds.), *Cellular thalamic mechanisms* (pp. 435-446). Amsterdam: Elsevier Science Publishers BV.

Shatz, C. J., & Kirkwood, P. (1984). Prenatal development of functional connections in the cat's retinogeniculate pathway. *Journal of Neuroscience, 4,* 1378-1397.

Shatz, C. J., Lindstrom, S., & Wiesel, T. N. (1977). The distribution of afferents representing the right and left eyes in the cat's visual cortex. *Brain Research, 131,* 103-116.

Shatz, C. J., & Stryker, M. P. (1978). Ocular dominance in layer IV of the cat's visual cortex and the effects of monocular deprivation. *Journal of Physiology, 281,* 267-283.

Shatz, C. J., & Stryker, M. P. (1988). Tetrodotoxin infusion prevents the formation of eye-specific layers during prenatal development of the cat's retinogeniculate projection. *Science, 242,* 87-89.

Sherk, H., & Stryker, M. P. (1976). Quantitative study of cortical orientation selectivity in visually inexperienced kitten. *Journal of Neurophysiology, 39,* 63-70.

Sherman, S. M., & Spear, P. D. (1982). Organisation of visual pathways in normal and visually deprived cats. *Physiological Review, 62,* 738-855.

Soodak, R. E. (1987). The retinal ganglion cell mosaic defines orientation columns in striate cortex. *Proceedings of the National Academy of Sciences USA, 84,* 3936-3940.

Sretavan, D. W., & Shatz, C. J. (1986). Prenatal development of retinal ganglion cell axons: Segregation into eye-specific layers within the cat's lateral geniculate nucleus. *Journal of Neuroscience, 6,* 234-251.

Sretavan, D. W., & Shatz, C. J. (1987). Axon trajectories and pattern of terminal arborization during the prenatal development of the cat's retinogeniculate pathway. *Journal of Comparative Neurology, 255,* 386-400.

Sretavan, D. W., Shatz, C. J., & Stryker, M. P. (1988). Modification of retinal ganglion cell morphology by prenatal infusion of tetrodotoxin. *Nature, 336,* 468-471.

Stent, G. S. (1973). A physiological mechanism of Hebb's postulate of learning. *Proceedings of the National Academy of Sciences USA, 70,* 997-1001.

Stryker, M. P. (1977). The role of early experience in the development and maintenance of orientation selectivity in the cat's visual cortex. In E. Poppel, R. Held, & J. E. Dowling (Eds.), *Neurosciences research program bulletin* (Vol. 15, N. 3, pp. 454-462). Cambridge, MA: MIT Press.

Stryker, M. P. (1986). The role of neural activity in rearranging connections in the central visual system. In R. J. Ruben, T. R. Van De Water, & E. W. Rubel (Eds.), *The biology of change in otolaryngology* (pp. 211-224). Amsterdam: Elsevier Science B. V.

Stryker, M. P., & Harris, W. (1986). Binocular impulse blockade prevents the formation of ocular dominance columns in cat visual cortex. *Journal of Neuroscience, 6,* 2117-2133.

Stryker, M. P., Sherk, H., Leventhal, A. G., & Hirsch, H. V. (1978). Physiological consequences for the cat's visual cortex of effectively restricting early visual experience with oriented contours. *Journal of Neurophysiology, 41,* 896-909.

Stryker, M. P., & Strickland, S. L. (1984). Physiological segregation of ocular dominance columns depends on the pattern of afferent electrical activity. *Investigative Opthalmology Supplements, 25,* 278.

Stryker, M. P., & Zahs, K. R. (1983). On and off sublaminae in the lateral geniculate nucleus of the ferret. *Journal of Neuroscience, 3,* 1943-1951.

Sur, M. (1988). Development and plasticity of retinal X and Y axon terminations in the cat's lateral geniculate nucleus. *Brain, Behavior and Evolution, 31,* 243-251.

Sur, M., Merzenich, M. M., & Kaas, J. H. (1980). Magnification, receptive-field area, and 'hypercolumn' size in areas 3b and 1 of somatosensory cortex in owl monkeys. *Journal of Neurophysiology, 44,* 295-311.

Sur, M., Wall, J. T., & Kaas, J. H. (1984). Modular distribution of neurons with slowly adapting and rapidly adapting responses in area 3b of somatosensory cortex in monkeys. *Journal of Neurophysiology, 51,* 724-744.

Swindale, N. V. (1980). A model for the formation of ocular dominance stripes. *Proceedings of the Royal Society of London Series B., 208,* 243-264.

Swindale, N. V. (1988). Role of visual experience in promoting segregation of eye dominance patches in the visual cortex of the cat. *Journal of Comparative Neurology, 267,* 472-488.

Toyama, K., Kimura, M., & Tanaka, K. (1981a). Cross-correlation analysis of interneuronal connectivity in cat visual cortex. *Journal of Neurophysiology, 46,* 191-201.

Toyama, K., Kimura, M., & Tanaka, K. (1981b). Organization of cat visual cortex as investigated by cross-correlation technique. *Journal of Neurophysiology, 46,* 202-214.

Tsien, R. W., Lipscombe, D., Madison, D. V., Bley, K. R., & Fox, A. P. (1988). Multiple types of neuronal calcium channels and their selective modulation. *Trends in Neurosciences, 11,* 431-438.

Tso, D. Y., Gilbert, C. D., & Wiesel, T. N. (1986). Relationships between horizontal interactions and functional architecture in cat striate cortex as revealed by cross correlation analysis. *Journal of Neuroscience, 6,* 1160-1170.

Tusa, R. J., Palmer, L. A., & Rosenquist, A. C. (1978). The retinotopic organization of area 17 (striate cortex) in the cat. *Journal of Comparative Neurology, 177,* 213-235.

Udin, S. B. (1983). Abnormal visual input leads to development of abnormal axon trajectories in frogs. *Nature, 301,* 336-338.

Udin, S. B. (1985). The role of visual experience in the formation of binocular projections in frogs. *Cellular and Molecular Neurobiology, 5,* 85-102.

Udin, S. B., & Fawcett, J. W. (1988). Formation of topographic maps. *Annual Reviews of Neuroscience, 11,* 289-327.

Wall, J. T. (1988). Variable organization in cortical maps of the skin as an indication of the lifelong adaptive capacities of circuits in the mammalian brain. *Trends in Neurosciences, 11,* 549-557.

Wall, J. T., Kaas, J. H., Sur, M., Nelson, R. J., Felleman, D. J., & Merzenich, M. M. (1986). Functional reorganization in somatosensory cortical areas 3b and 1 of adult monkeys after median nerve repair: Possible relationships to sensory recovery in humans. *Journal of Neuroscience, 6,* 218-233.

Whitelaw, V. A., & Cowan, J. D. (1981). Specificity and plasticity of retinotectal connections: A computational model. *Journal of Neuroscience, 1,* 1369-1387.

Wiesel, T. N., & Hubel, D. H. (1965). Comparison of the effects of unilateral and bilateral eye closure on cortical unit responses in kittens. *Journal of Neurophysiology, 28,* 1029-1040.

Wiesel, T. N., & Hubel, D. H. (1974). Ordered arrangement of orientation columns in monkeys lacking visual experience. *Journal of Comparative Neurology, 158,* 307-318.

Willshaw, D. J., & Malsburg, C. von der. (1976). How patterned neural connections can be set up by self-organization. *Proceedings of the Royal Society of London Series B, 194,* 431-445.

Willshaw, D. J., & Malsburg, C. von der. (1979). A marker induction mechanism for the establishment of ordered neural mappings: Its application to the retinotectal problem. *Philosophical Transactions of the Royal Society of London Series B, 287,* 203-243.

Worgotter, F., & Eysel, U. Th. (1989). On the influence and topography of excitation and inhibition at orientation-specific visual cortical neurons in the cat. Manuscript submitted for publication.

Zahs, K. R., & Stryker, M. P. (1988). Segregation of on and off afferents to ferret visual cortex. *Journal of Neurophysiology, 59,* 1410-1429.